

Design of Transceiver Module for Dual Polarized Doppler Solid State Radar for CASA Student Test Bed

by

Alexandra Litchfield-Santana

A thesis submitted in partial fulfillment of the requirements for the degree of

MASTER OF SCIENCE
in
ELECTRICAL ENGINEERING

UNIVERSITY OF PUERTO RICO
MAYAGÜEZ CAMPUS
2009

Approved by:

Sandra L. Cruz-Pol, PhD.
Member, Graduate Committee

Date

José Colóm Ustáriz, PhD.
Member, Graduate Committee

Date

Rafael Rodríguez Solís, PhD.
President, Graduate Committee

Date

Omar Colón Reyes, PhD.
Representative of Graduate Studies

Date

Isidoro Couvertier Reyes, PhD.
Chairperson of the Department

Date

ABSTRACT

The design of a Transmit Receive Solid State Module for a Solid State, X-band (9.5 GHz), Doppler, Dual Polarized meteorological radar system for the CASA student Test Bed is presented in this thesis. This Solid State Transceiver Module is capable of outputting a 1dBm power when transmitting and it receives a minimum detectable signal of -110dBm with as low as 4dB of Noise Figure. This device is able to handle an input signal no greater than -55dBm and it has a 24 channel system dynamic range of 41.19dBm. A twenty four channel Solid State Radar is to be designed in the future, then two Transceiver Modules are needed to fulfill each channel (one per polarizations) for a total of forty eight Solid State Modules. The scope of this project is to design a fully operational Transceiver Module and test it with one channel. This system will be the first Solid State system designed and developed at UPRM for precipitation measurements.

RESUMEN

Este trabajo presenta el diseño y desarrollo de la tarjeta de transmisión y recepción para un radar de estado sólido, banda X (9.5GHz), doppler y de doble polarización para el "CASA Student Test Bed". Este Módulo de Transmisión y Recepción de estado sólido es capaz de proveer una salida de 1dBm cuando está transmitiendo y recibe una señal mínima de -110dBm, con una figura de Ruido tan baja como 4dB. Este dispositivo es capaz de manejar señales no mayores de -55dBm y el sistema con 24 canales posee un rango dinámico de 41.19dBm. En el futuro se diseñará un radar de estado sólido con 24 canales. Entonces dos módulos de transmisión y recepción se necesitarán por cada canal (uno para cada polarización) para un total de 48 módulos de estado sólido. En este proyecto se diseñará un módulo de transmisión y recepción completamente operacional y se realizarán pruebas para un solo canal. Este sistema para medir precipitación será el primer sistema de estado sólido diseñado y desarrollado en la Universidad de Puerto Rico en Mayagüez.

To GOD, to my father Fernando Litchfield, my mother Norma Santana, my brother Fernando J. Litchfield, my sister Alicia Litchfield and my boyfriend Oscar R. Guzman Rivera, for encouraging and believing in me, for all your support and advice over the past years and for always being there when I most needed it.

ACKNOWLEDGEMENTS

There were a lot of people that helped me through the journey of completing my Master's degree. I have to admit that without the enthusiasm and inspiration of my advisor, Dr. Rafael Rodríguez Solís, this thesis would not have been possible. I have to thank him for his invaluable guidance through my research and course work. He has been not only an advisor to me but a great friend. Throughout my thesis-writing period, he provided encouragement, sound advice, good teaching, good company, and lots of good ideas. I would have been lost without him.

I would like to thank the many people who have taught me engineering through my entire bachelor and masters degree: all my undergraduate professors, (especially Dr. Sandra Cruz Pol and Dr. José Colóm Ustáriz), my Raytheon Co-workers (especially Brenda Ortiz Valle and Richard Chiasson), and finally my graduate teachers (especially Dr. Sandra Cruz Pol, Dr. José Colóm Ustáriz and Dr. Rafael Rodríguez Solís). For inspiring me to pursue my masters and always giving me good advice.

I am indebted to my many student colleagues for providing a stimulating and fun environment in which to learn and grow. I am especially grateful to Jaime Di Cristina, Alix Rivera, Pablo Lozada, Maria Fernanda, and Enid Serrano at the University of Puerto Rico. I would also like to extend my thanks to Solimar Reyes for her unconditional friendship, emotional support and for helping me through the difficult times.

I am grateful to the secretaries of the Electrical Engineering Department (especially Sandra Montalvo) for help the department to run smoothly and for assisting me in many different ways.

Finally, I would like to give all my gratitude to my parents, my extended family, and to my beloved, Oscar R Guzman Rivera. These people mean the most to me because they give me all their support and all their unconditional love and the journey was very pleasant with their presence by my side.

Table of Contents

ABSTRACT.....	II
RESUMEN	III
ACKNOWLEDGEMENTS.....	V
TABLE OF CONTENTS	VII
TABLE LIST.....	IX
FIGURE LIST	X
1 INTRODUCTION.....	2
1.1 MOTIVATION.....	4
1.2 OBJECTIVE	5
1.3 LITERATURE REVIEW	6
1.4 SUMMARY OF FOLLOWING CHAPTERS	10
2 THEORETICAL BACKGROUND	11
2.1 RADAR BASICS PRINCIPLES	11
2.1.1 <i>Basic Operation of a Radar</i>	12
2.1.2 <i>Radar Equation</i>	12
2.2 RECEIVER	14
2.2.1 <i>Bandwidth Considerations</i>	14
2.2.2 <i>Dynamic Range</i>	15
2.2.3 <i>Minimum Detectable Signal (MDS)</i>	16
2.3 TRANSMITTER.....	16
2.3.1 <i>Pulsed vs. Continuous Wave (CW) Transmitter</i>	17
2.3.2 <i>Vector Modulators</i>	17
2.4 SOLID STATE TRANSMITTER	18
2.5 METEOROLOGICAL RADAR	19
2.5.1 <i>Radar Range Equation for meteorological targets</i>	20
2.5.2 <i>Range Resolution</i>	20
2.5.3 <i>Maximum Unambiguous Range and Velocity</i>	21
2.5.4 <i>Doppler Frequency</i>	23
2.5.5 <i>Dual Polarization</i>	24
2.5.6 <i>Radar Reflectivity</i>	25
2.6 INTERMODULATION DISTORTION	27
3 METHODOLOGY	29
3.1 DESIGN METHODOLOGY	31
3.1.1 <i>Receiver Component Selection</i>	31
3.1.2 <i>Transmitter Component Selection</i>	35
3.2 SIMULATIONS.....	37
3.2.1 <i>Receiver Power Analysis</i>	37
3.2.2 <i>Transmitter Power Analysis</i>	42
3.2.3 <i>Receiver Dynamic Range Analysis</i>	49
3.2.4 <i>Transmitter Dynamic Range Analysis</i>	52

3.2.5	<i>Receiver Noise Figure Analysis</i>	53
3.2.6	<i>Receiver and Transmitter Harmonic Balance Two Tone Analysis</i>	55
3.2.7	<i>Vector Modulator Phase Shifting Simulation</i>	58
3.3	TRADEOFFS	61
4	TEST RESULTS	64
4.1	VECTOR MODULATOR HARDWARE TEST RESULTS	64
4.1.1	<i>Vector Modulator Phase Shifting Test</i>	65
4.1.2	<i>Vector Modulator Amplitude Change and Phase Shifting Test</i>	69
4.2	RECEIVER HARDWARE TEST RESULTS.....	74
4.3	TRANSMITTER HARDWARE TEST RESULTS	87
5	CONCLUSIONS AND FUTURE WORK	98
APPENDIX A.	MATLAB CODE FOR SENSITIVITY	103
APPENDIX B.	EXCEL FILE	106
APPENDIX C.	RADAR BUILD OF MATERIAL.....	107
APPENDIX D.	NOISE FIGURE.....	110
APPENDIX E.	TR MODULE COST	112
APPENDIX F.	RADAR BLOCK DIAGRAM	115

Table List

Tables	Page
TABLE 2.1 Rain Rates for precipitation Types.....	24
TABLE 3.1 Solid State Radar System Parameters	25
TABLE 3.2 Transmitter Input Values.....	48
TABLE 3.3 Noise Figure for Receiver Components.....	49
TABLE 4.1 I&Q vs. Phase.....	64
TABLE 4.2 Vector Modulator Amplitude Change and Phase Shift.....	69
TABLE 4.3 Receiver First portion Hardware Test.....	73
TABLE 4.4 Receiver Dynamic Range Hardware Test.....	79
TABLE 4.5 Transmitter first portion power analysis.....	85
TABLE 4.6 Mixer HMC521LC4 corrected output.....	88
TABLE 4.7 Transmitter second portion power analysis.....	93

Figure List

Figures	Page
Figure 1-1 MERA Module Block Diagram, MERA Transmitter frequency multiplier and receiver and MERA modules showing dual phase shifters and local oscillator source [1].....	6
Figure 2-1 Working Principle of Doppler Weather Radar.....	9
Figure 2-2 Resolved and Unresolved Targets.....	19
Figure 3-1 Basic Concept of a Solid State TR Module Block Diagram.....	26
Figure 3-2 Layout Design of a 90° hybrid with 50 Ohm line impedance.....	30
Figure 3-3 Layout Design of a Directional Coupler.....	32
Figure 3-4 Circuit Design for Receiver before Vector Modulator.....	34
Figure 3-5 Power at First Voltage Node (After the Circulator).....	35
Figure 3-6 Power at Second Voltage Node (After first LNA).....	36
Figure 3-7 Power at Third Voltage Node (After second LNA).....	36
Figure 3-8 Power at Fourth Voltage Node (After Dual Mixer).....	37
Figure 3-9 Circuit Design for Transmitter after Vector Modulator.....	39
Figure 3-10 Power at Second Voltage Node (After Power Splitter).....	40
Figure 3-11 Power at Fourth Voltage Node (After Dual Mixer).....	40
Figure 3-12 Power at Fifth Voltage Node (After first Power Amplifier).....	41
Figure 3-13 Power at Sixth Voltage Node (After second Power Amplifier).....	42
Figure 3-14 Power at the antenna Voltage Node (After Circulator).....	43
Figure 3-15 Leakage into Receiver (Transmit Mode).....	44
Figure 3-16 Power Signal after Isolation Switch (Transmit Mode).....	44
Figure 3-17 Receiver Dynamic Range.....	45
Figure 3-18 Radar Range Sensitivity.....	46
Figure 3-19 Transmitter Dynamic Range.....	47
Figure 3-20 Receiver Harmonic Balance Simulation.....	51
Figure 3-21 Transmitter Harmonic Balance Simulation.....	52
Figure 3-22 ADS Schematic for Vector Modulator.....	55
Figure 3-23 Power at Vector Modulator output.....	56
Figure 3-24 Phase at Vector Modulator output.....	56
Figure 3-25 Phase shift at Vector Modulator output.....	57
Figure 4-1 Vector Modulator PCB Layout (taken from [29]).....	63
Figure 4-2 Vector Modulator Hardware test setting.....	65
Figure 4-3 Vector Modulator phase shifting test configuration (block diagram).....	66
Figure 4-4 Vector Modulator amplitude and phase shifting test hardware configuration.....	67
Figure 4-5 Vector Modulator 20 degrees phase.....	69
Figure 4-6 Vector Modulator 50 degree phase.....	70
Figure 4-7 Vector Modulator 150 degree phase.....	70

Figure 4-8 Receiver up to 9.5GHz mixer.....71

Figure 4-9 Receiver test configuration (block diagram).....72

Figure 4-10 Mixer output with Rx -110dBm input.....74

Figure 4-11 Mixer output with Rx -90dBm input.....74

Figure 4-12 Mixer output with Rx -80dBm input.....75

Figure 4-13 Mixer output with Rx -70dBm input.....75

Figure 4-14 Mixer output with Rx -60dBm input.....76

Figure 4-15 Mixer output with Rx -55dBm input.....76

Figure 4-16 Mixer output with Rx -50dBm input.....77

Figure 4-17 Receiver up to the vector modulator.....78

Figure 4-18 Receiver second portion configuration.....78

Figure 4-19 Mixer output with Rx -110dBm input.....80

Figure 4-20 Mixer output with Rx -100dBm input.....80

Figure 4-21 Mixer output with Rx -90dBm input.....81

Figure 4-22 Mixer output with Rx -70dBm input.....81

Figure 4-23 Mixer output with Rx -80dBm input.....82

Figure 4-24 Mixer output with Rx -60dBm input.....82

Figure 4-25 Mixer output with Rx -55dBm input.....83

Figure 4-26 First Transmitter portion to be tested (up to the mixer HMC340LP5).....85

Figure 4-27 First Transmitter portion hardware configuration (up to the mixer HMC521)...86

Figure 4-28 Mixer HMC340LP5 output with 13dBm input.....86

Figure 4-29 Mixer HMC340LP5 output with 5dBm input.....87

Figure 4-30 Mixer HMC521LC4 output with 13dBm transmitter input.....89

Figure 4-31 Mixer HMC521LC4 output with 5dBm transmitter input.....90

Figure 4-32 21dB Power Amplifier HMC590LP5.....91

Figure 4-33 20dB Power Amplifier HMC487LP5.....91

Figure 4-34 Transmitter second portion hardware configuration.....92

Figure 4-35 21dB Power Amplifier output with a 13dB input signal to the transmitter.....93

Figure 4-36 21dB Power Amplifier output with 5dB input signal to the transmitter.....94

1 INTRODUCTION

The Solid State Transceiver Module (TR Module) that is described in this thesis is a compact design that provides low power and has moderate loss. It is designed to operate at X-Band Frequency (9.5GHz) and have a 24 channel system dynamic range of 41.2dBm. The design was performed on a Rogers 3006 substrate which has a permittivity of 6.15 and thickness of 25mils. Surface Mount Components (Mainly from Hittite) were used for this design because of the size and ease of mounting. The simulations were done using Agilent's Advanced Design System (ADS). All data presented through this thesis was simulated using ADS as well.

The goal of the National Science Foundation (NSF) Engineering Research Center (ERC) for Collaborative Adaptive Sensing of the Atmosphere (CASA) is to explore and develop new methods for improving observation, detection and prediction of atmospheric phenomena [15]. The center is focused on developing Distributed Collaborative Adaptive Sensing (DCAS) as a systems technology to improve our ability to monitor the earth's lower troposphere. Improving today's weather monitoring and forecasting requires an increase in both the resolution and volume coverage of observations in the lowest kilometers of the troposphere. The DCAS system will be created with a network of X-band radars. The center comprises four partners: University of Massachusetts (UMass), Colorado State University (CSU), University of Oklahoma (OU) and University of Puerto Rico, Mayagüez (UPRM).

To achieve a DCAS system, a series of technology and full-system test-beds were planned and distributed throughout the different collaborators. An innovative approach of

the center is to integrate students from the four different campuses in a unique research experience under what has been called the Student Led Test-bed (SLT). The SLT's main goals are to establish a Quantitative Precipitation Estimation (QPE) sensing network starting at the western end of Puerto Rico with its first node (PR1) located on top of the Electrical and Computer Engineering (ECE) building of UPRM.

Current radars used for Quantitative Precipitation Estimation (QPE) depend on mechanical parts and a high voltage modulator to operate [27]. This introduces certain limitations to our network system (such as not been able to distinguish moving targets from background clutter) because of the inability to work as coherent radar. This means that the radar phase control cannot be achieved. It also represents a drawback in terms of about power consumption since they operate using a magnetron, which is a high-powered vacuum tube that generates microwaves, and it operates at different power levels (1kW, 4kW, etc). Replacing current sensing network node (PR1) and future nodes with Solid State Radars will bring certain advantages to our system. Solid State components in Radars have better reliability since no mechanical action is involved and consequently the availability of the system will improve [1]. This thesis summarizes the work performed to design and develop a Solid State Transmit Received Module for the first solid state radar to be used on the DCAS radar network that is being developed for Puerto Rico. It covers all aspects taken into account during the design, implementation and initial testing of this Transceiver Module.

1.1 Motivation

Current Radars used for Quantitative Precipitation Estimation (QPE) depends on mechanical parts and a high voltage modulator to operate. This introduces certain limitations to our network system because of the inability to work as coherent radar. This means that the radar phase control cannot be achieved. It also represents a drawback in terms of about power consumption since they operate using a magnetron which is a high-powered vacuum tube that generates coherent microwaves and it operates at 25kW (This value is for the radar on top of the electrical engineering building). This type of radar needs very large peak power to be able to produce very short pulses which increases the range resolution. In solid state radars pulse compression is used to improve range resolution. Replacing current sensing network node (PR1) and future nodes with Solid State Radars will bring certain advantages to our system. Solid State components in Radars have better reliability since no mechanical action is involved and consequently the availability of the system will improve [1]. Having no mechanical parts eliminates radar malfunctions by parts wear out. Solid State Radars use less power because no magnetron is needed to operate the radar. They also have the ability to use pulse compression, which increases radar resolution and range.

Utilizing solid state devices in our design provides us with several advantages because of the inherent solid state superior performance, lower cost and higher factors of availability and reliability. Cost advantages can be achieved because no high power microwave feed system or high voltage DC power supply is required to operate a solid state radar. Additionally mass production of the transmit receive module will minimize cost and

the inherent modularity and reliability of the system will insure ease of maintenance and reduced cost ownership [3].

This Solid State X-Band Radar is designed to operate at a frequency of 9.5 GHz and have a short range of 6km because interference with mountains made long range radar useless and only 6km are needed to cover the area of interest. For the STB/OTG it is expected that with better reliability of the system, a significant improvement in precipitation estimates in western Puerto Rico will be achieved.

1.2 Objective

The main objective of this project is to develop a Transmit Receive Solid State Module for a Solid State (based only on semiconductor technology), X-band, Doppler, Dual Polarized meteorological radar system for UPRM Quantitative Precipitation Estimation sensing network. The complete system is comprised of 24 channels. Each channel has two polarizations (vertical and horizontal), then two TR Module are needed per channel, having a total of forty eight Solid State Modules. The scope of this project is to design a fully operational TR Module and test it with one channel. This system will be the first Solid State system designed and developed at UPRM for precipitation measurements. Being the first Transmit Receive Solid State Module designed for CASA Student Test Bed will lay the groundwork for future Solid State Radar development at UPRM. This solid state dual polarized transmit received module could be modified/ upgraded and reused in future projects, and therefore, bring down the cost of future radar research at UPRM.

On the other hand, the development of this Solid State Radar will provide new opportunities for undergraduate students to develop radar skills by engaging in a real life collaborative system design experience. In addition, this X-Band Solid State TR Module can be the source of challenging projects and the step stone to move forward to new technologies.

1.3 Literature Review

Solid State Technology had its earliest beginnings in 1958 when Texas Instruments began research work on microwave applications of semiconductors. This effort resulted in low noise parametric amplifiers and varactor frequency multipliers, and, in 1960 the first crystal controlled, solid state microwave source was developed and reported in technical journals by the author [1]. Solid State technology is based entirely on the semiconductor devices which need no use of the electrical properties of a vacuum or any mechanical action. Also a considerable amount of electromagnetic and quantum mechanical action takes place within it. The Air Force avionics lab did some research on solid state technology to develop integrated circuits in airborne computer and other avionics systems. In 1964 a program called Molecular Electronics for Radar Applications (MERA) was proposed in order to improve reliability of airborne radar systems and to promote the usage of integrated circuits [2]. That very same year Texas Instrument decided not to follow Air Force request but to propose a whole new approach in which solid state modules would be developed to build and active element phased array radar. The array consisted of 604 modules transmitting 1W peak

power each. The limited power where to be increased using chirp pulsed compression. Because funding was not found for 1 GHz they had to design for 9 GHz.

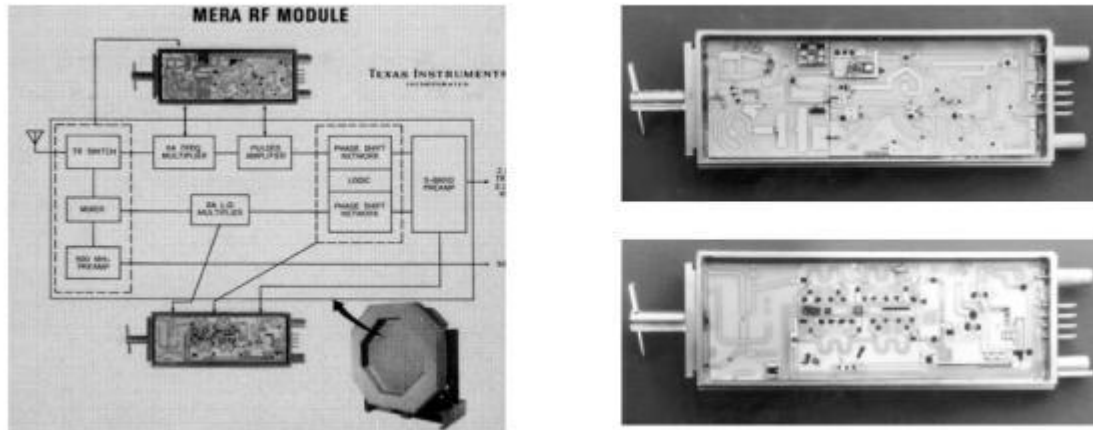


Figure 1-1 MERA Module Block Diagram, Radar MERA Transmitter frequency multiplier and receiver and MERA modules showing dual phase shifters and local oscillator source. [1].

The MERA program started with the initial objective of simply advancing the state of the art in microwave integrated circuits. The effort was expanded to the development of a laboratory model X-band all Solid State phased array radar. Frequency multiplication was accomplished in the module to generate the transmit signal. Similarly, the local oscillator signal was multiplied to X-band to allow the received signal to be down converted to a 500MHz intermediate frequency (IF). Figure [1-1] shows one side of the MERA Module with the transmitted power chain, frequency multiplier, TR switch, balanced mixer, and amplifier. Once the modules where designed a subarray was built. MERA was the first major effort to extend integrated circuits technology into the microwave region and to apply high density microelectronics into the phased array radars. It consisted of an all solid state

electronically scanned X-band radar with an active aperture consisting of 604 identical Modules.

The RASSR (Reliable Advanced Solid-State Radar) followed MERA and had two major objectives. First, to demonstrate that a practical system could be built that would meet operational requirements and second, to demonstrate that the reliability improvements promise by the technology was achievable [2].

After the Reliable Advanced Solid-State Radar approach an X-Band active element module were developed using GaAs FETS Technology. The application of GaAs monolithic circuits offers to provide module realization at an acceptable cost and enhanced reliability. Large production of electrically identical GaAs monolithic circuits is needed in order to send solid state radars to production.

In 1985 Delft University was given the opportunity of releasing a frequency modulated continuous-wave solid-state X-band weather surveillance radar developed as a fully operational system. The idea of designing this FM-CW X-band Radar was inspired mainly by the FM-CW Doppler radar facility developed by NOAA which mainly used for clear air turbulence measurements [30]. This type of radar is currently used for rain rate determination and rain cell contouring [31]. It was designed to be a purely solid state radar with a continuous wave power of 1Watt or 30dBm and is capable of suppressing coherent ground clutter as well as detecting rain cells. In 1988 the designed Radar by Delf University was placed on top of the electrical engineering building of that very same university.

Weather radars systems nearly always operate at S or C band due to the increase attenuation at higher frequencies. Now a days is possible to design at X-band (8-12GHz)

because of the progress of quasi real time processing tools which allows real time corrections for attenuations. These FM-CW radars are able to sweep the transmitter frequency to encode and determine range. This type of radar can only process one target normally which limits its use.

Pulsed Doppler radars and FM-CW solid state weather radars at X-band has been designed in the past. The system we designed combined both solid-state and pulsed Doppler radar technologies to create a unique weather radar. This system is an X-band, solid-state, polarimetric, coherent pulsed Doppler radar that will be able to measure the radial velocities of winds and to process velocities of precipitations by being a pulsed radar. This radar will also be capable of measuring the intensity of the rain. The advantage of combining Doppler processing to pulsed radars is to provide accurate velocity information. This type of radar is able to describe the rate at which a target moves toward or away the radar [32].

Significant advances have been achieved recently in the field of solid state active module so it is now possible to improve weather radar systems capabilities to meet operational requirements for the next generation of CASA Doppler radars. The active elements phased array radar can provide weather forecast with the ability to sense hydrometeors and winds. High performance, Low cost solid state active transmit / receive modules are key to the successful implementation of an active element solid state phased array radar.

1.4 Summary of Following Chapters

Chapter 2 develops the necessary background in basic radar theory. The point target radar equation all the way through to the weather radar equation is covered in this chapter along with basic microwave receiver design techniques. Chapter 3 deals with the design of the Solid State Transceiver Module. It covers the initial power analysis, part selection, Dynamic Range, Noise Figure and Intermodulation product analysis for the transmit and receive portions. The fourth chapter presents test results on the Transceiver Module. Conclusions and future work are presented in Chapter 5.

2 THEORETICAL BACKGROUND

2.1 Radar Basics Principles

The term RADAR stands for Radio Detection and Ranging. A radar operates by radiating electromagnetic energy and detecting the echo returned from reflecting objects known as our target. In which our case will be the rain. A weather radar detects rain in the atmosphere by emitting pulses of microwave and measuring the reflected signals from the raindrops. In general, the more intense the reflected signals, the higher will be the rain intensity. The distance of the rain is determined from the time it takes for the microwave to travel to and from the rain.

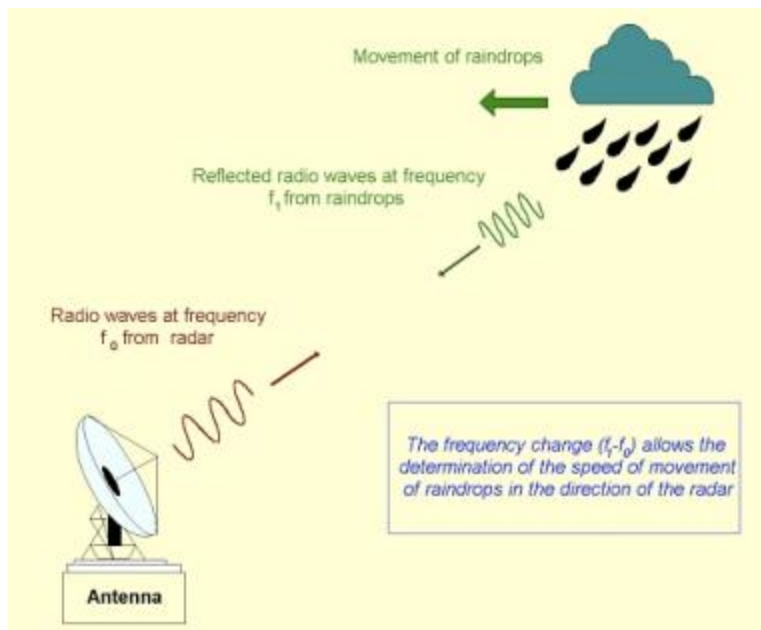


Figure 2-1 Working Principle of a Doppler Weather Radar. [25].

2.1.1 Basic Operation of a Radar

The operation of a radar can be described in more detail starting with the transmitter. The radar equation shows that the range of a radar is proportional to the fourth root of the transmitter power. Thus, to double the range requires that the transmitted power be increased by 16 [23]. This tells us that there is an optimal amount of power that should be employed to increase the range of a radar. The radar transmitter produces short duration high-power radio frequency pulses of energy that are radiated into space by the antenna. The antenna concentrates the energy into a narrow beam and also receives the echo that bounces back from the target. The signal collected by the antenna is sent to the receiver which separates the desired signal from the noise and other interference signals. The receiver also amplifies the signal that is to be display. It is important to mention that at microwave frequencies the noise at the receiver output is usually generated by the receiver itself rather than external noise.

2.1.2 Radar Equation

The radar equation represents the physical dependences of the transmit power, that is the wave propagation up to the receiving of the echo-signals. In other words, it relates the transmitted and received powers and antenna gains of a primary radar system to the echo area and distance of the radar target. Then we have that the amount of received power P_r returning to the receiving antenna is given by the radar equation for a point target:

$$P_r = \frac{G_t A_r \lambda^2 \sigma F^4 P_t}{(4\pi)^2 R_t^2 R_r^2} \quad \text{Equation 2.1}$$

Where:

P_t = transmitted power.

G_t = gain of the transmitting antenna.

A_t = effective aperture (area) of the receiving antenna.

σ = radar cross section, or scattering coefficient, of the target.

F = pattern propagation factor.

R_t = distance from the transmitter to the target.

R_r = distance from the target to the receiver.

λ = radar wavelength.

In the case of distributed targets the radar equation will be:

$$\bar{P}_r = \left(\frac{P_t G^2 \lambda^2 \theta^2 h}{512 \pi^2 R^2} \right) \sum_i \sigma_i \quad \text{Equation 2.2}$$

This shows us that the received power for point targets declines as the fourth power of the range which indicates that the reflected power distant target is very small. And it also shows that for distributed targets the received power declines as the second power of the range.

2.2 Receiver

The receiver accepts weak radio frequency echoes from the antenna system and routes them to the indicator as discernible video signals. Because the radar frequencies are very high and difficult to amplify, a superheterodyne receiver is used to convert the echoes to a lower frequency, called the intermediate frequency (IF), which is easier to amplify. The function of a radar receiver is to amplify the echoes of the radar transmission without adding noise or introducing any kind of distortion, filtering echoes in a manner that will provide the maximum discrimination between desired echoes and undesired interference. The echo, after modest amplification, is shifted to an intermediate frequency by mixing it with a local oscillator (LO) frequency. The receiver optimizes the probability of detection of the signal utilizing its bandwidth characteristics.

2.2.1 *Bandwidth Considerations*

The bandwidth of a system is the frequency band over which the system can simultaneously amplify two or more signals to within a specified gain. One of the most important factors is the receiver noise added to its input signal. Even with very careful design, noise due to thermal motion of electrons in resistive components is unavoidable. The amount of such thermal noise is proportional to receiver bandwidth. Therefore, bandwidth reduction is a possible solution to the problem of receiver noise. However, if the bandwidth is made too

small the receiver does not amplify and process signal echoes properly. In practice, the receiver bandwidth of a pulse radar is normally close to the reciprocal of the pulse duration. For example, a radar using 1 μ s pulses is expected to have a bandwidth of about 1 MHz.

2.2.2 *Dynamic Range*

The dynamic range is the operating range for which a component or system has desirable characteristics. Linear Dynamic Range is also known as the minimum detectable power levels and this definition is more appropriate for a receiver system. The receiver system provides large dynamic range as well as to reject interfering signals so that the required information can be optimally detected. The receiver must amplify the received signal without distortion. If a large clutter signal sends the system into saturation, the result is a modification to the spectrum of the signal. This change in spectral content reduces the ability of the signal processor to carry out Doppler processing. Furthermore, if the receiver enters saturation, then there can be a delay before target detection is restored. In principle, the dynamic range of the receiver must exceed the total range of signal strength from noise level up to the largest clutter signal. In practice dynamic ranges of 80 dB's or so meets system requirements.

2.2.3 Minimum Detectable Signal (MDS)

The minimum receivable power for a given receiver is important because the minimum receivable power is one of the factors which determine the maximum range performance of the radar. All receivers are designed for a certain sensitivity level based on requirements. One would not design a receiver with more sensitivity than required because it limits the receiver bandwidth and will require the receiver to process signals it is not interested in. Basically the Minimum Detectable Signal is the minimum input signal power to the system. For accurate demodulation the input power to the receiver should be greater than Minimum Detectable Signal. This Minimum Discernable Signal thus determines the sensitivity of the receiver.[28].

2.3 Transmitter

The radar transmitter generates powerful pulses of electromagnetic energy at precise intervals. It produces the short duration high-power radio frequency pulses of energy that are radiated into space by the antenna. The required power is obtained by using a high-power microwave oscillator, such as a magnetron, a microwave amplifier, or a klystron.

The range of a radar varies as the fourth root of power because both the outgoing transmitted power density and the returning echo energy density from the target become diluted as the square of the signal traveled:

$$R^4 \propto P_x A_x T$$

Equation 2.3

Trying to increase range by increasing transmitter power is costly so there is a need to reduce range requirements in order to produce remarkable savings during production.

2.3.1 Pulsed vs. Continuous Wave (CW) Transmitter

Pulsed transmitter are used because in a radar system if the transmitter is on all the time, it will be very hard to keep the transmitter from interfering with the receiver that is trying to receive faint echoes from distant targets. CW radars have been made to work by using separate transmit and receive antennas to isolate the receiver from the transmitter. Since CW radars required two antennas, it is actually wasting 3dB of range equation performance that could be gained if only one antenna were use to transmit and receive as it is in the case of the pulsed radars. Maximum Range Capabilities of the CW radars is often limited by the fact that leakage into the receiver of transmitter noise sidebands sets a limit below which small moving targets signals cannot be seen. A pure CW radar system can detect moving targets by their Doppler offset, but no range information is obtained. In a pulsed radar system, short-range and long-range echoes arrive at different times, and the receiver sensitivity can be adjusted accordingly with STC (Sensitivity Time Control).

2.3.2 Vector Modulators

The heart of the radar system is the modulator. The function of an IQ Vector Modulator is to simultaneously control the phase and amplitude characteristics in the

processing of a microwave signal. This Vector Modulator Device will convert a signal to a desired vector location via a digital command. The theory of operation is to divide the input signal into two equal signals 90 degrees apart, I (in-phase) and Q (quadrature). This allows the magnitude of each signal to be re-located along its vectors' axis. The two signals are then combined. Using The Pythagorean Theorem, the sum of the vectors produces the resultant output signal.

2.4 Solid State Transmitter

Compared with tubes, solid state devices offer certain advantages:

- No hot cathodes are required; therefore; there is no warm-up delay, no wasted heater power, and virtually no limit on operating life.
- Device operation occurs at much lower voltages; therefore; power supply voltages are on the order of volts rather than kilovolts. This avoids the need for large spacing, oil filling, or encapsulation, thus saving size and weight and leading to higher reliability of the power supplies as well as of the microwave power amplifier themselves.
- Transmitters designed with solid state devices exhibit improved mean time between failures (MTBF) in comparison with tube-type transmitters. Module MTBFs greater than 100,000 hours have been measured.
- No pulse modulator is required. Solid state microwave devices for radar generally operate in Class-C, which is self pulsing as the RF drive is turned on and off.

- Graceful degradation of system performance occurs when modules fail. This results because a large number of solid-state devices must be combined to provide the power for a radar transmitter, and they are easily combined in ways that degrade gracefully when individual units fail. Overall power output, in decibels, degrades only as $20 \log(r)$, where r is the ratio of operating to total amplifiers.
- Extremely wide bandwidth can be realized. While high power microwave radar tubes can achieve 10 to 20 percent bandwidth, solid state transmitter modules can achieve up to 50 percent bandwidth or more with good efficiency.
- Flexibility can be realized for phased array applications.

2.5 Meteorological Radar

A weather radar is a type of radar used to locate precipitation, calculate its motion, estimate its type (rain, snow, hail, etc.), and forecast its future position and intensity. Modern weather radars are mostly pulse-Doppler radars, capable of detecting the motion of rain droplets in addition to intensity of the precipitation. Both types of data can be analyzed to determine the structure of storms and their potential to cause severe weather. This type of system provide quantitative and automated real time information on storms, precipitation, hurricane, tornadoes, and a host of other important weather phenomena, with higher spatial and temporal resolution.

2.5.1 Radar Range Equation for meteorological targets

The radar range equation relates the range performance of a radar system to other radar components and characteristics such as:

- Transmitter (transmitted power)
- Receiver (minimum detectable signal)
- Antenna (gain)
- Target (radar cross section)

In relating these characteristics to radar range, the radar range equation provides an insight into the trade-offs and compromises that must go into designing and operating a radar system.

The received power from distributed targets can be derived from the next equation:

$$P_r = \frac{\beta\sigma}{r^4} \quad \text{Equation 2.4}$$

where β is a constant dependent upon radar system parameters, r is the range, and σ is the radar cross section.

2.5.2 Range Resolution

The Range Resolution of a radar is the ability to distinguish between targets that are close in either range or bearing. The degree of range resolution depends on the width of the transmitted pulse, the types and sizes of the target and the efficiency of the receiver. Radars

are normally designed to operate between a minimum range R_{min} and a maximum range R_{max} . The distance between these ranges is divided into range gates. The width of each range gate is ΔR and the radar must be able to resolve targets in adjacent range bins.

The echoes are separated in space by $2s$ and in time $\Delta t = \frac{2s}{c}$ to avoid overlap the $\Delta t \geq \tau$.

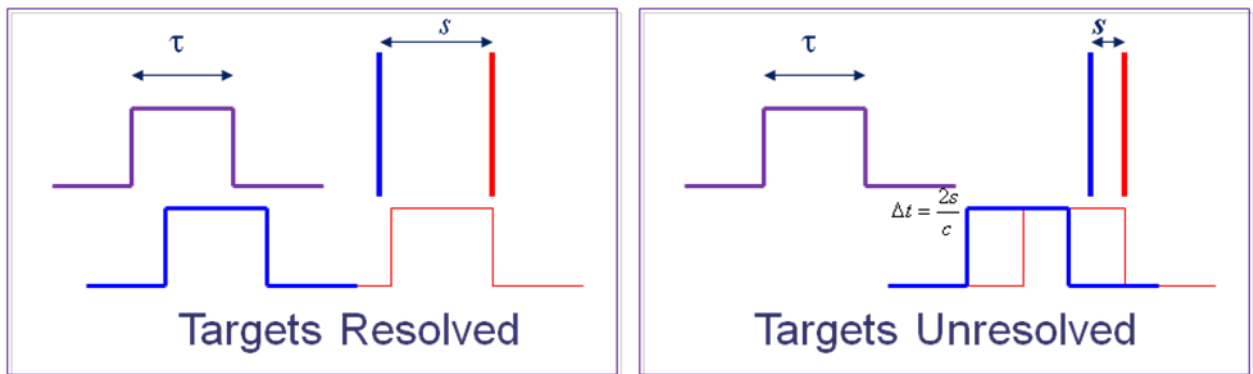


Figure 2-2 Resolved and Unresolved targets. [26].

Generally we want better range resolution and smaller ΔR :

$$\Delta R = \frac{c\tau}{2} \quad \text{Equation 2.5}$$

But to do that τ needs to be shrank and that result in higher bandwidth and smaller average transmitted power.

2.5.3 Maximum Unambiguous Range and Velocity

The pulse repetition frequency (PRF) of a radar system determines the maximum operating range of a radar before ambiguities start to occur. This is what we call the

maximum unambiguous range of a radar. The maximum unambiguous range of a radar is different from the maximum range of the radar. Maximum range of a radar is due to power and maximum unambiguous range is a timing issue.

The unambiguous Doppler frequency for a pulse repetition frequency is give by:

$$\Delta f = \pm \frac{PRF}{2} \quad \text{Equation 2.6}$$

Then the unambiguous range will be given by:

$$\Delta r = \pm \frac{c}{2PRF} \quad \text{Equation 2.7}$$

Since the Doppler shift f and the target radial velocity v are linearly related by the expression:

$$v = \frac{\lambda}{2} f \quad \text{Equation 2.7}$$

Then it follows that the product of unambiguous range and unambiguous velocity is:

$$\Delta v \Delta r = \frac{\lambda c}{4} \quad \text{Equation 2.9}$$

and is maximized by maximizing the transmitted wavelength. For the range to be unambiguous, the echo must return before the next pulse is transmitted.

2.5.4 Doppler Frequency

The Doppler effect is the apparent change in frequency between the source of a wave and the receiver. It happens because of the relative motion between the source and the receiver.

The Doppler frequency is given by the following formula:

$$f_d = \frac{2v}{\lambda} \cos \alpha \quad \text{Equation 2.10}$$

Where:

f_d = Doppler frequency

λ = wavelength

v = speed of the aircraft

α = angle between the direction of the transmitted / reflected signal and the direction of flight of the target.

The Doppler velocity is calculated from the pulse to pulse change in the received signal and is expressed by the following formula:

$$v_d = -\frac{\lambda}{4\pi T} \theta \quad \text{Equation 2.11}$$

On weather radars the Doppler frequency and Doppler velocity are used to determine the motion of rain droplets in addition to intensity of the precipitation.

2.5.5 Dual Polarization

Most liquid hydrometeors have a larger horizontal axis due to the drag coefficient of air while falling (water droplets). This causes the water molecule dipole to be oriented in that direction so radar beams are generally polarized horizontally to receive the maximal return. If we were to use two pulses with orthogonal polarization, vertical and horizontal, we are able to extract two set of data for vertical and horizontal polarization. Some of the fundamental variables measured by a polarimetric radar are listed below:

- Differential Reflectivity (Z_d); The differential reflectivity is a ratio of the reflected horizontal and vertical power returns. It indicates drop shape and with this information the average drop size can be estimated.
- Correlation Coefficient (ρ_{hv}); A statistical correlation between the reflected horizontal and vertical power returns. Values near one indicate homogeneous precipitation types and low values indicate low precipitation types.
- Linear Depolarization Ratio (LDR); This ratio of a vertical power return from a horizontal power return from a vertical pulse.
- Specific Differential Phase (θ_{pd}); The specific differential phase is a comparison of a returned phase difference between the horizontal and vertical pulses. This change in phase is caused by the difference in the number of wave cycles (wavelength) along the propagation path for horizontal and vertically polarized waves. It should not be

confused with the Doppler frequency shift, which is caused by the motion of the clouds and precipitation particles.

As mentioned above, polarimetric radars gain additional information about the precipitation characteristics of clouds by essentially controlling the polarization of the energy that is transmitted and received. Polarimetric radars transmit and receive both horizontal and vertical polarization radio wave pulses. Therefore, they measure both the horizontal and vertical dimensions of clouds and precipitation particles. This additional information leads to improved radar estimation of precipitation type and rate.

2.5.6 Radar Reflectivity

The radar reflectivity is a measure of the efficiency of a radar target in intercepting and returning radio energy. It depends upon the size, shape and dielectric properties of the target and includes the effect of reflection, scattering and diffraction. It is important to mention that the radar reflectivity of a meteorological radar depends on factors such as:

- The number of hydrometeors per unit volume
- Size of hydrometeors
- Physical state of hydrometeors (ice or water)
- Shape of individual element of the group
- If the shape is asymmetrical it will depend on their aspect with respect to the radar

The radar reflectivity has dimensions of area per unit volume usually 1/m and is defined by:

$$\eta = \sum_i N_i \sigma_i \quad \text{Equation 2.12}$$

Where N_i is the number of hydrometeors per unit volume with backscattering cross section σ_i . This radar reflectivity is related to the radar reflectivity factor which is determined by the drop size distribution of precipitation. Then the radar reflectivity factor Z may be written as:

$$Z = \int_0^{\infty} N(D) D^6 dD \quad \text{Equation 2.13}$$

Where N(D) is the Drop size distribution and D is the drop diameter.

This reflectivity factor is used to estimate Rain rate (which is simply the amount of precipitation occurring in a unit of time, generally expressed in mm per hour) by using the Rosenfeld relation that is given by the next expression [22]:

$$Z = 250 R^{1.2} \quad \text{Equation 2.14}$$

The table below show different rain rates corresponding to different precipitation types. The values shown in the table were estimated using equation [2.14] and then taking the logarithm (base 10) of that value.

Table 2.1 Rain Rates for Precipitation Types

Type of Precipitation	Rain Rate (mm/hour)	dBz
Drizzle	0.25	less than 16
Light rain	1	less than 30
Moderate rain	4	30-40

Heavy Rain	16	40-45
Thunderstorm	35	45-50
Intense Thunderstorm	100	50-57

2.6 Intermodulation Distortion

Frequency conversion in a mixer is made possible through the use of a nonlinear device. These nonlinearities give rise to a number of undesired harmonics and mixer products. These spurious signals increase the conversion loss of a mixer, and can also lead to signal distortion. In general, a system using a non linear device has a voltage transfer function that can be written as a Taylor series:

$$V_{out} = a_0 + a_1 v_{in} + a_2 v_{in}^2 + a_3 v_{in}^3 + \dots \quad \text{Equation 2.14}$$

For a mixer the a_0 term correspond to the DC bias voltage, while the desired mixed output is part of the v_{in}^2 . The operation of a subharmonically pumped mixer depends on the v_{in}^3 term. Thus, depending on the application, one of these terms provides the desired output while the remaining terms produced the desired spurious signals. If the input of the system consists of a single frequency or tone, let's say $V_{in} = \cos(w_1 t)$ then the output of equation 2.14 will consist of all harmonics, mw_1 of the input signal. In a mixer, single tone distortion products are generally eliminated by filtering.

More serious problems arise when the input to the system consist of two relatively closely spaced frequency or two tone, let's say $V_{in} = \cos(\omega_1 t) + \cos(\omega_2 t)$. Then the output spectrum will consist of all harmonics of the form $m\omega_1 + n\omega_2$, where m and n may be positive or negative integers. The v_{in}^2 will produce harmonics at the frequencies $2\omega_1$, $2\omega_2$, $\omega_1 - \omega_2$ and $\omega_1 + \omega_2$ which are all second order products. These combinations of the two input frequencies are called intermodulation products. These frequencies are generally far away from the fundamentals ω_1 and ω_2 , and so can easily be filtered (either pass or rejected) from the output. Products that arise from mixing two input signals are called intermodulation distortion [20].

3 Methodology

The Solid State Transmit Receive Module is designed at X-band frequency band. Operating at X band makes the design more cost-efficient than S-band since mature technology for X-band marine radars such as the Raytheon MK2 is commercially available [14]. Another advantage is that component size is inversely proportional to its operating frequency. Therefore, we are able to build smaller and compact modules which make our device more portable and easy to handle. In order to start the design, there is a need to consider the following design requirements, which are based on the specifications of the current radars operating on the UPRM Quantitative Precipitation Estimation sensing network. Table 3.1 summarizes the complete system parameters.

Table 3.1 Solid State Radar System Parameters

Parameter	symbol	Specification
Radar Frequency	F	9.5 GHz (X Band)
Wavelength	λ	31.88 mm
Peak Transmitter Power	P_t	24W
H Antenna HPBW	θ_x	6°
V Antenna HPBW	θ_y	6°
Antenna Gain	G	24 dB
Range Resolution	ΔR	1500m
Radial Resolution	$\tau/2$	5us
Unambiguous Range	URmax	15000m
Noise Figure	F_n	<4dB

Minimum Detectable Signal	MDS	-110 dBm
Intermediate Frequency	IF	5.0MHz
Maximum Range	R	6-10 km
Pulse Width	τ	10us
Pulse Repetition Interval	PRI	100us
Pulse Repetition Frequency	PRF	10000Hz
Sensitivity	Z	3dBz-40dBz
Maximum Winds	w	40 m/s, 89mph

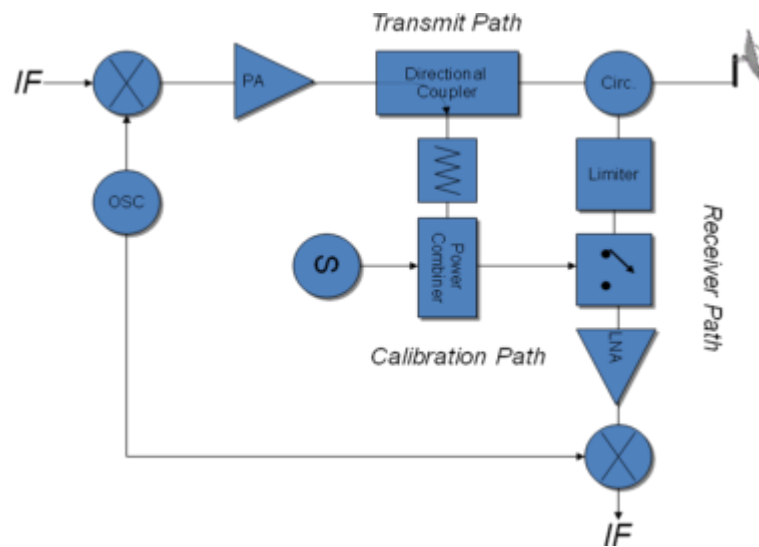


Figure 3-1 Basic Concept of a Solid State TR Module Block Diagram.

Solid State Transmit Receive Module design is based on modifications of the PR-1 block diagram shown in Figure [3.1]. First step to start the design is to carefully analyze the

requirements. The analysis will begin with the study and selection of the solid state components to be used on this design. Components were carefully selected in order to meet the Radar requirements listed above. Also, most components allow surface mount manufacturing techniques to avoid the need for wire bonding; this will simplify the construction of our system. After design is complete with all its microwave solid state components there is a need to verify that design is meeting requirements. Then, several analysis and tests need to be run in order to ensure compliance with specifications. To complete the analysis we used ADS (Agilent Advanced Design and Simulation Software) to simulate the behavior of the Receiver, Transmitter and Vector Modulator under different environments. Among the analyses that were performed we have the Power Analysis, Noise Analysis, Dynamic Range, Harmonic Balance, Two Tone Simulations and Phase Simulations. Also the help of Matlab and Excel has been used to determine how sensitive is our system, to plot Signal to Noise Ratio (SNR) vs. Range and to plot the dynamic range in terms of sensitivity.

3.1 Design Methodology

3.1.1 Receiver Component Selection

A three port circulator used to route outgoing and incoming signals between the antenna, the transmitter and the receiver is placed after the antenna such that when the received and transmitted signal is fed into its corresponding port it is only transferred to the

next port. A circulator is placed instead of a switch because it provides more isolation and avoids temporal overlap between sent and received pulses. A ferrite circulator is chosen for our design because of its power handling capabilities, linearity and signal-to-noise ratio of circulators made with active components such as transistors is not as high as those made from ferrite. The circulator chosen for this design (31MS95-1 from Dorado) provides 20dB of Isolation and has a low Noise Figure of 0.5. After the circulator a Limiter should be added to the design in order to allow signals below the specified input power to pass unaffected while attenuating the peaks of stronger signals that exceed the input power. Placing a limiter at this point will reduce the effect of a weaker signal on the output. Instead of a limiter a High Isolation SPDT switch is placed before the LNA string to prevent damage on the receiver caused by leakage that comes from the transmitter when TR Module is in transmit mode. The HMC607 switch provides 60dB of Isolation that in conjunction with the 20dB Isolation Circulator will provide the necessary isolation to prevent the leakage from saturating the LNA's when transmitting. Then a cascade of low noise amplifiers (LNA) is located after the switch to amplify weak signals captured by the antenna. These LNAs are located near the antenna so losses in the feed line become less critical. With the low noise amplifier, the noise of all the subsequent stages is reduced by the gain of the LNA and the noise of the LNA is injected directly into the received signal. The LNA's boost the input signal power while at the same time they add some noise and distortion so that the retrieval of the signal become possible in the later stages of the system. The LNA's chosen for this design is the HMC564LC4 and the same provides a gain of 17dB and have a Low Noise

Figure of 1.7. Only a string of two LNA's are needed in order to amplify the weakest signal detected by this receiver, in which this case is required to be -110dBm. After the amplification stages a GaAs downconverter frequency mixer operating from 9 to 12 GHz is added. The power that we have after the amplifiers will be around 73dBm considering an input received signal of -110dBm and this is enough to operate the double mixer to be placed after the LNA stage. This double mixer is a time varying circuit that will take the signal at 9.5 GHz from the LNA and will mix it with a 7.1 GHz oscillator signal to downconvert received signal from 9.5 GHz to 2.4 GHz since a signal of 2.4 GHz is needed as an input to the Vector Modulator. The mixer that is going to be used for this design is the HMC568LC5 which provides a small signal conversion gain of 14 dB with a noise figure of 2 dB and 33 dB of image rejection. The HMC568LC5 utilizes an LNA followed by an image reject mixer which is driven by an LO buffer amplifier. The image reject mixer eliminates the need for a filter following the LNA, and removes thermal noise at the image frequency. But there is still a need of having a 90 degree hybrid at the end of the mixer in order to phase shift received signal by 90 degrees before they go into the vector modulator. Next an external coplanar waveguide 90° hybrid was designed to select the required sideband. Figure [3-2] shows an Auto Cad layout for the suggested design with dimensions to attain a line impedance of 50Ω.

The Vector Modulator used in this design (HMC631LP3) is a complete X-Band phase shifter system using vector polar modulation, suitable for solid state phased array radar applications [17]. When signal comes out from Vector Modulator it will be divided by a

power splitter operating from 1.5 to 2.5 GHz that feeds the next dual mixer. This dual mixer (HMC340LP5) will be responsible of downconverting one more time the received signal from 2.4GHz to the required Intermediate Frequency (IF) of 5.0MHz. When combining with an external Hybrid the Dual Mixer provide two Outputs which are the IF phase and the IF quadrature signals. The hybrid design suggested for this stage is the same as the one shown in figure [3-2]. Signal Processing needed after this stage of the design is out of the scope of this project. It is also important to mention that the substrate to be used in this design is the Rogers 3006 with a thickness of 25mils, a relative permittivity of 6.15, a relative permeability of 1 and a loss tangent of 0.002. This substrate was selected because it allows us to design smaller circuits compare to lower permittivity substrate.

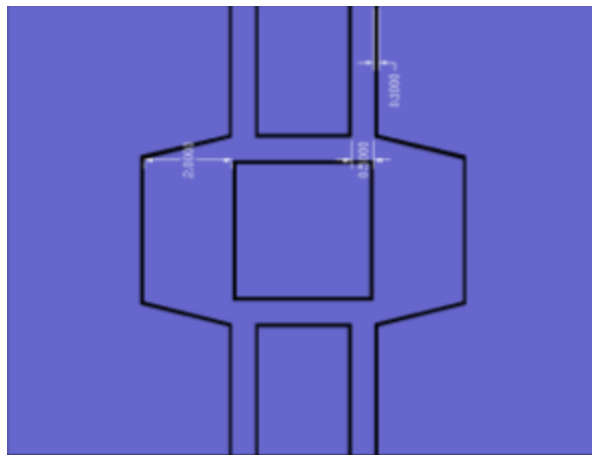


Figure 3-2 Suggested Layout Design of a 90° hybrid with 50 Ohm line impedance.

3.1.2 Transmitter Component Selection

A generated 5.0MHz Intermediate signal (IF) is to be mixed with a local oscillator signal to convert from IF 5.0MHz to RF 2.4GHz. The HMC340LP5 double mixer is entitled to perform this task. This double mixer provides an IF bandwidth from DC to 3.5GHz an image rejection of 38dB and a high input third order intermodulation product of 50dB. The HMC385LP4 is the local oscillator connected to the double mixer mention above, it operates from 2.25GHz to 2.5GHz. This oscillator is in charge of upconverting the signal from IF to 2.4GHz. A frequency of 2.4GHz is needed for the vector modulator to operate. The Vector Modulator used in this design (HMC631LP3) is a complete X-Band phase shifter system using vector polar modulation, suitable for solid state phased array radar applications [17]. After the RF signal is phase shifted in the vector modulator it pass through a Mini Circuit BP2U power splitter (operating from 1.5 to 2.5 GHz) that feed another dual mixer. This dual mixer is responsible of upconverting one more time the transmitted signal from 2.4 GHz to the desired operating frequency at 9.5 GHz. The HMC521LC4 dual mixer provides a bandwidth of 1.7 to 4.5GHz making itself suitable to perform this operation. The HMC505LP4 is the local oscillator placed in conjunction with the dual mixer in order for the signal to be upconverted. It oscillates at 7.1GHz which when mixed with 2.4GHz will produced the desired 9.5GHz. A quadrature hybrid is placed between the power splitter and the dual mixer to phase shift the signal by 90 degrees. The suggested hybrid design for the transmitter is the same as the one designed for the receiver (please refer to the receiver component selection part). This is done because the mixer requires two inputs, one for phase

and one for quadrature. The output of the mixer powers a power amplifier string that provides necessary power to operate the transmit module. The power amplifiers chosen for this are the HMC590LP5 with 21dB gain followed by the HMC487LP5 with 20dB gain. Only a string of two power amplifiers are needed in order to amplify the signal at such a level that permits us to have approximately 30dB signal at the Antenna. After the power amplifiers a directional coupler will be added to couple part of the transmission power into the transmission line. Transmission line from calibration path is set close enough together with transmission line from transmit path such that energy passing through one is coupled to the other. An advantage of using a directional coupler is that the coupled output from the directional coupler might be used to obtain the information on the signal without interrupting the main power flow in the system.

This Directional Coupler needs to be designed for the calibration path and it has an isolation of 30dB. The model we used for the suggested design was the coupled line coupler and it was done and analyzed with the help of ADS and linecalc. This Directional Coupler is a four port input with one port isolated from the input port. The through port is connected to the antenna passing through the circulator first. This is to redirect most of the signal to the transmit path. The coupled port is the port used for calibration. This port let pass a fixed fraction of the input signal (30dB). After the directional coupler the 30dB variable attenuator (MA-COM AT-635) is placed followed by a power splitter (Mini Circuit BP2U) which has the noise source (Noise Con NC1128A) connected to it.

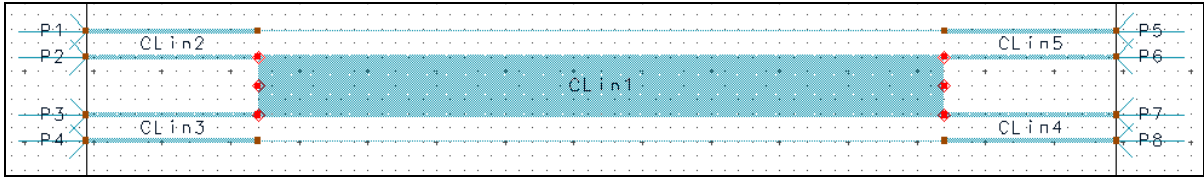


Figure 3-3 Layout Design of a Directional Coupler.

3.2 Simulations

3.2.1 Receiver Power Analysis

ADS Power simulations are used to determine how many amplification stages are needed in order to amplify the weakest signal received by the antenna. For this system the weakest signal to be amplified is -110dBm which is equivalent to 1×10^{-14} Watts. It also helps to avoid saturation on different stages of the circuit as well as to prevent burning of components. Basically this analysis ensures the well behavior of the circuit when all components are integrated. Figure [3-4] shows the schematic for the receiver. This diagram is not including the vector modulator.

In order to start the analysis several voltage Nodes are placed throughout the circuit. These nodes are needed to state power equations on each stage. The power equation used for this analysis is as follow:

$$P_i = wtdbm \left(\frac{|V_i^*| \|V_i\|}{50} \right) \quad \text{Equation 3.1}$$

This equation provides the power in dBm for each voltage node. An input power of -110dbm is been simulated at the source representing the antenna (as seen in figure [3-4]).

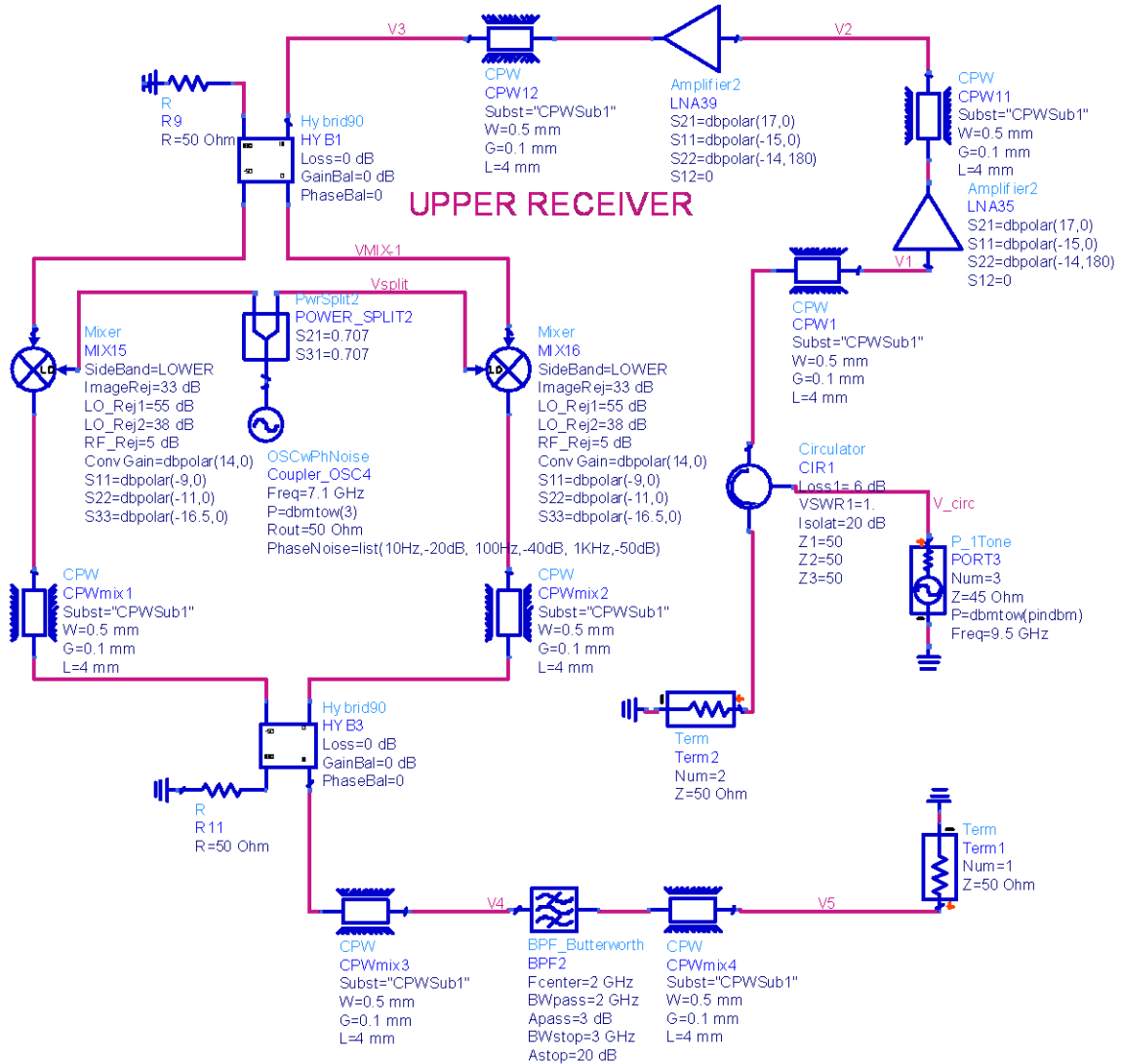


Figure 3-4 Circuit Design for Receiver before Vector Modulator . Done in Agilent Advanced Design System 2008.

After the circulator and before the first Low Noise Amplifier a value of -106dB appear (as shown in figure [3-5]). This is due to certain losses on the circulator which have an isolation of 20dB and losses of .5dB along with several other losses that the coplanar waveguide might introduce.

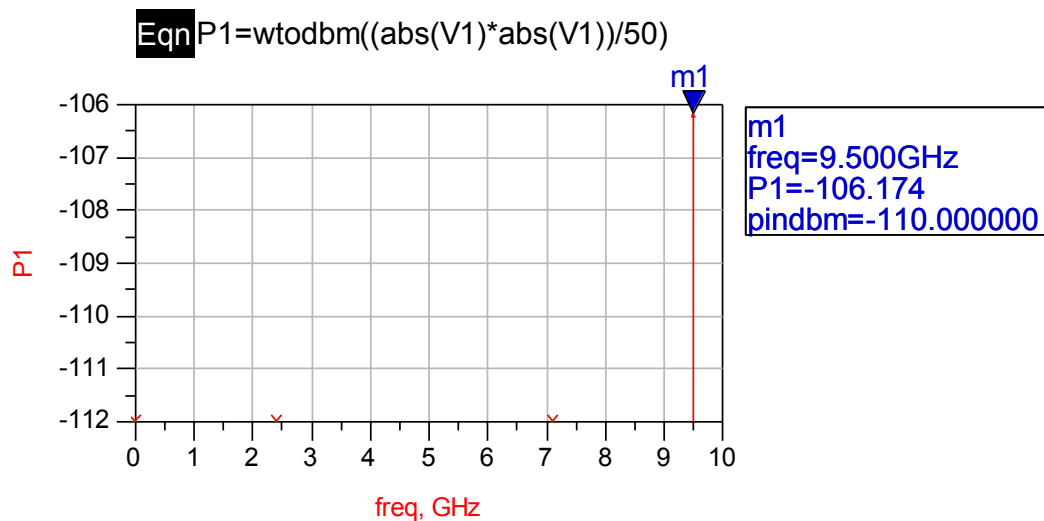


Figure 3-5 Power at First Voltage Node (After the Circulator).

Now the first Low Noise Amplifier is been fed with a power of -106.174dBm. This LNA has a gain of 17dB and an output 1dB compression point of 13dBm. Then, since -106.174dBm is an extremely low power it is not enough to saturate the LNA. The HMC564LC4 LNA enters into saturation when is fed with a power greater than -4dBm. Any value below that is not supposed to saturate the LNA. The second LNA is fed with a power of -88.8dBm and it provides an output of -73dBm. More than two amplifiers at this stage of the circuit will cause the Noise Figure to increase, besides they are not necessary since two LNAs are more

than enough to provide sufficient amplification of the Minimum Detectable Signal (-110dBm). Figure [3-6] and figure [3-7] display the power after the first and second LNA respectively.

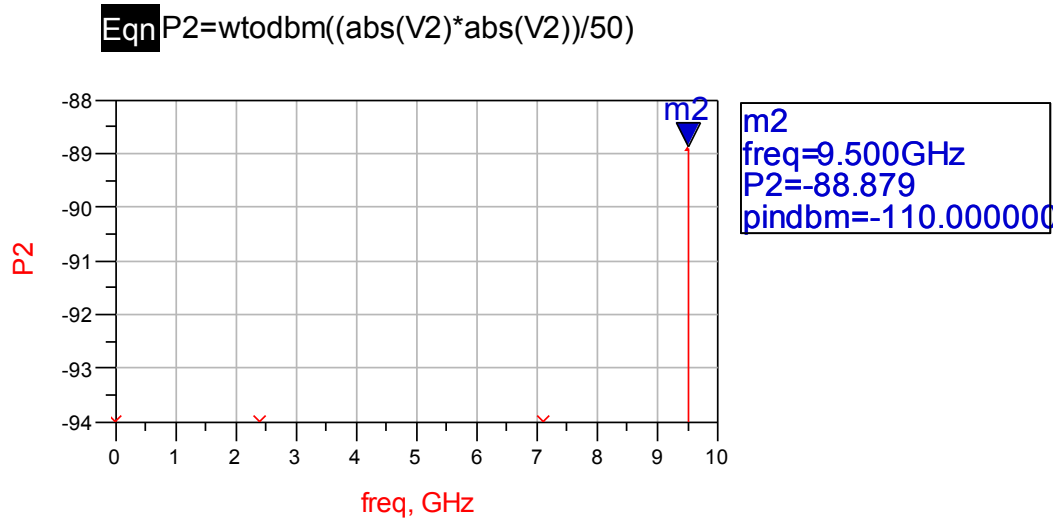


Figure 3-6 Power at Second Voltage Node (After first LNA).

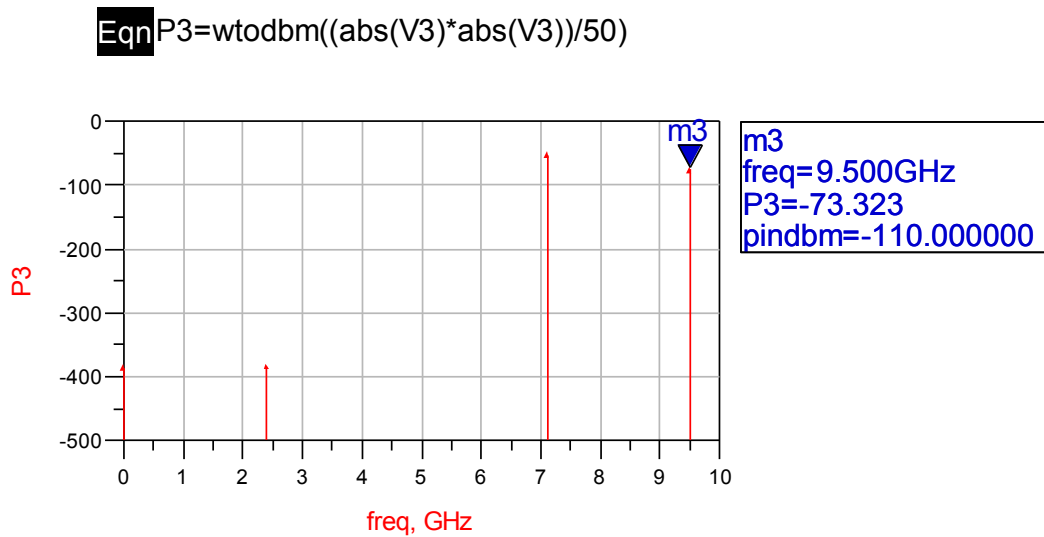


Figure 3-7 Power at Third Voltage Node (After second LNA).

Then the signal passes through the HMC568LC5 dual mixer which introduces a gain of approximately 15dB to the signal, having a power at its output of -57dBm as shown in Figure [3-8]. After the dual mixer the frequency is been downconverted from 9.5GHz to 2.4GHz. Then, outputs power after mixer needs to be taken at that frequency.

$$\text{Eqn } P4 = \text{wtodbm}((\text{abs}(V4) * \text{abs}(V4)) / 50)$$

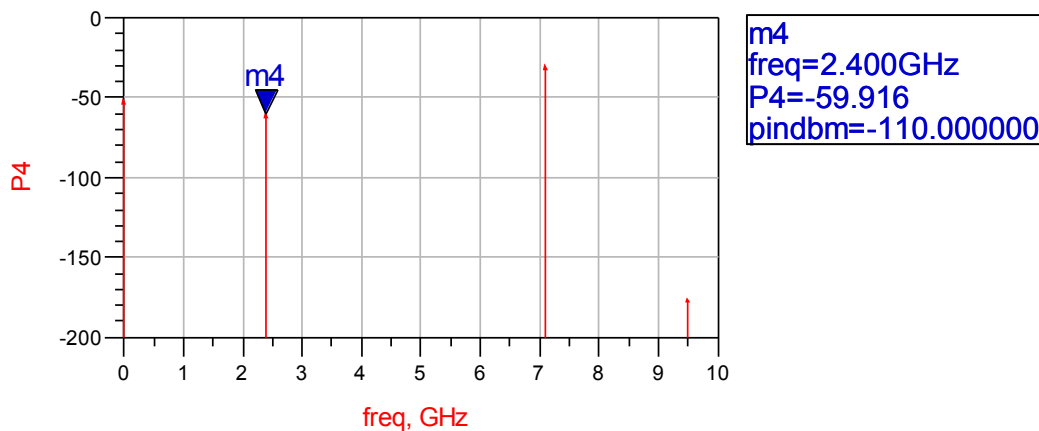


Figure 3-8 Power at Fourth Voltage Node (After dual Mixer).

A value of -60dBm will be the output of this dual mixer and the input of the vector modulator. The minimum detectable signal for the Vector Modulator is a function of the detection and measurement equipment. The Minimum detectable signal (MDS) is determined by the input noise power, additive noise (NF) and system Bandwidth. The input

noise power at room temperature is -174dBm/Hz . The additive noise, typically the noise figure, for a mixer is equal to the conversion loss. For devices like the vector modulator it can be assumed a value of 8dB . If we assume a 1MHz bandwidth this is 60dB . Therefore, the noise floor will be $-174\text{dBm/Hz} + 8\text{dB} + 60\text{dB Hz}$ which is equal to -106dBm . We also have to account for detecting the signal which is usually considered to be 10dB . Then it can be said that the Minimum detectable signal for the HMC631LP3 Vector Modulator will be around -96dBm . Then a -60dBm power signal is enough for the vector modulator to operate.

3.2.2 Transmitter Power Analysis

After the transmitter component selection is complete a power analysis through the transmit path is needed in order to ensure correct compatibility between components. This Analysis was done using Agilent ADS Software. Figure [3-9] shows the schematic for the Transmitter circuit after the vector modulator. Voltage nodes are placed after each stage of the circuit and power equations are stated through the design to prove that power levels are on range. An input power of 1dBm is placed at the source. This value represents the highest value that the vector modulator will feed into the transmitter to produce a transmit signal of approximately 30dBm (30dBm correspond to 1Watt) without saturating the power amplifiers. Keep in mind that this design is only for one polarization. Each channel has two polarizations and the 24 channel system should provide a combined power of about 24Watts per polarization.

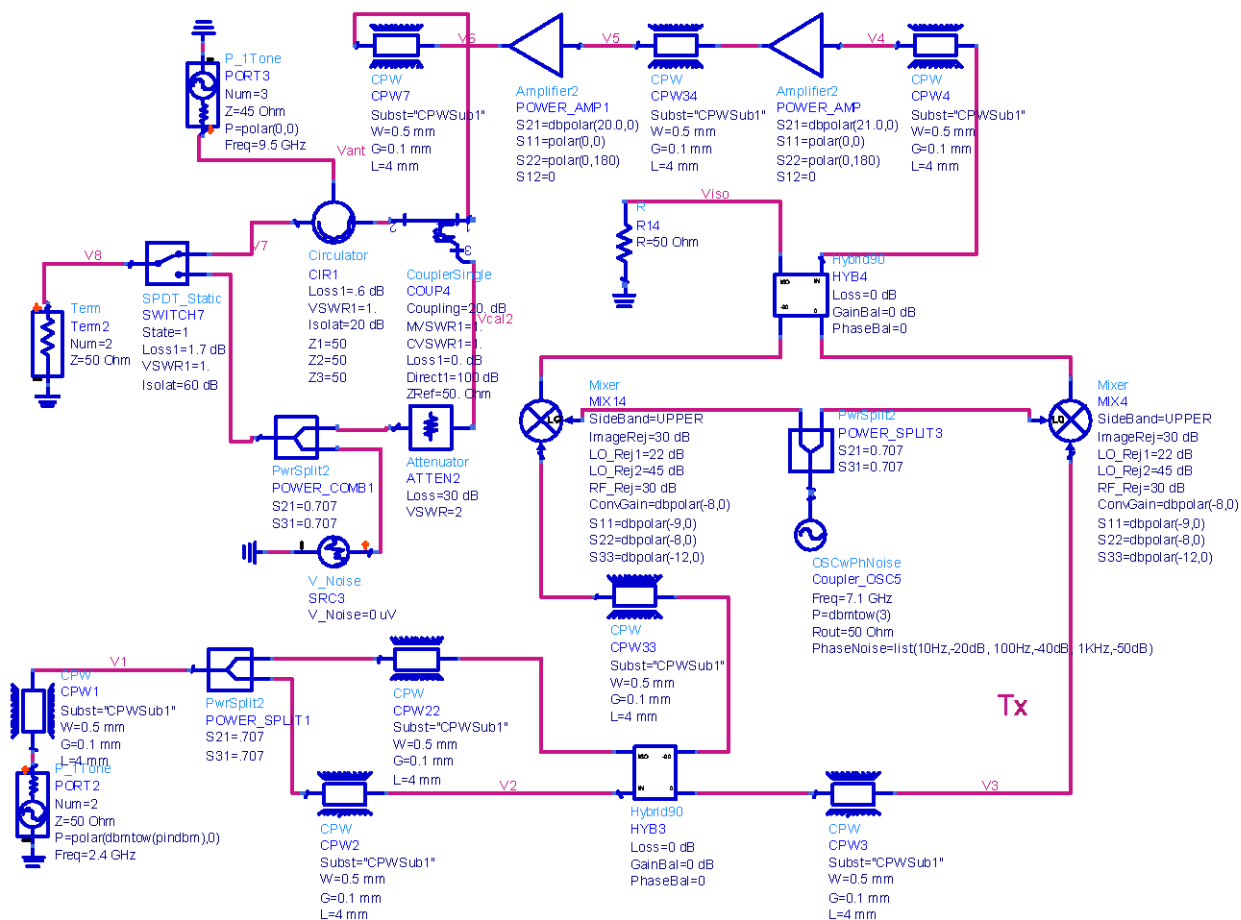


Figure 3-9 Circuit Design for Transmitter after Vector Modulator

A power of 1dBm enters the Mini Circuit BP2U power splitter that divides the power producing an output of approximately -1dBm at each end of the power splitter (Figure [3-10]). Then -1dB feed a quadrature hybrid which has an output of 3.537dB. This power of 3.537dBm will feed the HMC340LP5 dual mixer that have a conversion loss of 8dB producing an output of -7.895dBm as shown in figure [3-11].

Eqn $P2 = \text{wtodbm}((\text{abs}(V2) * \text{abs}(V2)) / 50)$

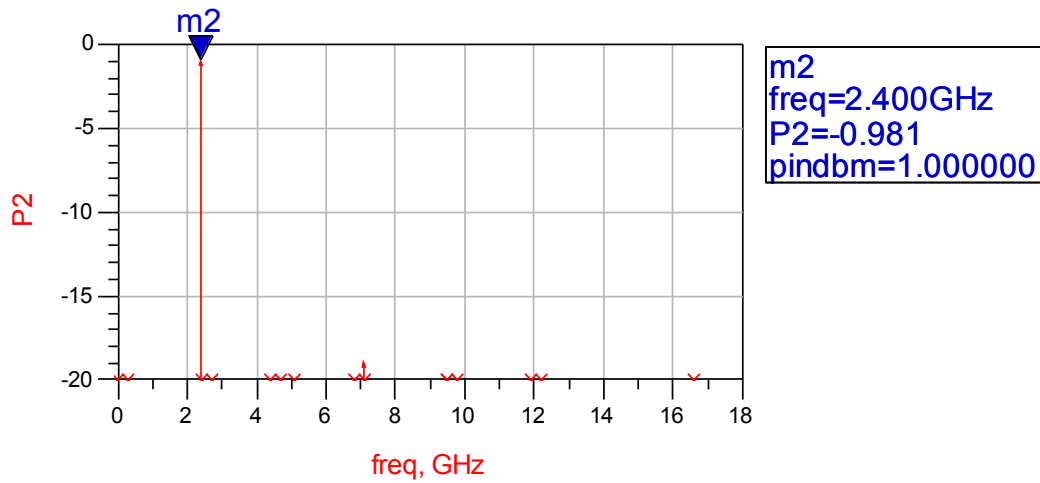


Figure 3-10 Power at second voltage node (After power splitter)

Eqn $P4 = \text{wtodbm}((\text{abs}(V4) * \text{abs}(V4)) / 50)$

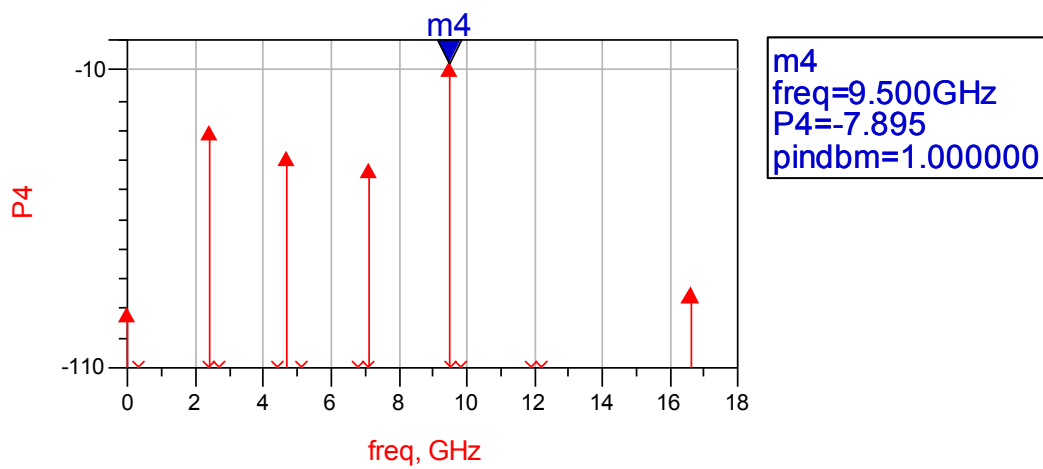


Figure 3-11 Power at fourth voltage node (After dual mixer)

Having an input value of -7.893dBm to the Power Amplifiers there is a need to determine how many Power Amplifiers are needed in order to transmit a power of 30dBm or 1W. It turns out that only two amplifiers are needed to accomplish this; the first one with a gain of 21dB (HMC590LP5) and the second one with a gain of 20dB (HMC487LP5). The reason of having two different power amplifiers with different gains is to avoid saturation of the second amplifier as well as to obtain the closest value to 30dBm. The first amplifier in the string has a gain of 21dB and a saturation output power of 31dBm. This means that it can manage power up to 10dBm, any value greater than that will saturate this power amplifier. Since the input of this first amplifier is -7.893dBm then this device is not on saturation as we see on figure [3-12].

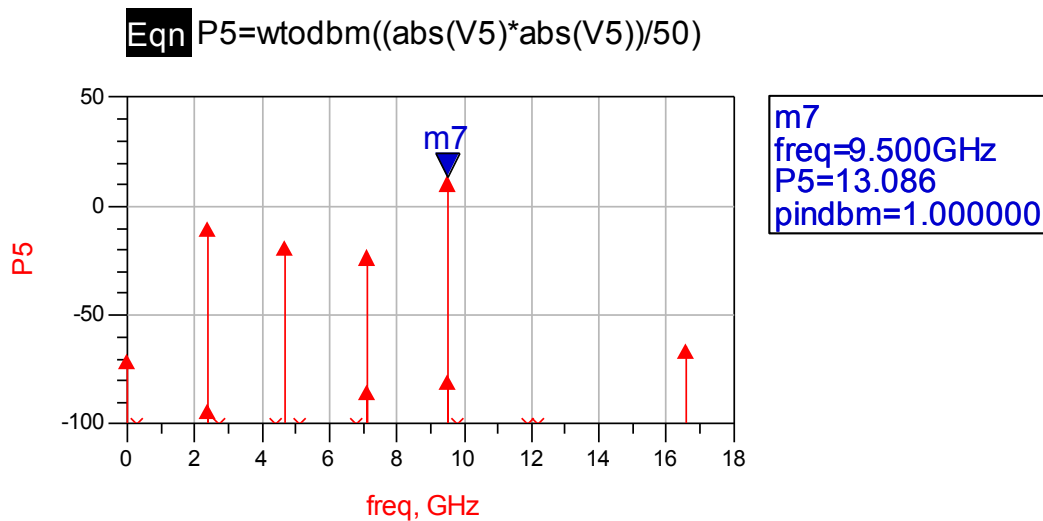


Figure 3-12 Power at fifth voltage node (After first power amplifier)

The second power amplifier in the string has a gain of 20dB and an output saturation power of 33dBm. This means that this device can manage up to 13dBm at its input. Having an input of 13.086dBm will make this amplifier to operate near saturation. The effect of operating a power amplifier near saturation can be overcome by placing a filter that eliminates all undesired harmonics produced. But operating the power amplifier near saturation means that I am operating with higher efficiency. Figure [3-13] shows the output power after second power amplifier. The value is supposed to be around 33dBm but since it is almost saturated the gain decreases by approximately 2dB giving us a value of 31dBm. It is almost inevitable to fall into saturation because there is no other combination of Hittite devices that will produce 30dBm and at the same time can stand an input power greater than 13dBm. We are sacrificing saturation to have better output power.

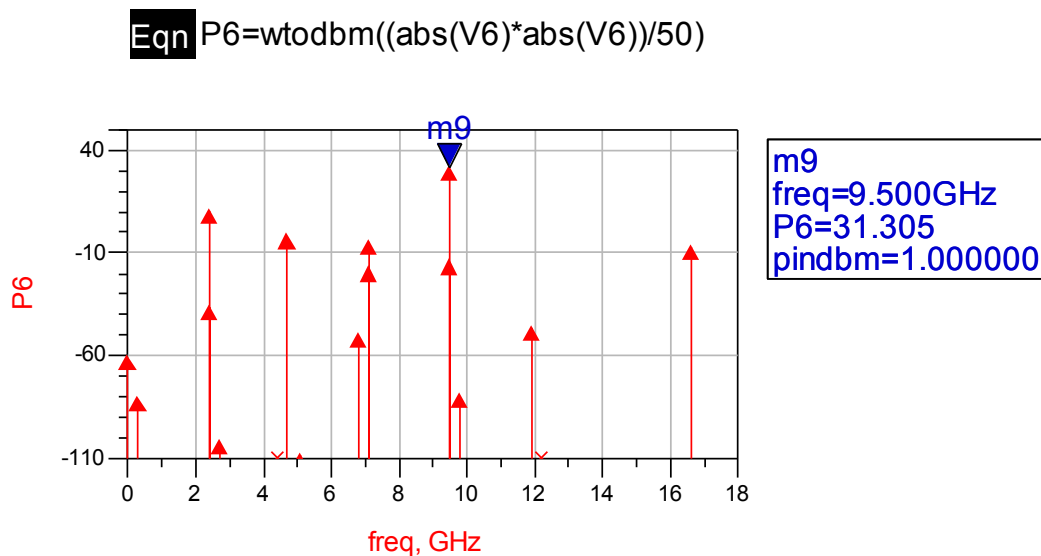


Figure 3-13 Power at sixth voltage node (After second power amplifier)

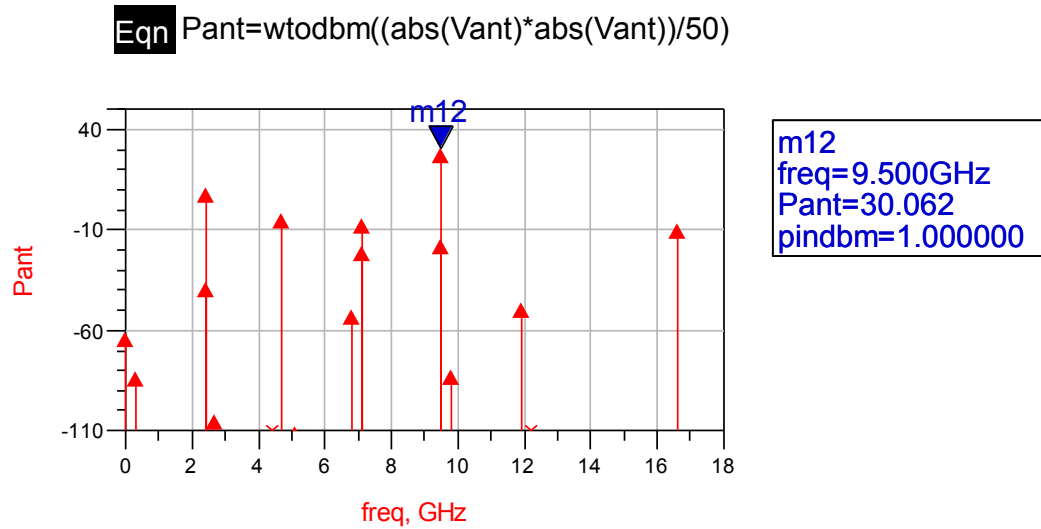


Figure 3-14 Power at the antenna voltage node (After circulator)

The power at the antenna will decrease by 1.24dB. This loss is due to losses in the circulator and the coplanar waveguide interconnecting components. It is important to mention that this loss value is only for simulation purposes and does not mean that the system will have this exact loss when built (For this simulation CPW are 2.5mm long and are done with Rogers 3006 substrate which has a loss tangent of .002). Figure [3-14] shows that the output to be transmitted by the antenna per each channel will be 30dBm or 1Watt. Since a channel has two polarizations, each polarization will transmit 1Watt (alternating horizontal and vertical). Our system comprises 24 of these channels then the total peak power is 24W. This way we meet the 24W peak value requirement.

A problem that we faced is that when the circuit is transmitting there is a leakage of 5.8dBm into the Receiver as shown in Figure [3-15]. This amount of power can burn the

receiver LNAs. To prevent this from happening, a 60dB high isolation switch (HMC607) is placed at the beginning of the receiver. When module is in transmit mode the circuit needs to calibrate. The power that goes into the calibration loop is 11.140dBm. Then, when transmitting, the first LNA only see -54.42 dBm as shown on figure [3-16]. This power is not enough to damage the device.

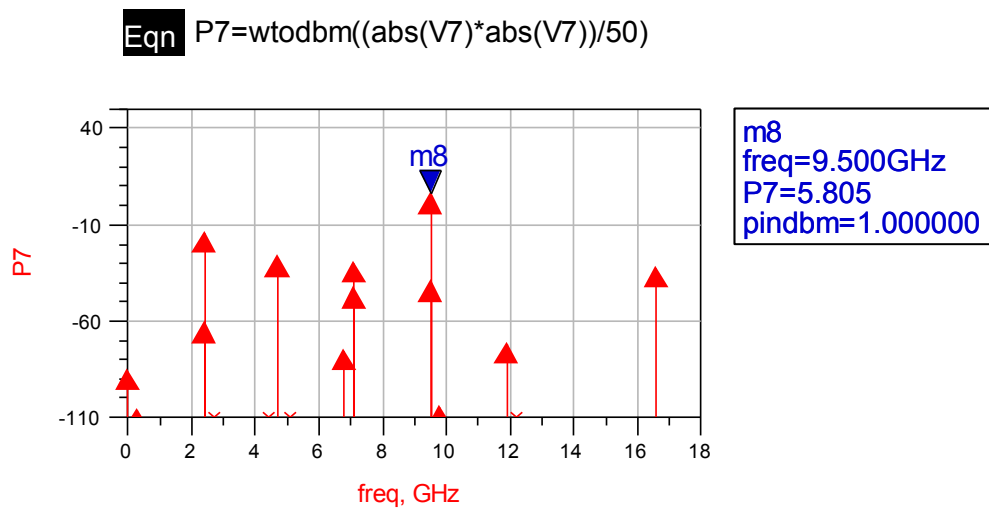


Figure 3-15 Leakage into receiver (transmit mode)

$$\text{Eqn } P8 = \text{wtodbm}((\text{abs}(V8) * \text{abs}(V8)) / 50)$$

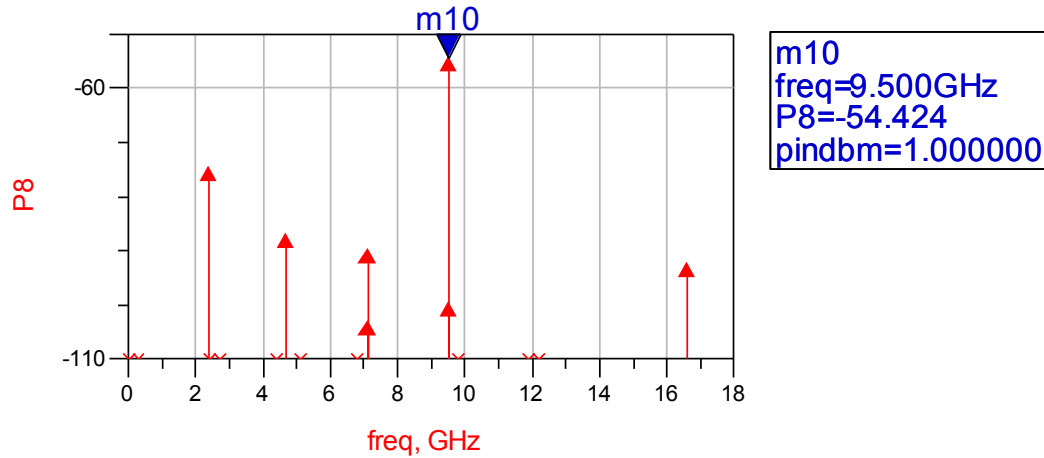


Figure 3-16 Signal Power after isolation switch (transmit mode)

3.2.3 Receiver Dynamic Range Analysis

The receiver dynamic range is the measure of the receiver ability to handle a range of signal strengths from the weakest to the strongest. For this design the receiver is able to receive power ranging from -110dBm to -55.0dBm approximately without causing saturation. Figure below show the dynamic range simulation result for the receiver.

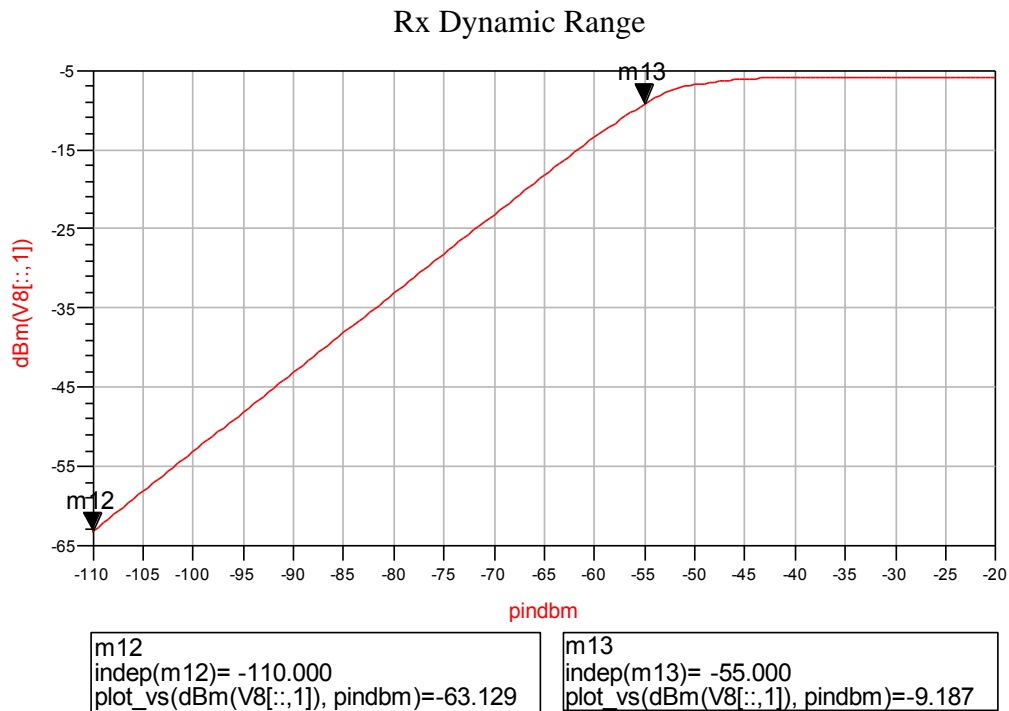


Figure 3-17 Receiver Dynamic Range

To calculate the exact dynamic range that our 24 channel system will have, we take those -55dBm and make the conversion to milliwatts using the next formula:

$$mW = 10^{\left(\frac{dBm}{10}\right)} \quad \text{Equation 3.2}$$

Then we multiply the result by 24 and do the conversion back to dBm to obtain a total dynamic range of 41.19dBm.

Using the help of a Matlab program (refer to Appendix A) we are able to determine the Radar Range Sensitivity which is basically the receiver dynamic range in terms of dBz.

This plot tells us the sensitivity of the radar depending on the range given in km. Sensitivity is calculated using Rosenfeld relation.

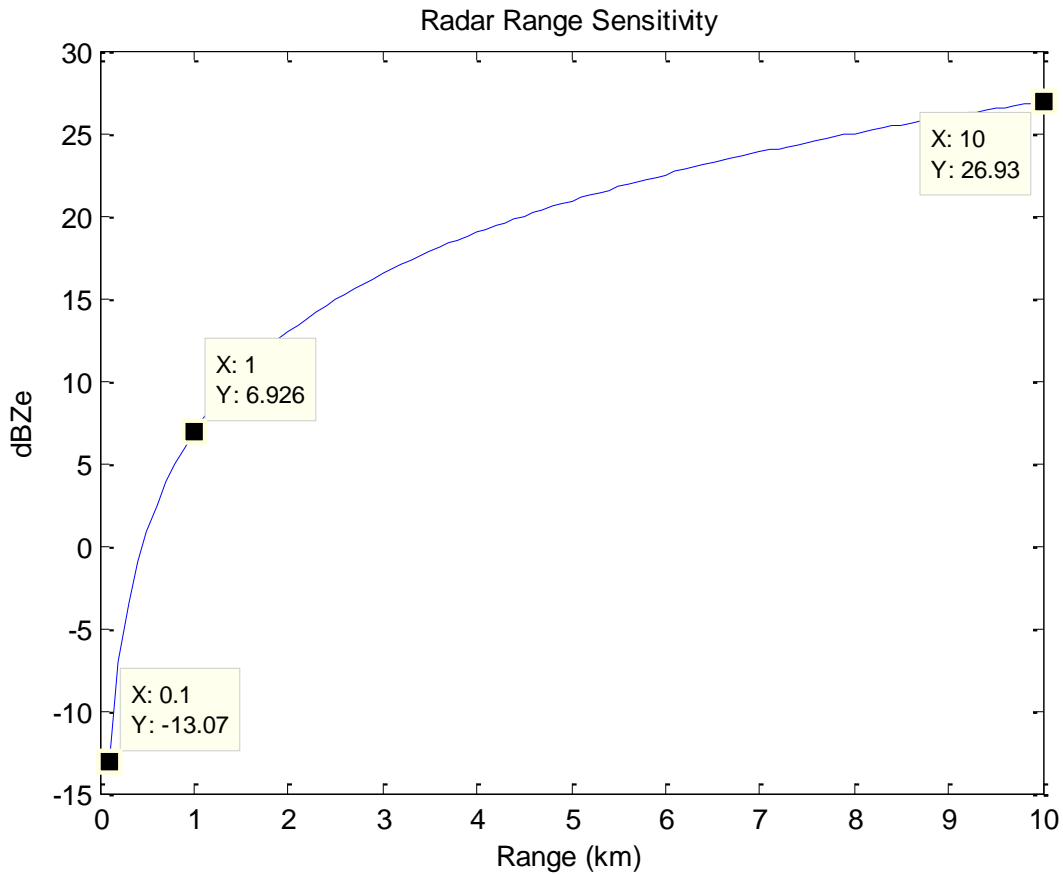


Figure 3-18 Radar Range Sensitivity.

For example it can be seen that the minimum sensitivity at 1km lies around 6.926dBz which by following table 2.1 that sensitivity correspond to a rain rate around .25mm/hr which is translated to drizzle. Same at 10km, the radar is capable to see a minimum sensitivity of around 27dBz which correspond to a rain rate of about 1mm/hr which translate to light rain.

At 10km, rain rates below 1mm/hr can't be seen because the return echo is so weak that gets buried in the noise.

3.2.4 Transmitter Dynamic Range Analysis

The Transmitter Dynamic Range is the amount of input values that the transmitter can hold before entering into saturation and at the same time transmitting close to the expected value. This range of values we will call the Transmitter Dynamic Range. Figure [3-19] below show the range of input power this circuit can operate with. Keep in mind that this system is designed to operate with a vector modulator output of 1dBm.

We see from Figure [3-19] that the circuit can sustain value ranging from -20dBm to 7dBm but only value ranging from 0.2dBm to 1.7dBm will provide a transmitted output close to 30dBm. The input power to the vector modulator should be around 12dBm in order to produce 1dBm at its output.

Table 3.2 Transmitter Input Values

Pin(dBm)	Power at Antenna (dBm)
0.2	29.53
1	30.06
1.7	30.5

Tx Dynamic Range

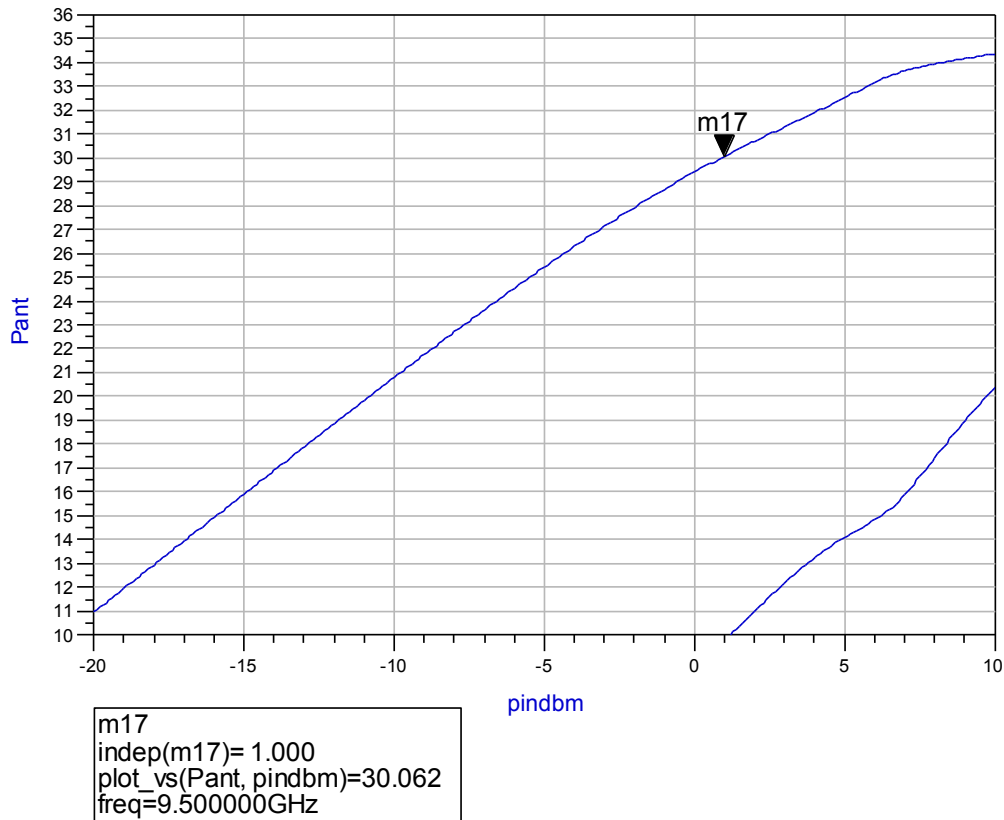


Figure 3-19 Transmitter Dynamic Range

3.2.5 Receiver Noise Figure Analysis

In order to comply with a noise figure of at least 4, a noise figure analysis was performed. Using Friis Formula as stated in equation [3.3] it has been determined how many low noise amplifier are needed to have enough power to operate the receiver and at the same time not to exceed the noise figure. It was also used to determine the receiver overall Noise Figure. This is assuming that the minimum power received will be -110dBm.

$$F = F_1 + \frac{F_2 - 1}{G_1} + \frac{F_3 - 1}{G_1 G_2} + \frac{F_4 - 1}{G_1 G_2 G_3} \dots \quad \text{Equation 3.3}$$

The Friis Formula state that the overall Noise Figure of the receiver front end is dominated by the first few stages. Thus, a higher gain and low Noise Figure LNA is chosen at the beginning of the cascade to provide high amplification in the first stage and to avoid saturation of subsequent stages. In the very beginning we achieve a low Noise Figure of 2.3 and a total gain of 33.6dB, but this Noise Figure was highly affected by the isolation switch we placed to prevent transmitter leakage from damaging the receiver. This isolation switch introduced an extra 1.7 Noise Figure which made our Overall Noise Figure a little higher than originally was.

Each component was simulated separately to verify that they were giving the correct noise figure (Refer to Appendix E). Then we calculate the Overall Noise Figure using Friis Formula stated above to obtain a Final Noise Figure value of 4.08.

Table 3.3 Noise Figure for Receiver Components

Component	Part Number	Gain [dB]	Noise Figure	Noise Figure from Simulation	Overall Noise Figure	Overall Gain [dB]
Circulator	41MS10-4	-0.5	0.5	0.49		
Isolating Switch	HMC607	-1.7	1.7	1.6945	4.085	38.1
LNA-1	HMC564LC4	17	1.8	1.7945		
LNA-2	HMC564LC4	17	1.8	1.7945		

Mixer with 90 QH	HMC568LC5	0.1	5.3	5.3
Vector Modulator	HMC631LP3	-11	11	11
Mixer with 90 QH	HMC340LP5	0.1	5.3	5.3

3.2.6 Receiver and Transmitter Harmonic Balance Two Tone Analysis

Harmonic balance is a frequency-domain analysis technique for simulating distortion in nonlinear circuits and systems. Within the context of high-frequency circuit and system simulation, harmonic balance offers several benefits over conventional time-domain transient analysis. Harmonic balance simulation obtains frequency-domain voltages and currents, directly calculating the steady-state spectral content of voltages or currents in the circuit. Harmonic Balance Simulation calculates the magnitude and phase of voltages or currents in this potentially nonlinear circuit.

Harmonic Balance is used to:

- Compute quantities such as P1dB, third-order intercept (TOI) points, total Harmonic distortion (THD), and intermodulation distortion components.
- Perform power amplifier load-pull contour analyses.
- Perform nonlinear noise analysis.
- Simulate oscillator harmonics, phase noise, and amplitude limits.

For the Transmitter we are going to use the Harmonic Balance simulation to perform a multiple frequencies or tones (in this case two tones) simulation to determine the intermodulation distortion components around the operating frequency (9.5GHz). In the case of the Receiver we use the two tone simulation to determine the intermodulation distortion components around the downconverted frequency (2.4GHz). Intermodulation distortion occurs because more than one input frequency is present in the circuit. Therefore, we have specified two closely spaced input frequencies when we set up the simulation. The frequency spacing used is small enough that the two tones are well within the signal bandwidth of the circuit. To obtain an accurate value for the intermodulation distortion we have worked with the maximum order, the LO order and the oversampling factor of the Fourier Transform. In the case of increasing the maximum order a larger number of spectral products will be summed to estimate the time domain waveform and therefore provide greater accuracy. When no significant change was observed, then we knew that the maximum order was large enough. When increasing the oversampling ratio, this controlled the number of time points taken when converting back from time to frequency domain in the harmonic balance simulation algorithm. A larger number of time samples also increased the accuracy. Figure [3-19] and Figure [3-20] show the two tone response for the Receiver and Transmitter respectively.

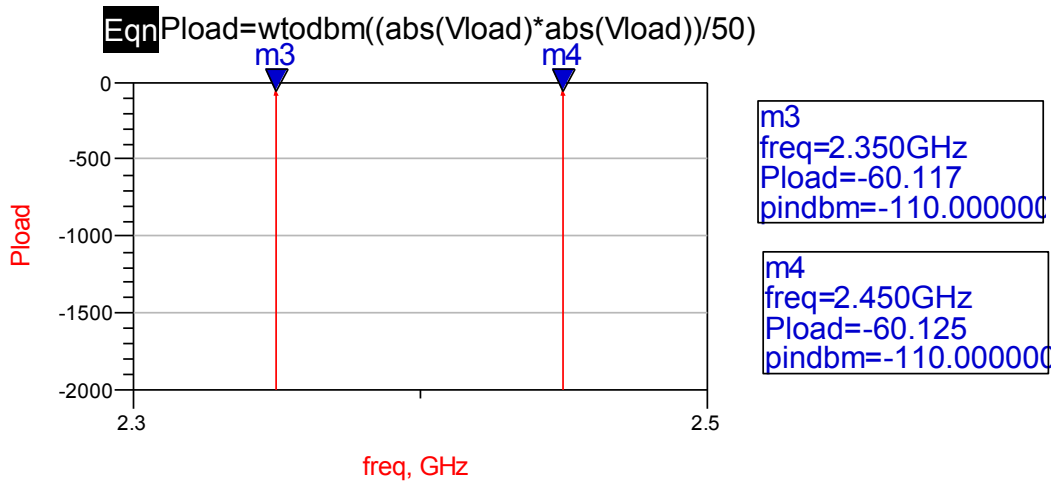


Figure 3-20 Receiver Harmonic Balanced Simulation

For the receiver it is seen that the two tones have values very close to the expected value at 2.4GHz. At this frequency the Receiver see a power of about -59.9dBm. For the transmitter it is seen from the plot that both tones diverges from the 9.5GHz expected value (which was 30dbm) by 2dB. Unfortunately, when this happens, no useful information is provided by the simulator. This type of problem generally arises when the circuit under simulation is or becomes highly nonlinear. In the case of mixers, there are inherent nonlinearities that are required for the mixing process, but these are usually not so bad unless you are seriously overdriving one of the inputs. In this circuit we are not overdriving any input.

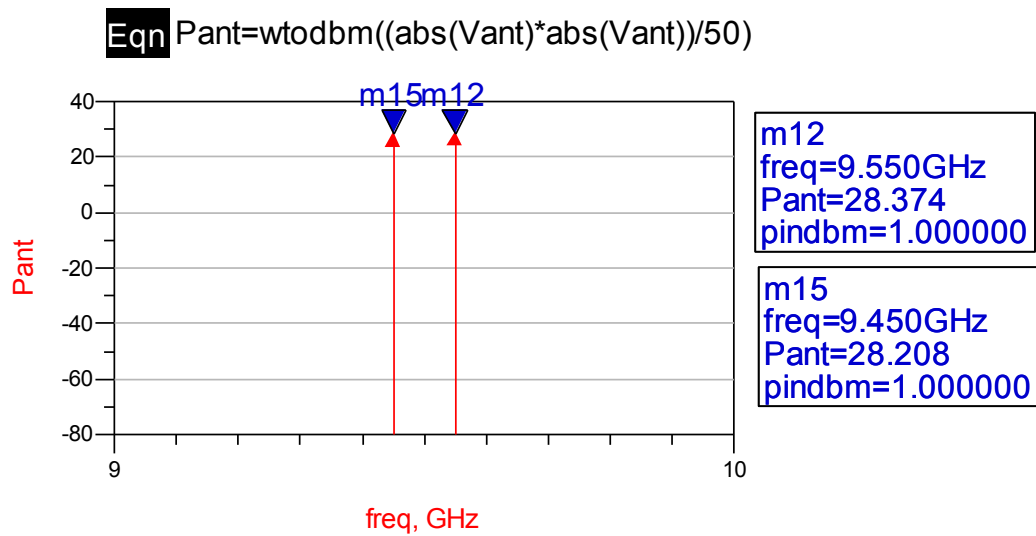


Figure 3-21 Transceiver Harmonic Balanced Simulation

3.2.7 Vector Modulator Phase Shifting Simulation

In order to determine the phase shifting capabilities of our Vector Modulator, a test has been performed on it. The Test consisted in changing the phase of the vector modulator mixers to verify if the vector modulator behaves as a phase shifting device. Figure [3-22] below shows the ADS schematics for the vector modulation portion.

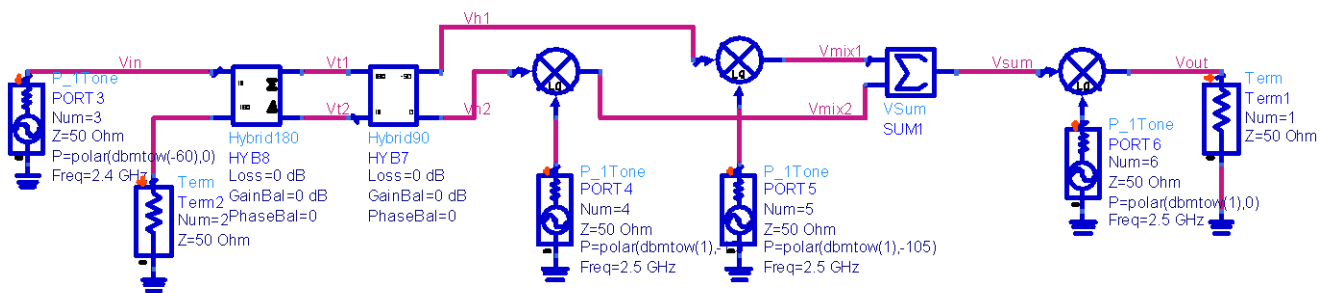


Figure 3-22 ADS Schematic for Vector Modulator

The vector modulator is been fed with a power of -60dBm because that is the output power of the stage before (which is the double mixer, refer to figure [3-8]). This is assuming the circuit is in receive mode. To start, a 0 phase is been assigned to the input power for the purpose of this simulation. This power enters the 180 degrees Hybrid and that power is equally split having an output of -63dBm. After the 180 degrees Hybrid the power enters the vector modulator which comprises a 90 degrees hybrid, two mixers and an integrator. For this simulation, the first vector modulator mixer is fed with a power of 1dBm and a 90 degree phase while the second one is fed with a power of 1dBm and a 0 degree phase. Another mixer is placed at the output of the vector modulator to upconvert the frequency from 100MHz to 2.4MHz (this is for simulation purposes only) and this produce and output of -53dBm and a -90 degree phase at 2.4GHz. At the vector modulator output we have a value of -53dBm with a -90 degree phase as shown in figure [3-23] and figure [3-24].

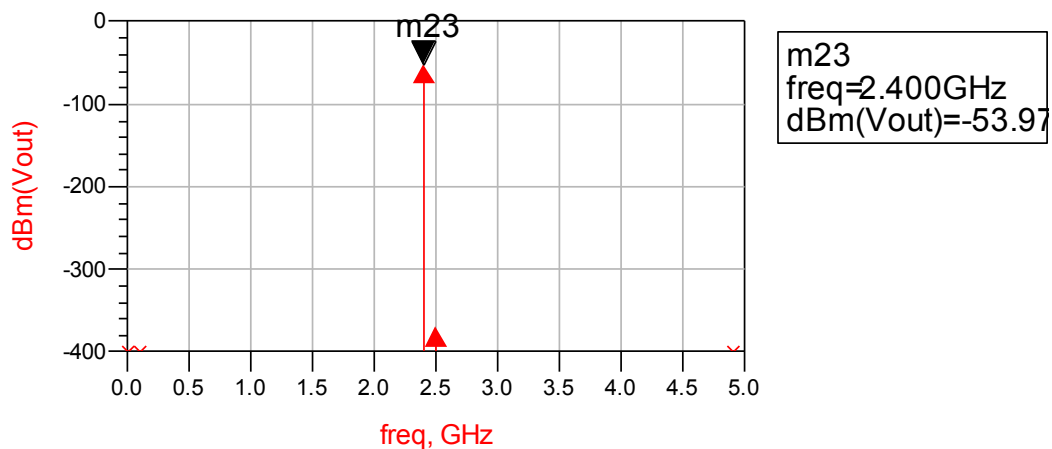


Figure 3-23 Power at vector modulator output

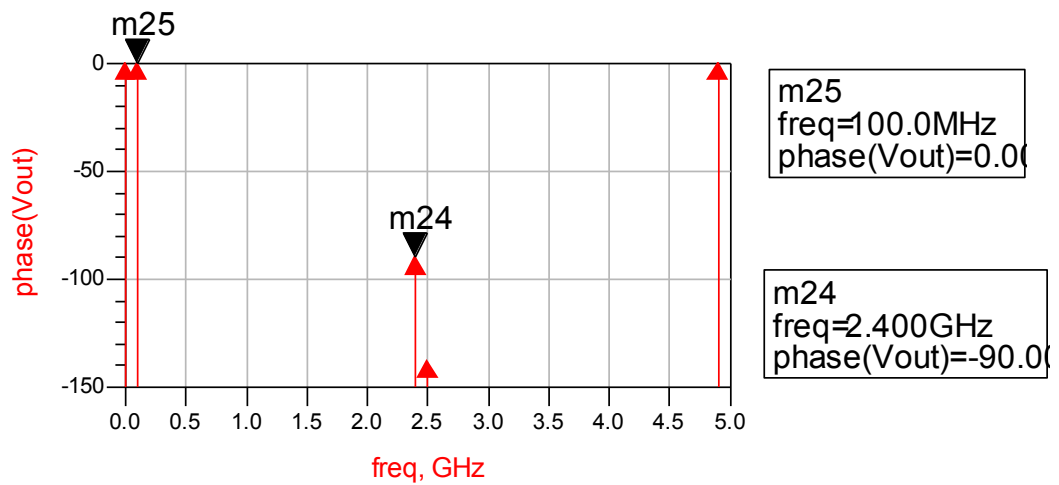


Figure 3-24 Phase at vector modulator output

If we were to change the phase using the vector modulator for an arbitrary value, let's say 15 degrees, then we just need to change the phase of the mixers. For example if the first mixer is fed using a 15 degree phase and the second mixer is fed with a -105 degree phase the vector modulator will have an output value with a 15 degree phase as shown in figure [3-25].

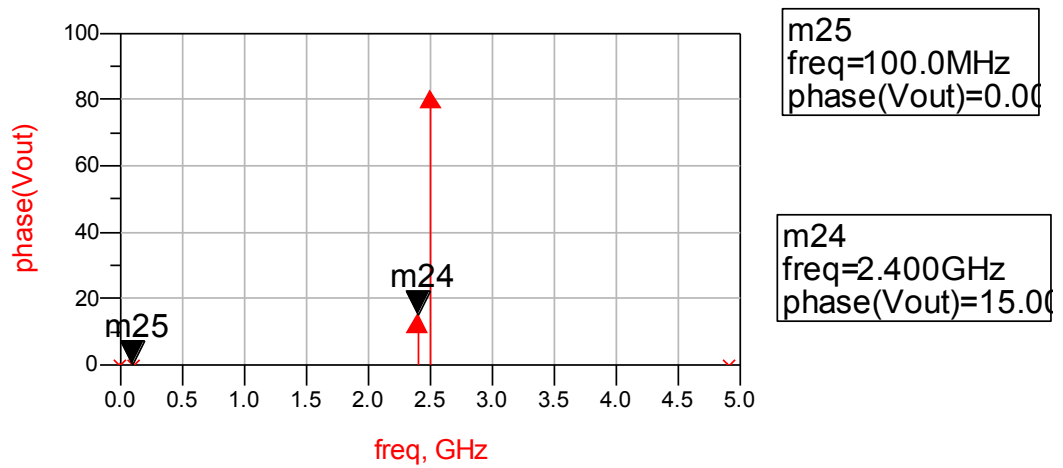


Figure 3-25 Phase shift at vector modulator output

3.3 Tradeoffs

When picking components for the Receiver there was a tradeoff with the maximum gain it was possible to achieve versus the noise figure requirement. The more low noise amplifiers we used the more amplification and gain we were going to have but the noise figure was highly affected by each LNA we placed. We end up having only two LNA's but an overall Noise Figure of 4. There was also a tradeoff between maximum gain and dynamic range for this receiver. Dynamic Range was also affected by how many amplifiers we wanted there. The more amplifiers the better dynamic range but the worse the noise figures. Two amplifiers gives just the right amount of dynamic range we need to operate this radar and at the same time does not hit the noise figure as hard as it would if we want more than

two LNA's. A tradeoff between maximum isolation achieved and noise figure was also at stake because we needed to isolate the receiver from the transmitter to avoid transmitter leakage from damaging receiver components. This was one of the hardest things because there were no packaged surface mount switches on the market that provided a very high isolation and at the same time a low noise figure. We needed to place two switches in order to have enough isolation and since the switches are at the beginning of the receiver chain they hurt the noise figure so much that we end up having a value around 7. This was not acceptable so we found a chip that provide 60dB of isolation and a noise figure of 1.7 and since we needed only one, that was not much of a problem. Finally with this chip and only two LNA's we achieved an overall receiver noise figure of 4, a total gain of 38.1dB and a system (24 channel) dynamic range of 41dBm. The only drawback is that to be able to use this chip on our circuit we need to do wire bonding and we were trying to avoid that to maintain certain simplicity. Then we have sacrificed ease of construction for a better noise figure.

When picking components for the transmitter we undergo several different tradeoffs between the specifications we have and the components available on the market. For example when choosing the right power amplifiers we needed to make sure that we had enough amplification to produce 30dBm at the antenna and at the same time we needed to be careful not to saturate any of the two amplifiers.

When designing interconnection lines there was a need to choose the width and longitude of the coplanar waveguides to provide an impedance of 50 ohms. Among the

several options we had we needed to consider the one that was able to send to production since some of the combinations required very narrow lines that were almost impossible to create on a board. When designing the directional coupler we also needed to pick the right dimensions to be able to fabricate this device.

Performing the power analysis on the TR Module it was noticed that the Receiver total dissipated power per TR Module is 11.7087W and the Transmitter total dissipated power per TR Module is 36.4259W. Both calculations are including the power dissipated in the Vector Modulator.

The estimated cost of producing one TR Module is \$1011.06 dollars. For the 24 channel system we need 48 TR Modules for a total cost of \$48530.88 per radar. For more details on components costs please refer to Appendix E.

4 Test Results

With the polarimetric, doppler and solid state transmit/receive module already designed, the next step was to test the hardware. The tests were designed to validate that this system is able to operate as expected and that it is truly meeting requirements. The first hardware test was conducted on the vector modulator and the goal was to verify that the vector modulator behaves as a phase shifting device. Additional tests were performed on the receiver and the transmitter portion of the module to verify the power flow through the circuit and their dynamic ranges.

4.1 Vector Modulator Hardware Test Results

To perform the Vector Modulator hardware test we used the Hittite component (HMC631LP3) already mounted on its PCB Board as shown in figure [4.1]. Two tests were performed with the vector modulator; the first consisted of verifying the operation of the vector modulator as a phase shifting device to verify the voltage levels for different amplitude and phase combinations, and the second was intended to document its

performance in the system when in receiving mode. Two mixers were placed at the input and the output of the vector modulator, to have a 9.5 GHz input signal and looking at the phase change at the IF frequency of 5.0MHz. This last test serves us to show the amplitude change and phase shifting capabilities of the system.

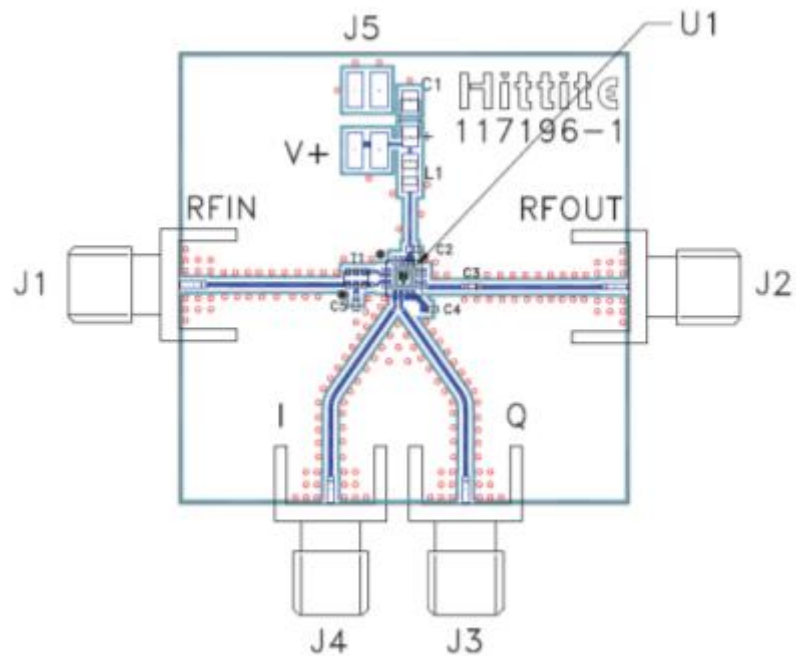


Figure 4-1 Vector Modulator PCB Layout (taken from [29])

4.1.1 Vector Modulator Phase Shifting Test

The Vector Modulator is fed with a -60dBm power signal coming from the network analyzer. This signal is been input through port J1 and the output is got from port J2. Port J5 is used to provide dc power to the circuit with a Vcc signal of 8V and 93mA. Ports J3 and J4

are used to input the phase (I) and quadrature (Q) signals described by equation [4.1] and equation [4.2].

$$I(G, \theta) = V_{mi} + 1.0V \left(\frac{G}{G_{\max}} \right) \cos(\theta) \quad \text{Equation 4.1}$$

$$Q(G, \theta) = V_{mq} + 1.0V \left(\frac{G}{G_{\max}} \right) \sin(\theta) \quad \text{Equation 4.2}$$

where V_{mi} and V_{mq} are the I and Q voltage settings corresponding to maximum isolation at room temperature and $F = 2$ GHz. Then $G = 10^x$ and $G_{\max} = 10^y$ where $x = \frac{G_{\text{setting}}(\text{dB})}{20}$ and $y = \frac{\text{Max}G_{\text{setting}}(\text{dB})}{20}$. Typically V_{mi} and V_{mq} have values of 1.5V for a 2GHz frequency. Also a -10dB maximum gain and -11dB Gain has been set. Phase and Quadrature input signals are used to produce an output signal with the desired phase shift. Table 4.1 below show some examples of the I and Q voltage settings to produce different desired angles at the output and the frequency at which each phase setting (angle) is met. I and Q signals can take values from 0.5V to 5.0V.

Table 4.1 I&Q vs. Phase

θ	I (V)	Q (V)	Frequency (GHz)
0	2.39	1.50	2.395
10	2.38	1.65	2.395
20	2.34	1.81	2.395
30	2.27	1.95	2.395
40	2.18	2.07	2.395
50	2.07	2.18	2.395

60	1.95	2.27	2.395
100	1.35	2.38	2.395
130	0.93	2.18	2.395
150	0.73	1.95	2.395

A Network Analyzer and two power supplies were needed to provide all necessary input signals to the circuit. The first power supply provides the necessary Vcc power to energize the circuit (8V) and the second power supply provides two voltage signals corresponding to the I and Q signals. Figure [4-2] shows the setting required to perform this test. Figure [4-3] is a block diagram showing the configuration required for this test.

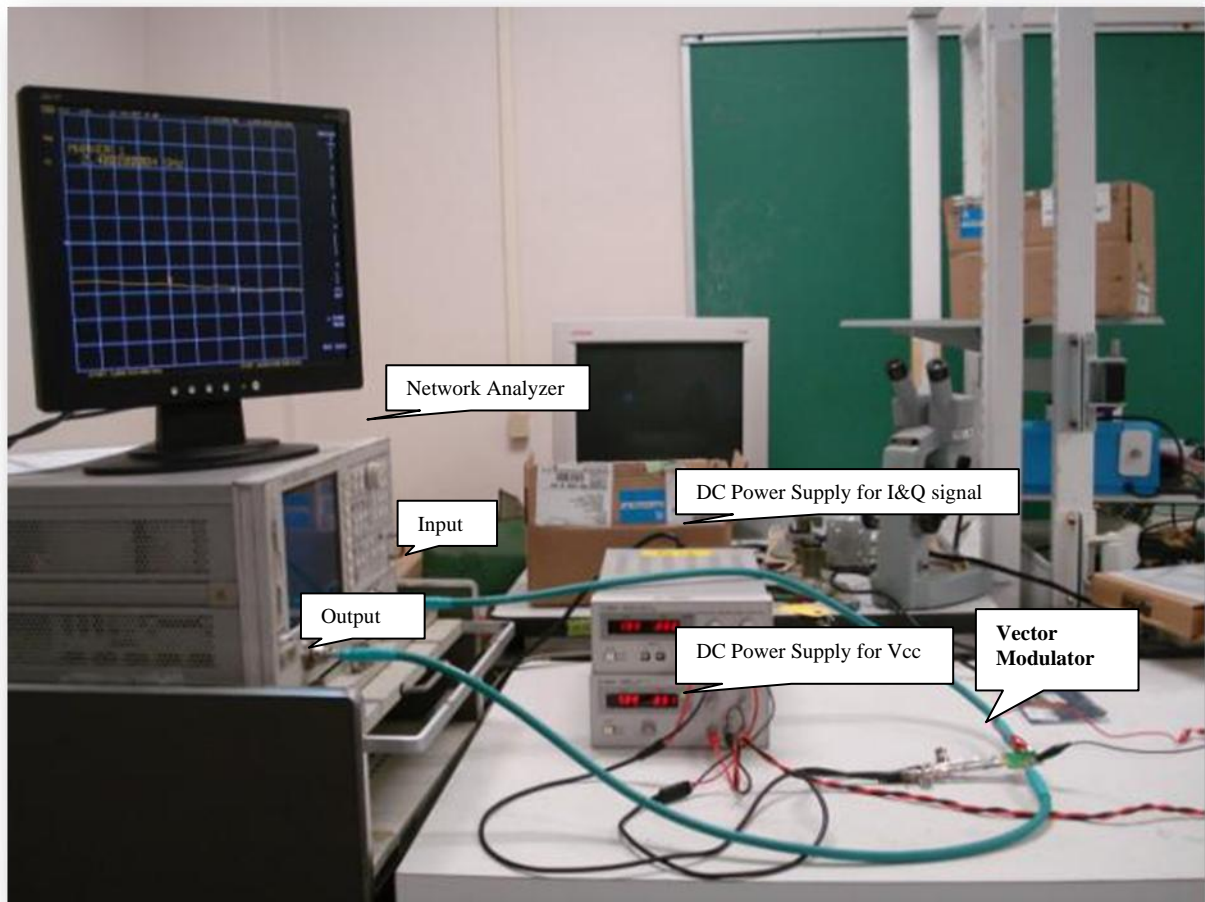


Figure 4-2 Vector Modulator Hardware test setting

Note from table 4.1 that the desired phase shift is achieved at a frequency of 2.395 GHz. To operate the Vector Modulator at 2.395GHz, the receiver must downconvert the 9.5GHz signal to a 2.395GHz signal by mixing the received signal with a 7.105GHz signal. Same thing for the Transmitter, it must upconvert the IF signal which is 5.0MHz to a 2.395GHz signal by mixing the IF with a 2.390GHz signal.

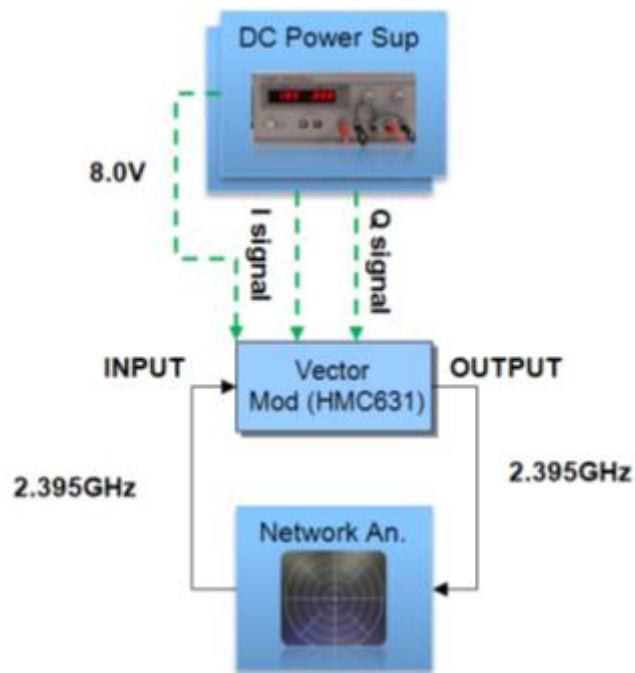


Figure 4-3 Vector Modulator phase shifting test configuration (block diagram)

4.1.2 Vector Modulator Amplitude Change and Phase Shifting Test

To verify the behavior of the vector modulator together with the system, the same has been tested with the mixers in receiver mode. Then the configuration consisted of the mixer HMC568LC5 followed by the vector modulator HMC631LP3 which provide the signal to the mixer HMC340LP5. To perform this test it was needed a network analyzer, 4 DC power supplies, one oscillator, one signal generator and one oscilloscope as shown in figure [4-4].

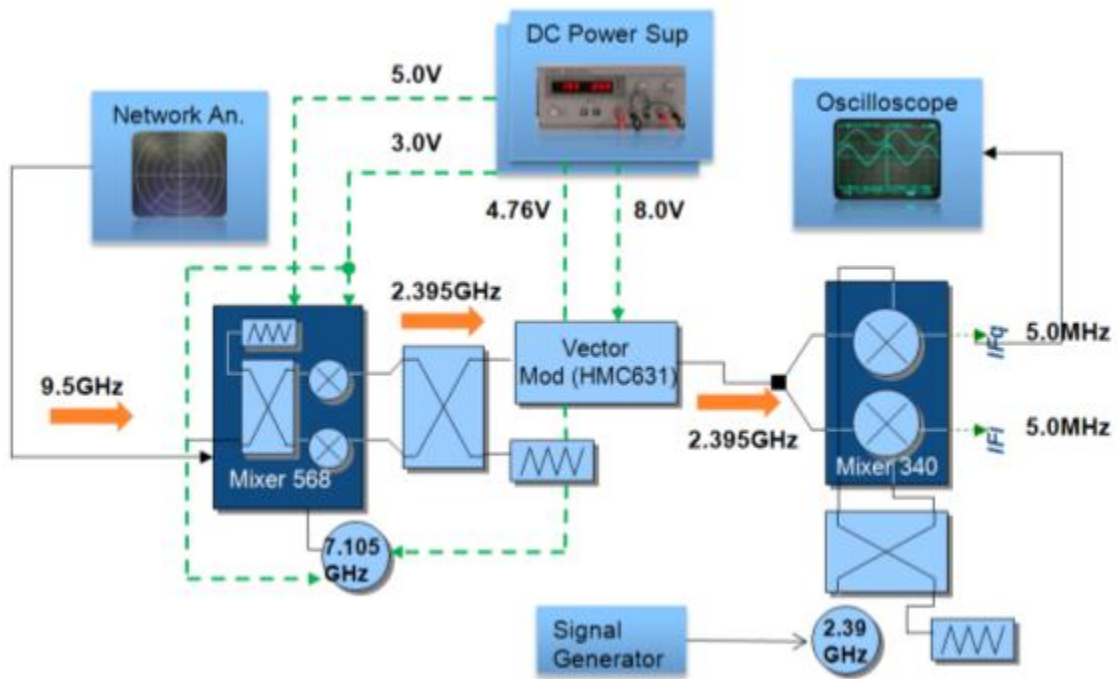


Figure 4-4 Vector Modulator amplitude and phase shifting test hardware configuration

After phase locking all signal generators and the network analyzer to 10MHz reference signal taken from one of the signal generators, we apply a voltage signal to the I and Q pins that correspond to the desired phase shift and amplitude change. Table 4.2 shows different combinations of I and Q signals to produce various desired phase shifts. For example, if a 10 degree phase shift is required, a voltage of 2.38V to the I (phase) input pin and 1.65V to the Q (quadrature) input pin should be applied. Once this is done, a reference marker at one of the signal peaks or zeroes should be placed to measure the phase shift when changing I and Q voltages. After voltages are changed, a second marker is placed at that very same peak or zero we chose with the first marker. With the oscilloscope, the time

difference between the two markers is taken and with the total period of the signal a percentage of 360 degrees is calculated as seen on Table 4.2. The phase shift from the signal calculated before, needs to be added to the phase shift we are calculating. This has to be done because of the way markers were chosen to develop this test. For example if the calculated phase shift value for a 10 degree signal resulted in an approximate 7 degree value, when we calculate the phase shift for a 20 degree phase shift, those 7 degrees needs to be added to the total phase shift (8 degrees for a 15 degree phase shift) to have a total of 15 degrees as it can be appreciated from table 4.2. It is important to mention that these measurements are approximate values, since the markers had to be placed manually. Figures [4.5] to [4.7] are examples of the measurements that were taken from the oscilloscope. The phase shift and amplitude change can be appreciated in these figures. It can be seen that the greater the phase shift the lower the amplitude of the signal.

Table 4.2 Vector Modulator Amplitude Change and Phase Shift

θ (degrees)	I (V)	Q (V)	Δt (ns)	$1/\Delta t$ (MHz)	% of 360 (degrees)	θ (degrees)	Phase Shift(degrees)
0	2.39	1.5	0	0	0	0	0
10	2.38	1.65	7	143	0.019444	7	7
20	2.34	1.81	8	125	0.022222	8	15
30	2.27	1.95	11	90.9	0.030556	11	26
40	2.18	2.07	15	66.7	0.041667	15	41
50	2.07	2.18	17	58.8	0.047222	17	58
60	1.95	2.27	19	52.6	0.052778	19	77
100	1.35	2.38	22	45.5	0.061111	22	99
130	0.93	2.18	20	50	0.055556	20	119
150	0.73	1.95	14	71.4	0.038889	14	133

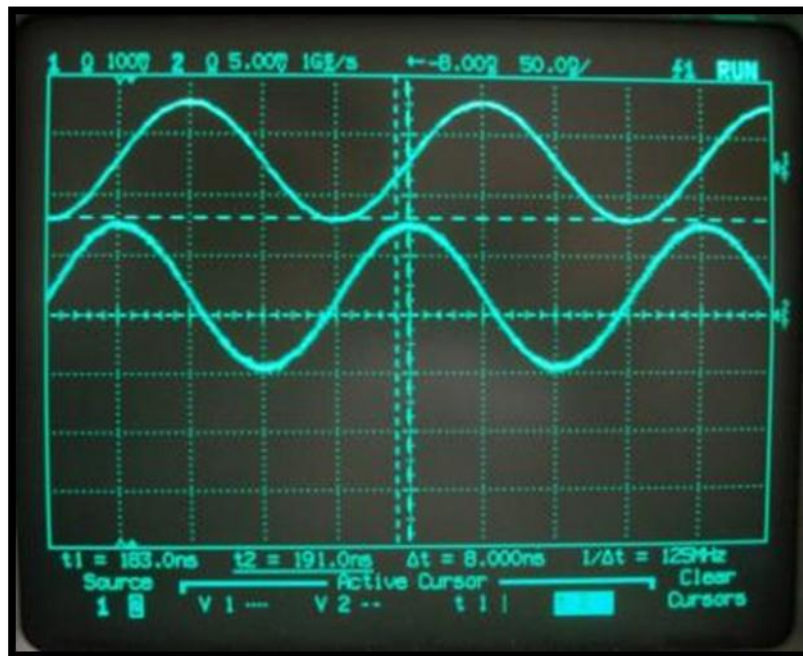


Figure 4-5 Vector Modulator 20 degrees phase

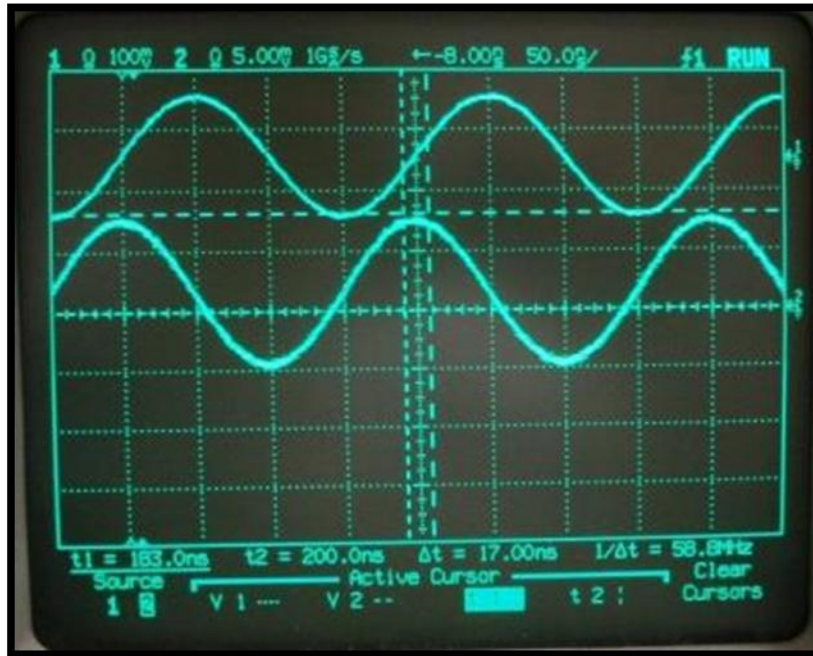


Figure 4-6 Vector Modulator 50 degree phase

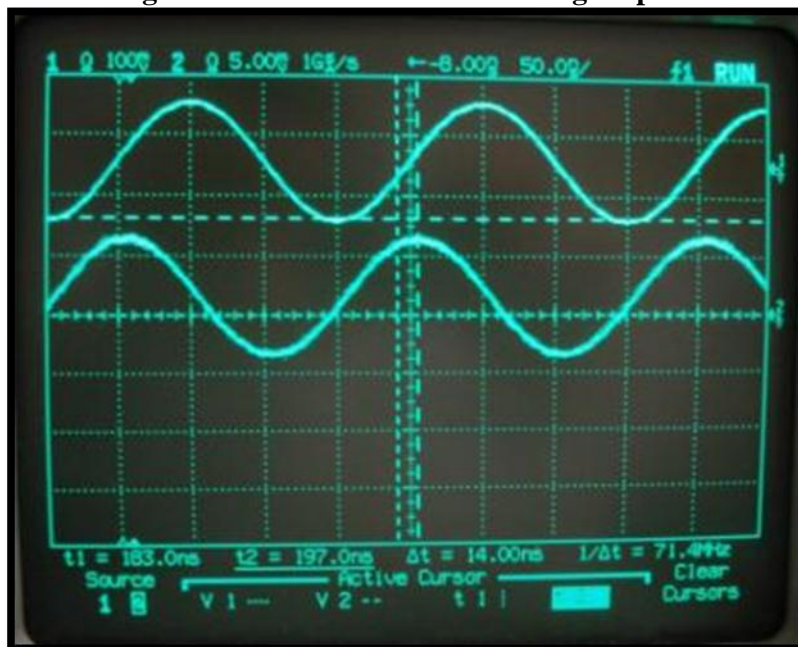


Figure 4-7 Vector Modulator 150 degree phase

4.2 Receiver Hardware Test Results

To perform the receiver hardware test we used the evaluation boards for all components listed on the bill of materials (refer to Appendix C). A power analysis test and a dynamic range test were conducted on the receiver. These tests are to ensure that we are having the expected (simulated) signal power through the circuits as well as to verify if some other components like attenuators or amplifiers are needed. For these tests we need a network analyzer, at least 5 different dc power supplies and a spectrum analyzer. Each evaluation board is tested separately. Once all circuits are being interconnected and all power signals are provided to energize the circuits we proceed to apply the receiver input signal to verify its output response. Instead of having all receiver components interconnected and test the output signal we decided to test the receiver in portions.

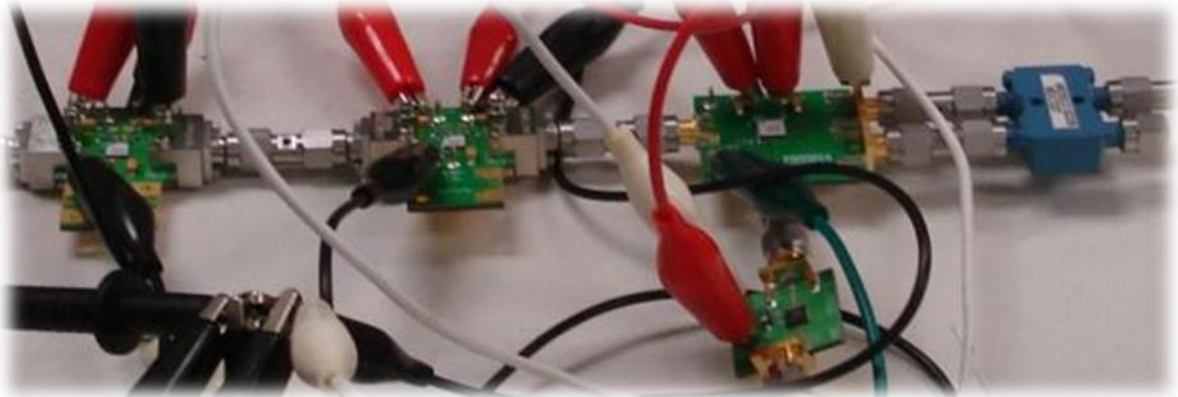


Figure 4-8 Receiver up to 9.5GHz mixer

Figure [4-8] shows the first tested receiver portion which consist of two Low Noise Amplifier, a 9.5GHz mixer, a local oscillator and a ninety degree quadrature hybrid. Figure [4-9] is a block diagram showing the receiver hardware test configuration including the equipment used and the supplied voltages.

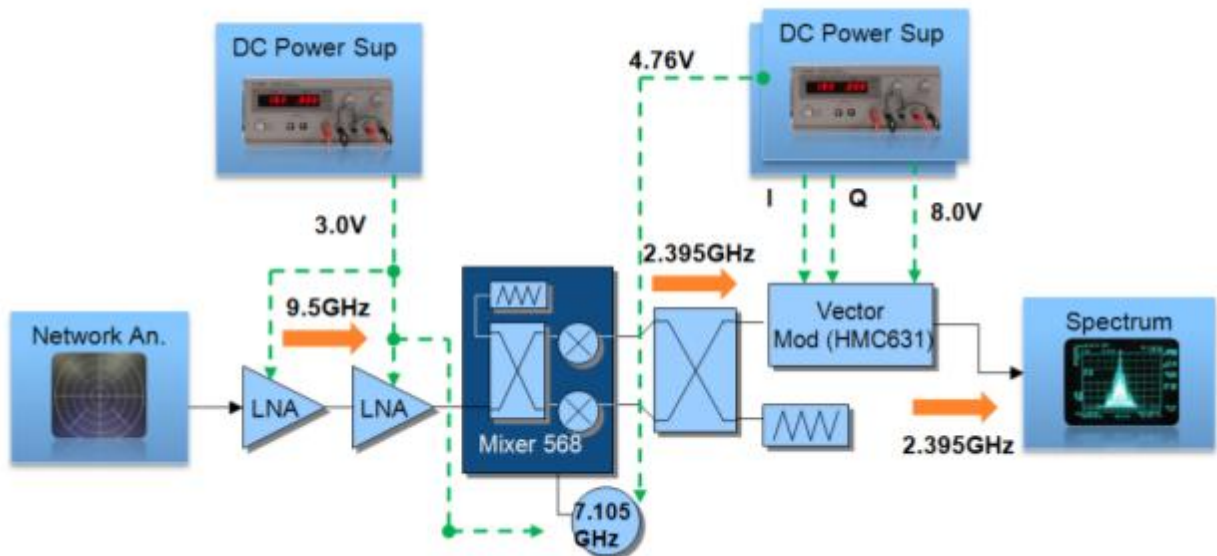


Figure 4-9 Receiver test configuration (block diagram)

To provide an input signal to this circuit we needed to make sure that the network analyzer has the capability to produce the minimum required signal and the maximum signal. Our system requires a minimum detectable signal of -110dBm and at least a maximum of -55dBm. Since the network analyzer only provide up to -65dBm of power, two 30 dB

attenuators were used to provide a total of 60dB attenuation necessary to achieve the minimum detectable signal of -110dBm. Then, different input signals were injected into the receiver and the output signal at the mixer was read using a power meter. Table 4.3 shows the different receiver input signal level versus the measured output signal level and the simulated value at the 9.5GHz mixer. The output is taken at 2.395GHz using the spectrum analyzer. Figures [4.10] to [4.16] show the mixer output as seen on the spectrum analyzer. Here we can appreciate how the mixers power output increase by 10dB's every time the Rx input increase 10dB

Table 4.3 Receiver First portion Hardware Test

Rx Input	Simulated Mixer Pout @ 2.395GHz	Tested Mixer Pout @ 2.395GHz
-110	-59.9	-58.8
-100	-49.916	-48.58
-90	-39.917	-39.9
-80	-29.919	-30.19
-70	-19.948	-19.8
-60	-10.948	-9.09
-55	-5.974	-3.74

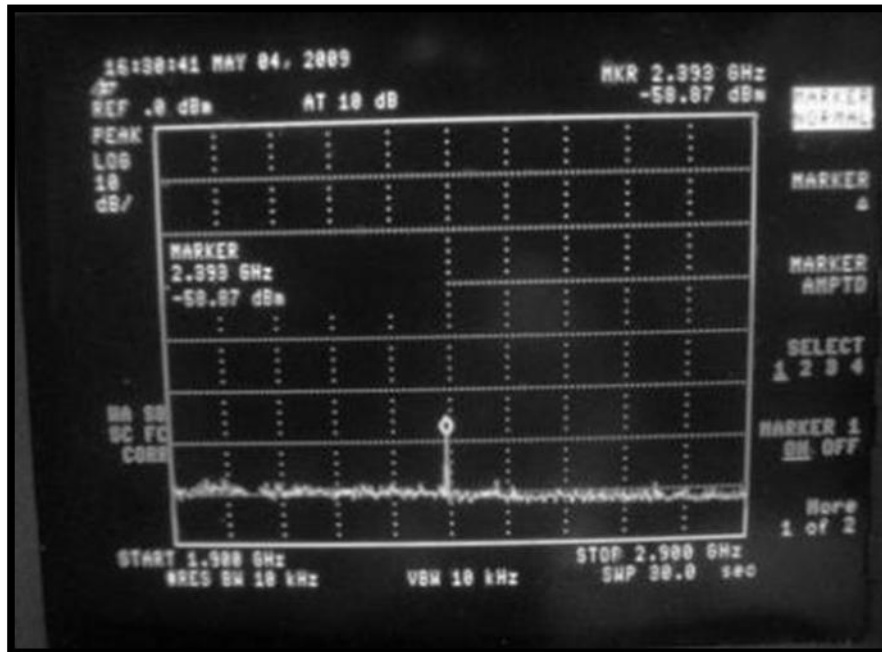


Figure 4-10 Mixer output with Rx -110dBm input

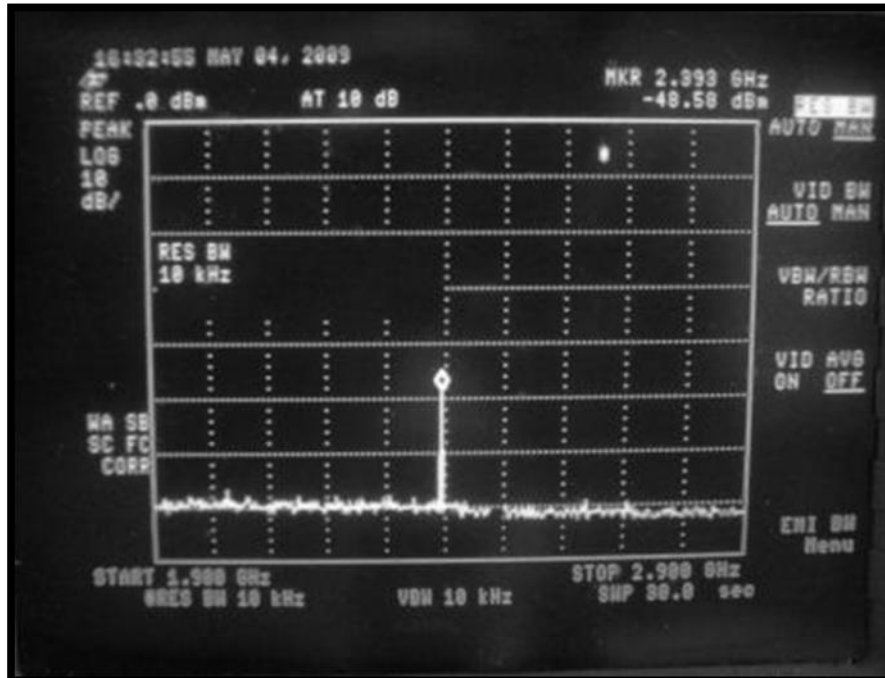


Figure 4-11 Mixer output with Rx -90dBm input

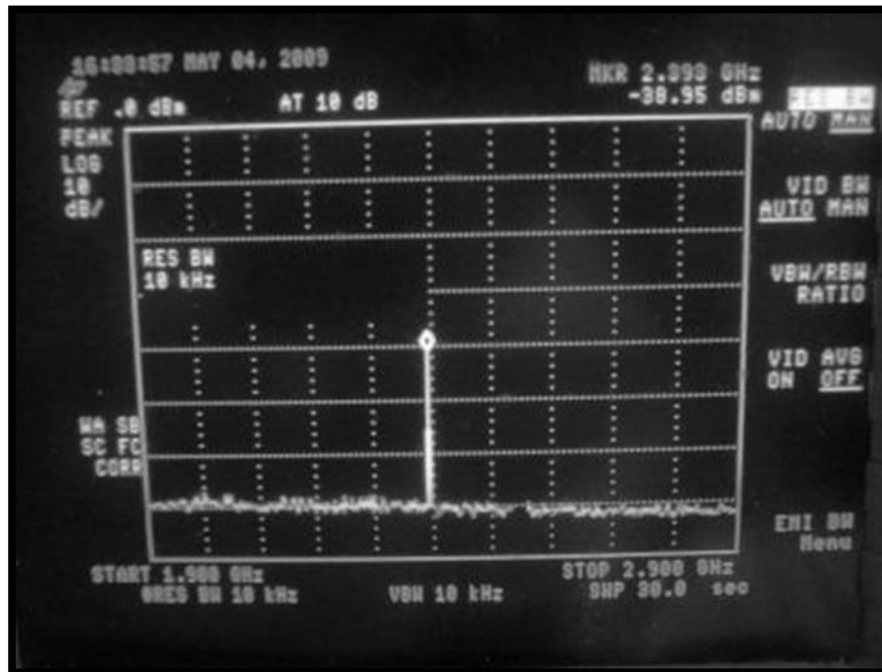


Figure 4-12 Mixer output with Rx -80dBm input

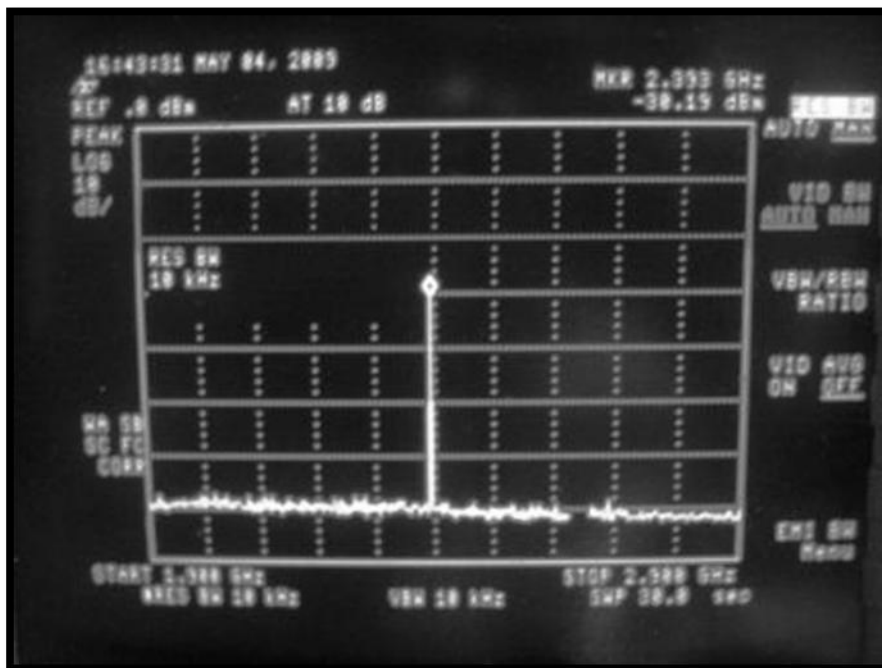


Figure 4-13 Mixer output with Rx -70dBm input

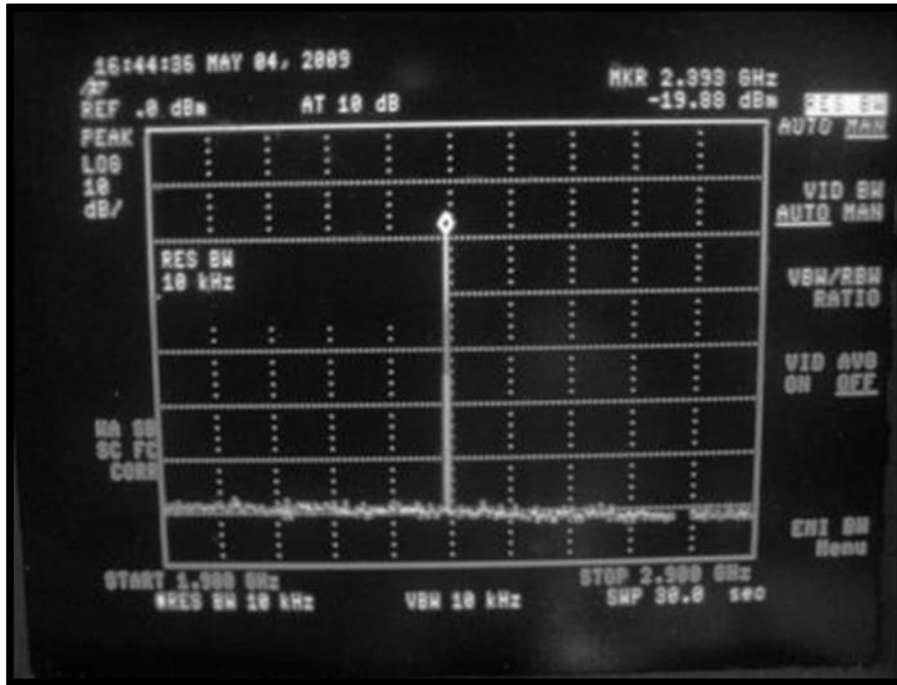


Figure 4-14 Mixer output with Rx -60dBm input

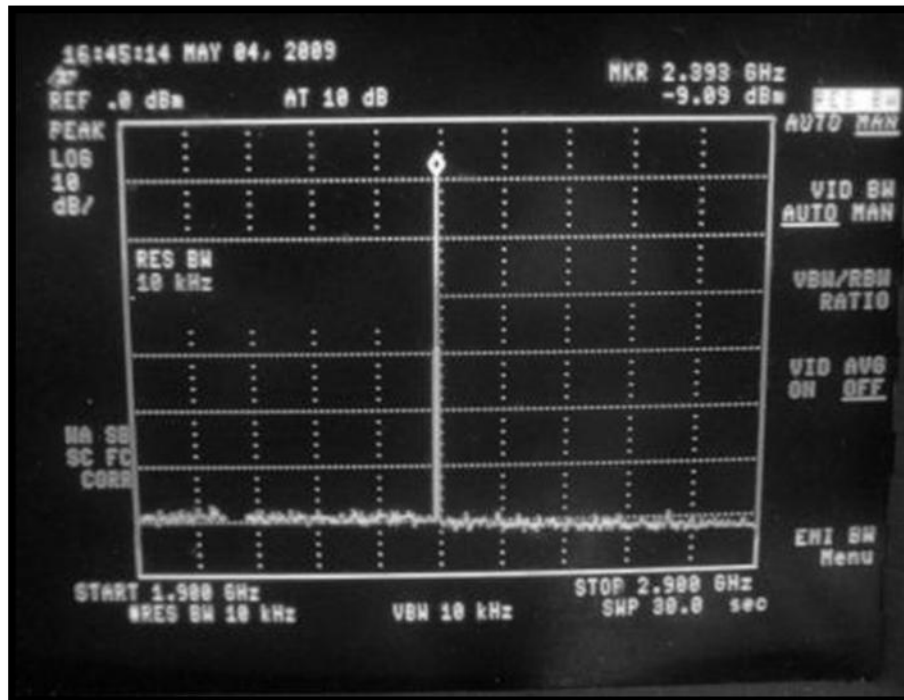


Figure 4-15 Mixer output with Rx -55dBm input

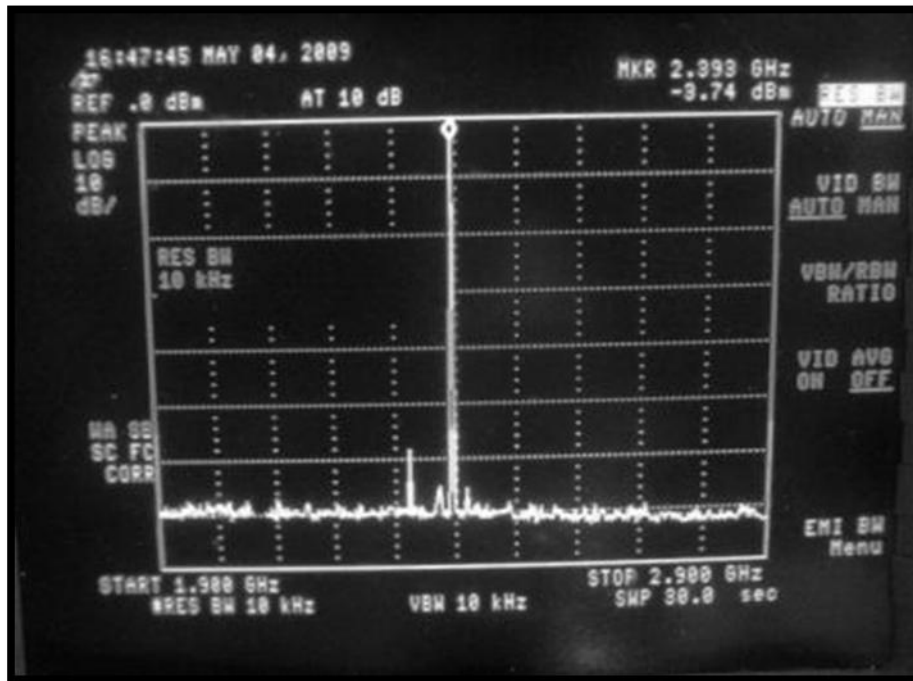


Figure 4-16 Mixer output with Rx -50dBm input

Note that the power at the output of the first mixer at different inputs is close to the simulated values. The vector modulator is then added to the circuit (as shown in figure [4-17]) and with a receiver input signal of -110dBm for example, we have an output of -53dBm.

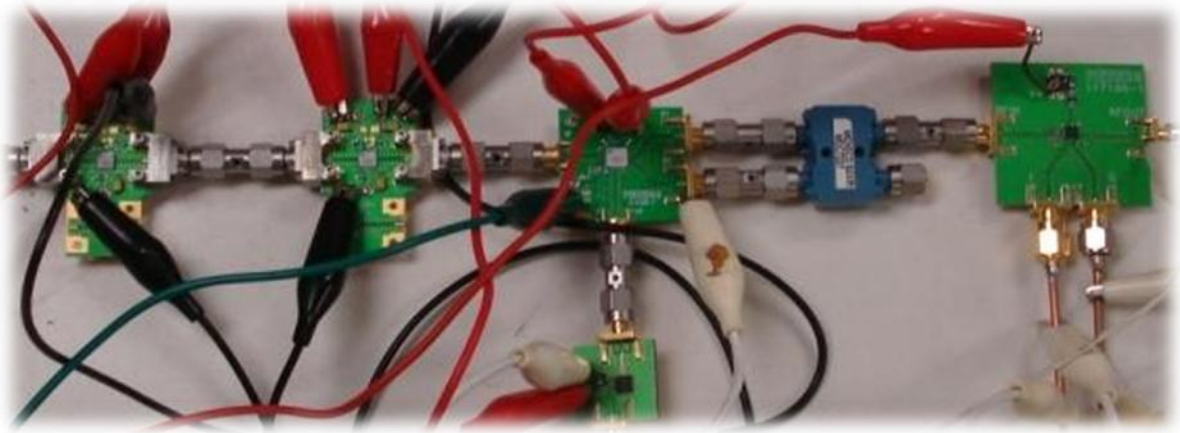


Figure 4-17 Receiver up to the vector modulator.

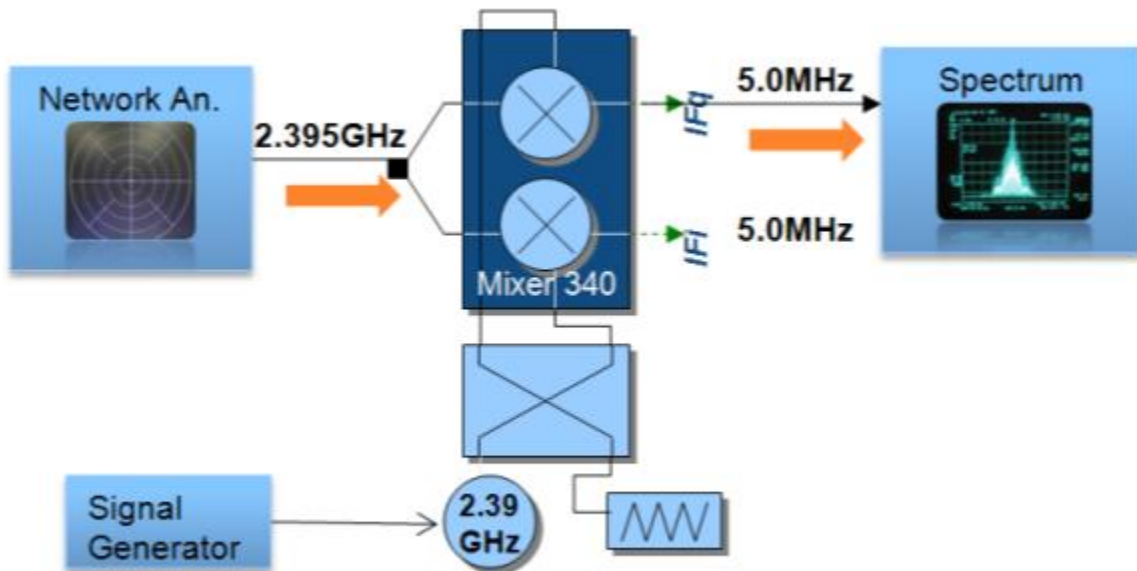


Figure 4-18 Receiver second portion configuration.

The next step is to test the second and final portion of the receiver which consists of a power splitter, a double mixer and a 2.390 GHz local oscillator. Figure [4-18] shows the configuration to perform this test with all necessary equipment and specifying supply voltages. Table 4.4 shows the receiver output response with different input signals. Measurements were taken with the spectrum analyzer at 5 MHz which is the intermediate frequency of our system.

Table 4.4 Receiver Dynamic Range Hardware Test

Rx Input (dBm)	Pout @ Mixer HMC568LC5 (dBm)	Pout @ Vector Mod (dBm)	Rx Pout @ 5MHz (dBm)
-110	-58.8	-53	-65.6
-100	-48.58	-43	-56.6
-90	-39.9	-33	-46.6
-80	-30.19	-23	-36.8
-70	-19.8	-13	-26.4
-60	-9.09	-3	-14.67
-55	-3.74	1	-8.9

.Figures [4-19] to [4-25] show the spectrum analyzer output readings for different input signals.

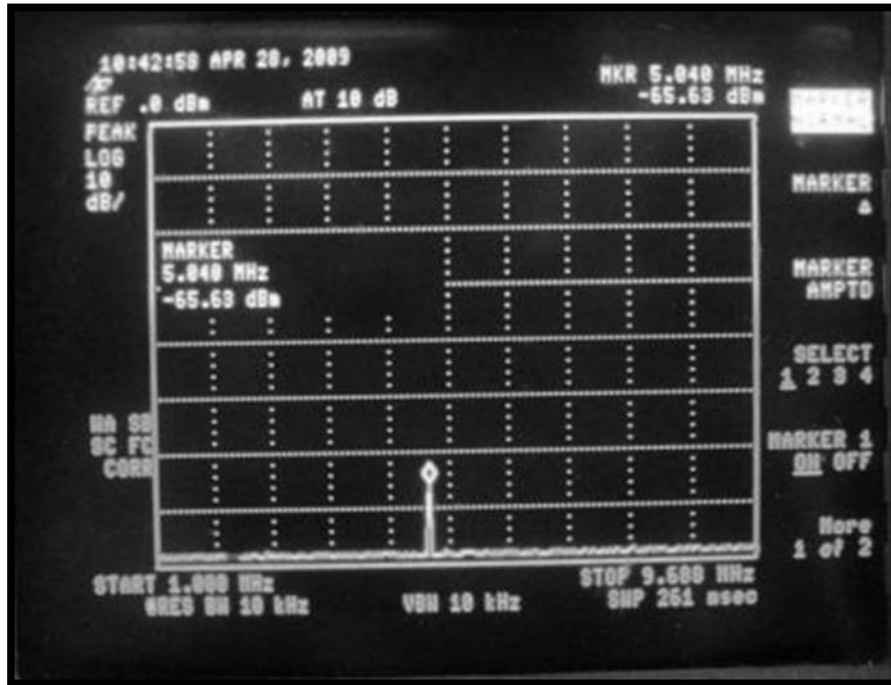


Figure 4-19 Mixer output with Rx -110dBm input

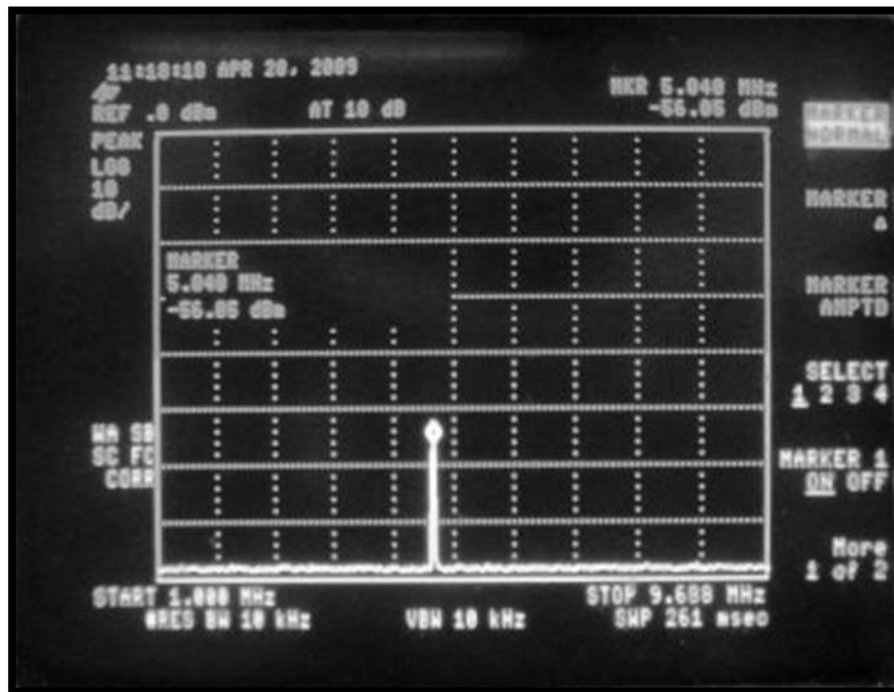


Figure 4-20 Mixer output with Rx -100dBm input

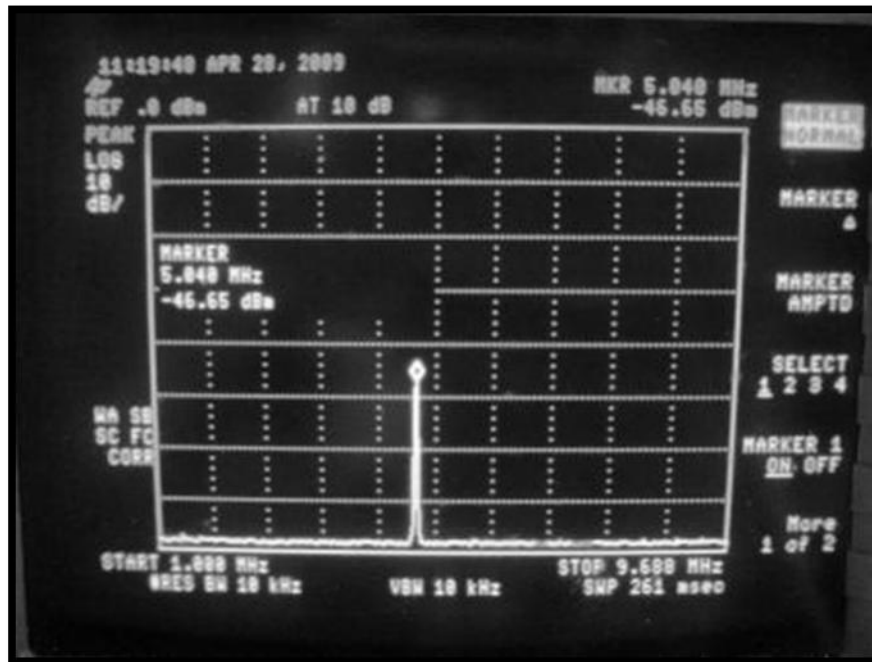


Figure 4-21 Mixer output with Rx -90dBm input

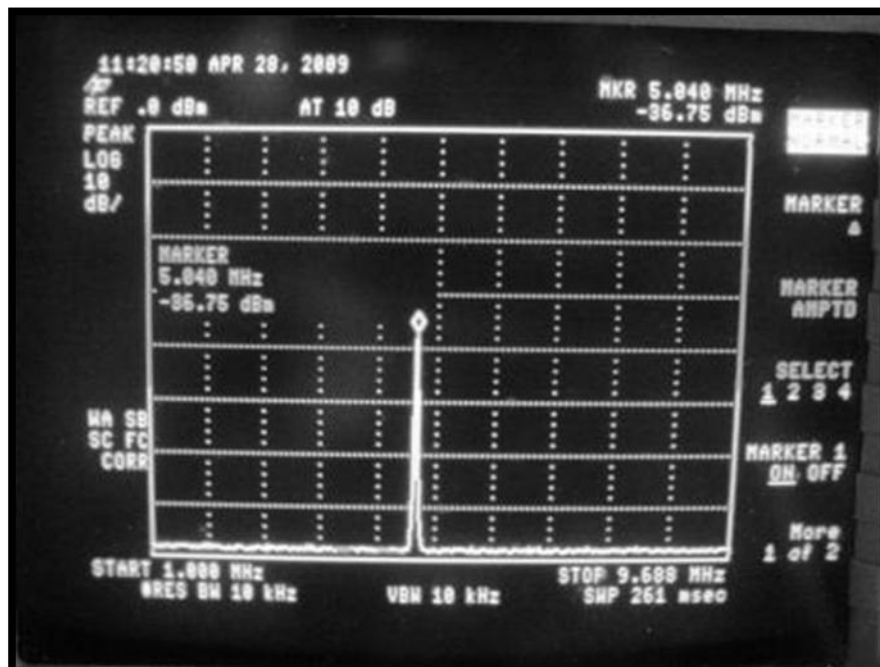


Figure 4-22 Mixer output with Rx -70dBm input

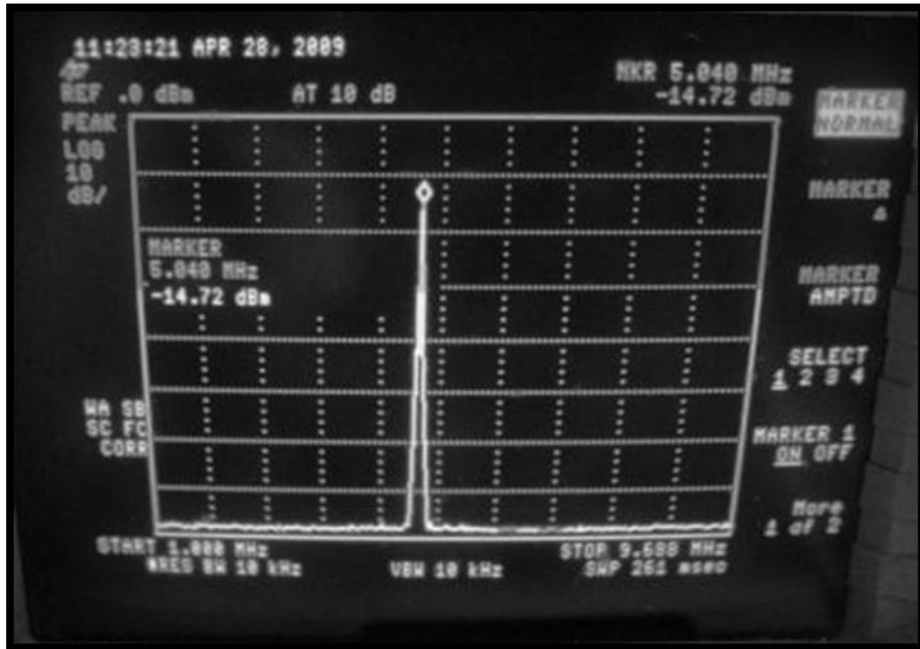


Figure 4-23 Mixer output with Rx -80dBm input

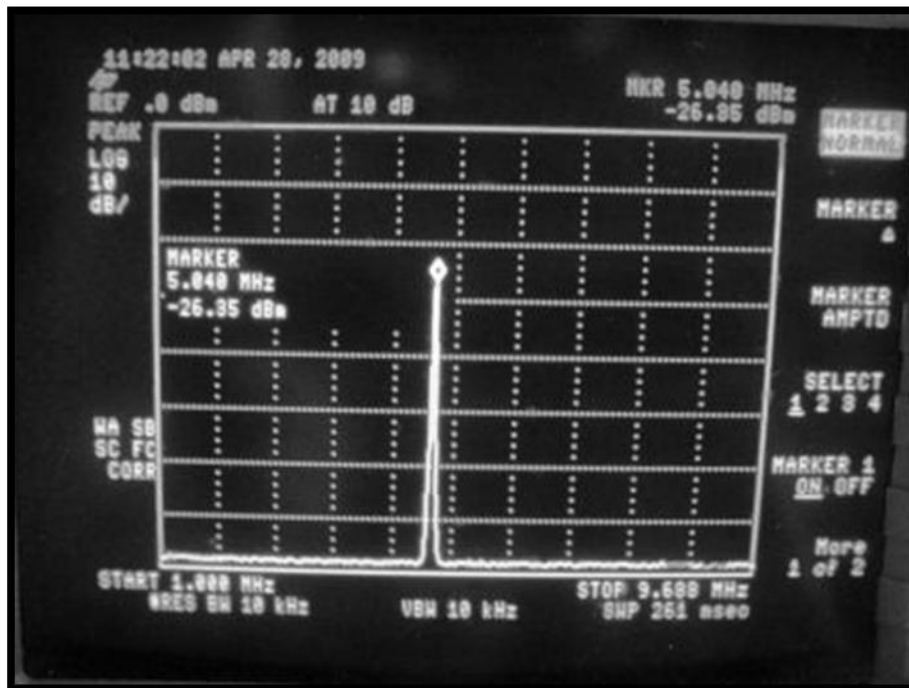


Figure 4-24 Mixer output with Rx -60dBm input

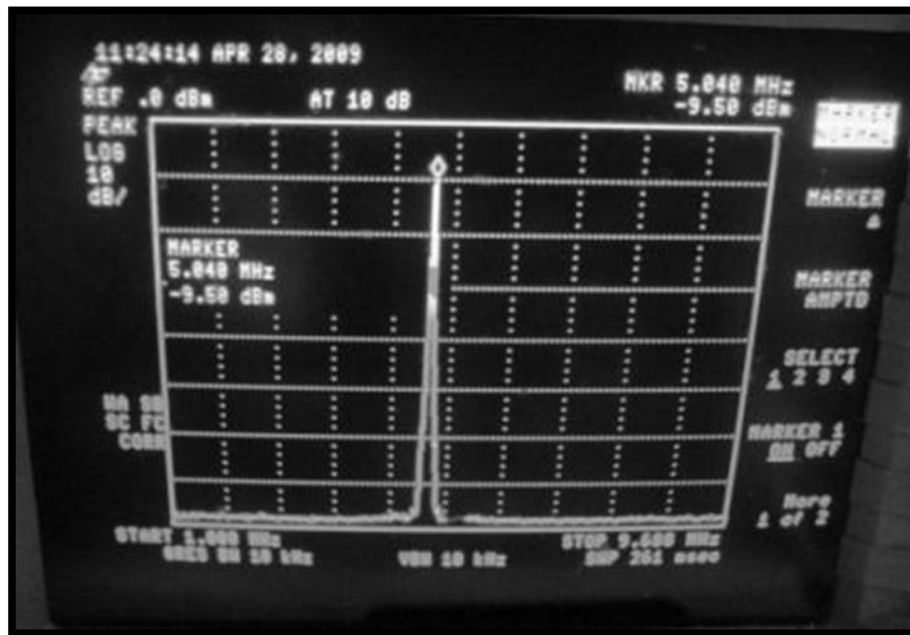


Figure 4-25 Mixer output with Rx -55dBm input

This receiver hardware test also served us to measure the dynamic range of our system. In simulations, it was determined a one channel dynamic range that permits us to have input signals ranging from -110dBm to -55dBm approximately. To measure the dynamic range with the hardware, we fed our system with signals ranging from -110dBm to -55dBm as shown in Table 4.3. We have also tested the circuit with signals greater than -55dBm and it was seen that the receiver saturates having an output value around -7dBm.

4.3 Transmitter Hardware Test Results

To perform the transmitter hardware test a 5MHz (Intermediate Frequency) signal was used to feed the transmit path. This signal was generated using a 500MHz oscillator and was feed directly into the first transmitter mixer (HMC340LP5). For testing purposes the transmitter is been divided in two portions; the first portion to be tested consisted of two quadrature hybrids, two upconverter mixers (HMC521LC4 and HMC340LP5), one power splitter (BP2U), a 10dB and 6dB attenuators, a local oscillator (HMC505LP4) and a 21dB power amplifier (HMC590LP5). The second transmitter portion to be tested consisted of a 21dB power amplifier (HMC590LP5) and the 20dB power amplifier (HMC487LP5). Figure [4-26] show the interconnections of all evaluation boards for the first transmitter portion and Figure [4-27] show the configuration used to perform this test including all necessary equipment and provided voltages. When connecting all boards for this first test we noticed that the local oscillator was not providing the necessary power to activate the mixer. The local oscillator provide an output power of 11dBm and the mixer need at least 15dBm (at the LO input) to operate. To solve this problem we placed the 21dB power amplifier (HMC590LP5) with a 10dB and 6dB attenuators in order to get the desired output. This was used in substitution of the phased locked loop board that needs to be design in the future. This board will control all local oscillators to phase lock them and will provide all necessary power signals. This is very important to synchronize all 24 channels that are going to be added in the future.

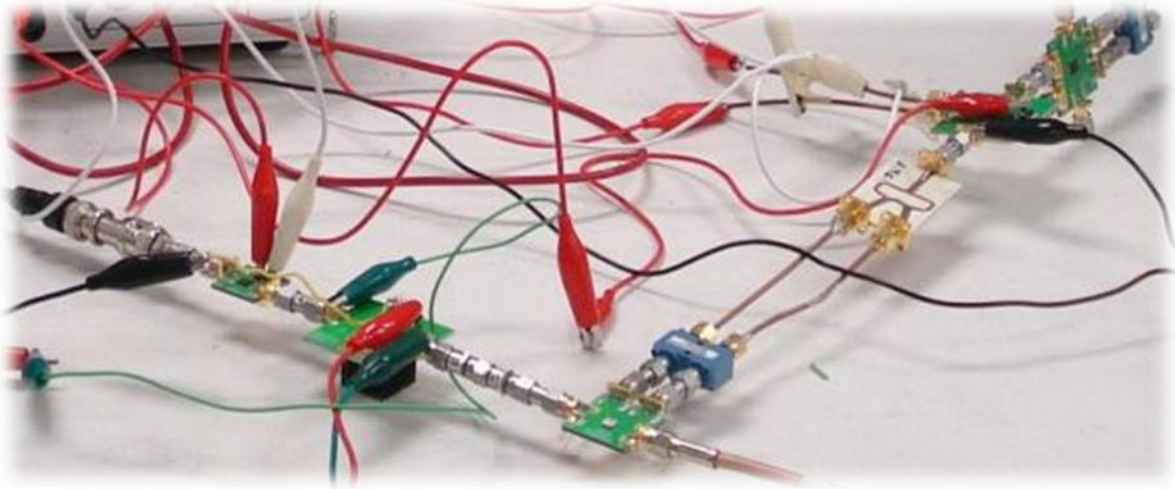


Figure 4-26 First Transmitter portion to be tested (up to the mixer HMC340LP5).

When all interconnections and all power signals were provided to the circuits the system was fed with different power signals at 5MHz. We decided to test the system with 13dBm, 5dBm, 1dBm, and -5dBm input signals at the mixer (HMC340LP5). The power signal obtain through the different stages of this transmitter portion are listed on table 4.5.

Table 4.5 Transmitter first portion power analysis

Tx Power Input (dBm)	Mixer HMC340LP5 Pout (dBm)	Vector Mod HMC63LP3 Pout (dBm)	Power Splitter Pout (dBm)	90 Degree Hybrid Pout (dBm)	Mixer HMC521LC4 Pout (dBm)
13	5.25	-1.57	-6.1	-11.16	-14
5	2.17	-3.62	-8.33	-12.97	-15.9
1	-1.66	-7.08	-11.87	-16.22	-18
-5	-8.77	-13.48	-18.14	-22.5	-20

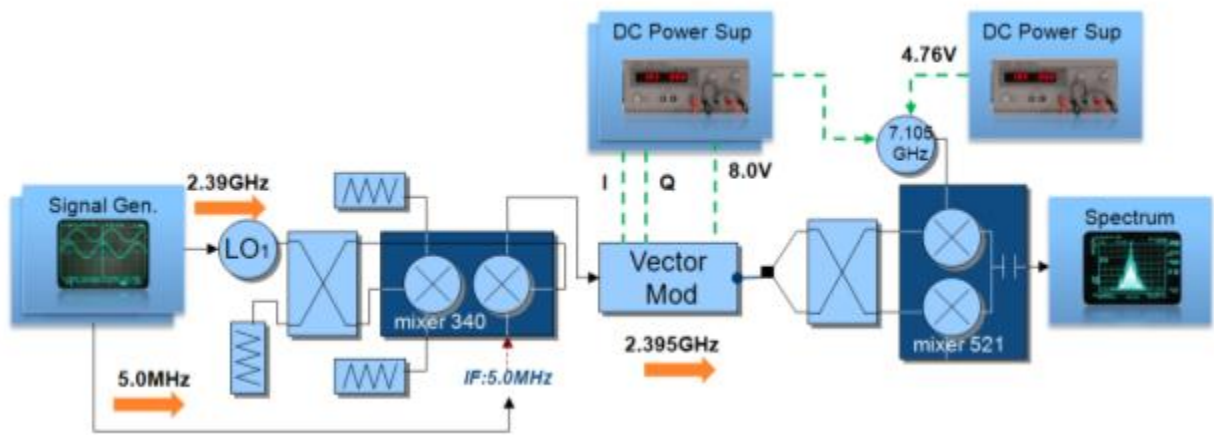


Figure 4-27 First Transmitter portion hardware configuration (up to the mixer HMC521).

Figures [4.28] and Figure [4.29] show the mixer (HMC340LP5) output as seen on the spectrum analyzer display. These outputs are taken at 2.395GHz frequency.

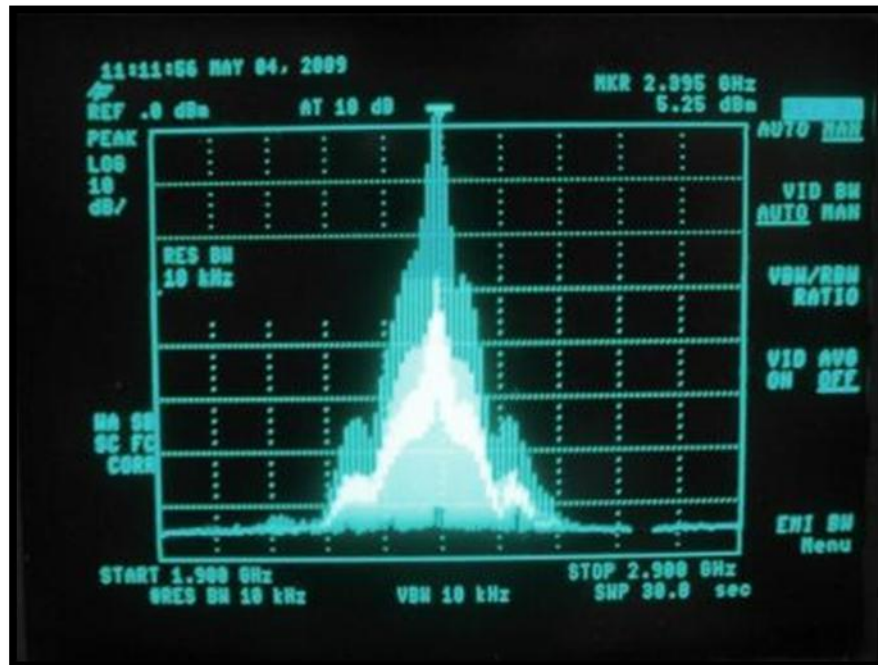


Figure 4-28 Mixer HMC340LP5 output with 13dBm input

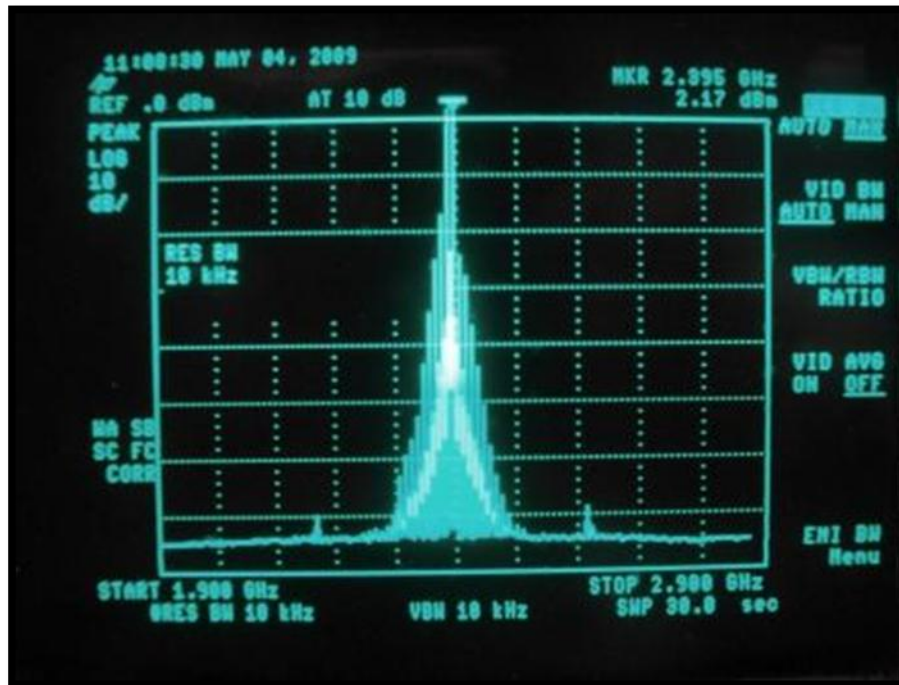


Figure 4-29 Mixer HMC340LP5 output with 5dBm input.

We will expect to see only two peaks on this plot, one for the addition of the signals at 2.395 GHz and one for the subtraction at 2.385 GHz. Instead we see a whole lot more peaks that correspond to the harmonics produced by the instability of the local oscillator. When the local oscillator was set to provide certain frequency the value kept fluctuating, and these fluctuations were responsible of producing all unwanted harmonics. Also some of the peaks correspond to the intermodulation distortion (please refer to theoretical background chapter 2 for more details on intermodulation distortion). For small input power the intermodulation products is small but will increase as input power increases as it can be seen in figure [4-28] and figure [4-29]

Returning to Table 4.5, if a 13dBm power signal is introduced to the mixer (HMC340LP5) it will provide an output power of 5.25dBm that feeds the vector modulator. With this 5.25dBm

signal at the vector modulator input it will be capable of having an output of -1.57dBm. This last signal enters the power splitter which produced an output of -6.1dBm on both ends. This two signals coming out from the power splitter gets in to the 90 degree hybrid producing an output of -11.16dBm. Finally a power of -11.16dBm is the input of the mixer (HMC521LC4) which have an output of -14dBm. In simulations we obtain an output value of -9.36dBm approximately for mixer (HMC521LC4) which is a little bit deviated from our tested value (-14dBm). When looking at all tested values against the simulated values for that mixer, it was notice that all measurements were off by the same approximate amount, 4.64dBm. Table 4.6 show simulated output values against tested output values for mixer HMC521LC4 at different input signals.

Table 4.6 Mixer HMC521LC4 corrected output

Tx Power Input (dBm)	Mixer HMC521LC4 Pout (dBm) Tested	Mixer HMC521LC4 Pout (dBm) Simulated	Error (dBm)	Corrected Mixer HMC521LC4 Pout (dBm)
13	-14	-9.36	-4.64	-9.57
5	-15.9	-11.26	-4.64	-11.57
1	-18	-13.36	-4.64	-13.57
-5	-20	-15.36	-4.64	-15.57

This behavior could be explained due to the network analyzer plus losses on the cables and the power splitter. When the network analyzer is set to deliver a power of 10dBm for example it is really delivering 7.5dBm (as we tested on the lab), this translate to 2.5dBm that we are not having in the input. Both cables connecting the power splitter provide 1dBm of losses each and the power splitter itself provides .43dBm. All this numbers adds to a total loss of 4.43dBm so we corrected the tested mixer (HMC521LC4) output signal by a factor of 4.43dBm. As it can be

seen from table 4.6 the discrepancy between measurements is 4.64dBm and we can only certify 4.43dBm, the other .21dB that is missing in the output could be due to other miscellaneous losses in the system but we are not going to include it to adjust the measurements. Then we have:

$$-14dBm + (2.5dB) + (1dB) + (1dB) + .43dB = -9.57dBm \quad \text{Equation 4.1}$$

Figures [4.30] and [4.31] show the mixer (HMC521LC4) output as seen on the power meter display. This output is taken at 9.5GHz frequency.



Figure 4-30 Mixer HMC521LC4 output with 13dBm transmitter input.



Figure 4-31 Mixer HMC521LC4 output with 5dBm transmitter input.

Now that we have finished testing the first transmitter portion we proceed with the second one. The second transmitter portion to be tested consisted of a 21dB power amplifier (HMC590LP5) and the 20dB power amplifier (HMC487LP5) as shown on figure [4-32] and [4-33]. In this test we basically fed the 21dB power amplifier with the adjusted mixer output we got on the first test. To provide the input signal to the power amplifier we used the network analyzer. Knowing this, it is expected to correct the output signal because the network analyzer provides 2.5dBm under the set value (as we explained on the first test). It is important to mention that the signal provided had a frequency of 9.5GHz because is the signal coming out from the last transmitter mixer (HMC521LC4).

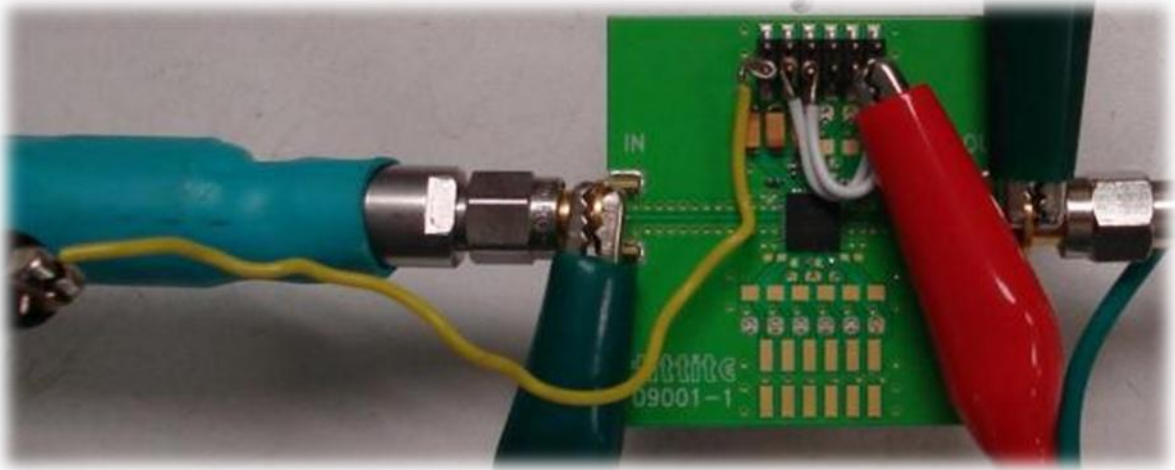


Figure 4-32 21dB Power Amplifier HMC590LP5.

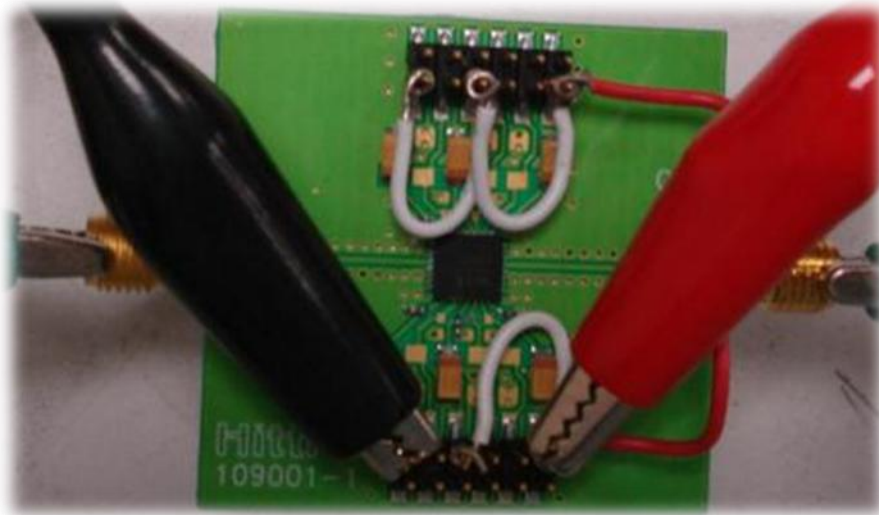


Figure 4-33 20dB Power Amplifier HMC487LP5.

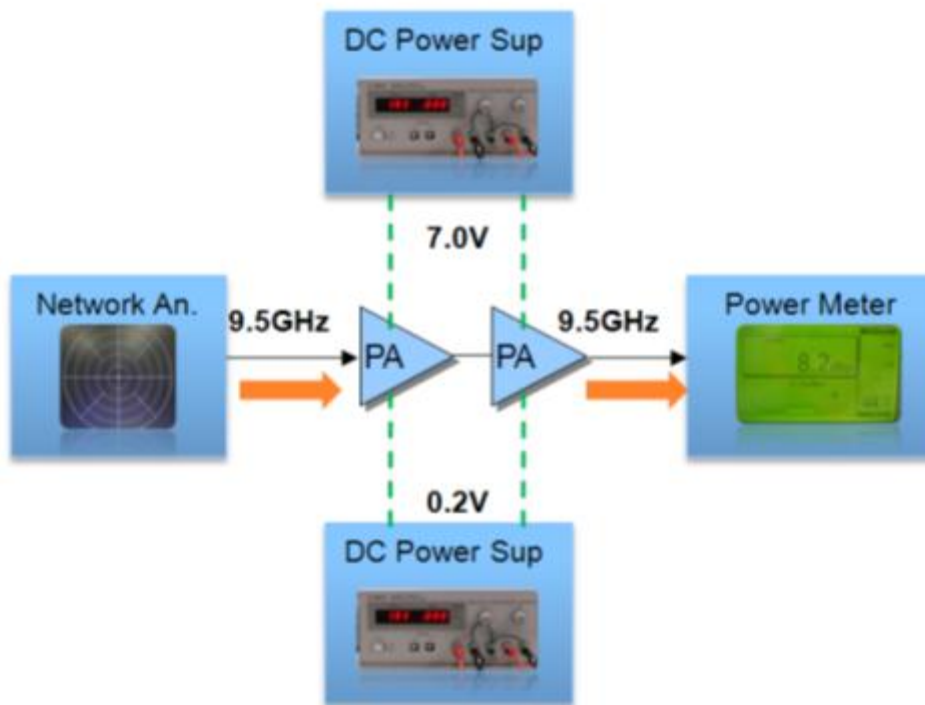


Figure 4-34 Transmitter second portion hardware configuration.

Figure [4-34] shows the configuration we used to test both power amplifiers. Table 4.7 contains both power amplifier outputs and their adjusted values. When feeding the 21dB power amplifier with -9.57dBm power signal at 9.5GHz, we obtain an output of 8.2dBm which is under the expected value by 3.23dBm. Since we already prove that the network analyzer is delivering a signal 2.5dBm under the set signal and we measure cable losses of .73 approximately, then the 21dB power amplifier (HMC590LP5) output has been adjusted by a factor of 3.23dBm.

Table 4.7 Transmitter second portion power analysis

Mixer HMC521LC4 Pout (dBm)	Mixer HMC521LC4 Corrected Pout (dBm)	21dB Power Amp HMC590LP5 Pout (dBm)	21dB Power Amp HMC590LP5 Corrected Pout (dBm)	20dB Power Amp HMC487LP5 Pout (dBm)
-14	-9.57	8.2	11.4	31.4
-15.9	-11.57	6	9.53	29.53
-18	-13.57	3.6	7.4	27.4
-20	-15.57	1.9	5.4	25.4

The next step was to use those 21dB power amplifier output as an input to the 20dB Power Amplifier (HMC487LP5). Again, we used the network analyzer as a source to provide the input signal. Table 4.7 shows the output values for the 20dB amplifier at 9.5GHz. Figures [4-35] and [4-36] are examples of the output measurements as seen on the power meter display.



Figure 4-35 21dB Power Amplifier output with a 13dB input signal to the transmitter



Figure 4-36 21dB Power Amplifier output with 5dB input signal to the transmitter.

5 CONCLUSIONS AND FUTURE WORK

A solid state, dual polarized, Transmit Receive Module for a doppler weather radar has been designed, simulated (using Agilent Advanced Design System) and tested (using components mounted on circuit boards). This TR Module will be the stepstone for further solid state radar design that will be part of the first collaborative and adaptive radar network system to measure lower atmospheric phenomena in the western part of Puerto Rico. The designed solid state TR Module operates at X-band with an operating frequency of 9.5GHz, having a wavelength λ of 31.88mm and a system total bandwidth of 100KHz. The system comprises 24 channels with two Transmit Receive solid state module per channel for a total of 48 TR Modules. Each Module is designed to have a total transmitter power of 1W or 30dBm, then the system have a total transmit power of 24W per polarization. A power analysis throught the circuit was performed in order to ensure compliance with the specifications. It was found from these analyses that the receiver portion of the module is capable to withstand powers no greater than -55dBm and no less than -110dBm. Values greater than -55dBm will cause saturation of the receiver and values less than -110dBm won't be enough power to operate the device. From this analysis it was also found that the transmit protion delivers a power of 30dBm, which means that this system is able to provide 24W of total transmitter power. Performing a Dynamic Range analysis it was found that Receiver portion has a dynamic range with values ranging from -110dBm to -55dBm per channel, (producing a total system dynamic range of 41.9dBm) while the transmitter have a dynamic range with values ranging from .2dBm to

1.7dBm. A Noise Figure analysis was also discussed and it returned a final noise figure value of 4dB. A Two Tone harmonic balanced test was run to determine the intermodulation distortion components around the operating frequency. From this analysis we concluded that no major problems were present in the receiver since both tones produce a value around the expected value (-60dBm). For the transmitter it was seen that both tones diverges from the expected value (30dBm) by 2dBm. This problem was probably caused by the inherent nonlinearities of the mixers and unfortunately when this kind of problem arise no useful information is given by the simulator. Finally this system was built to operate using pulse compression techniques to improve radar resolution and it is designed such that it has a minimum sensitivity around 27dBz at 10km and a maximum sensitivity of 82dBz at that very same range. With the polarimetric, doppler and solid state Transmit Receive Module already designed and tested, the first step will be to provide the corresponding digital signal processing that the signal will undergo before getting into the transmit path and after they are received and converted to Intermediate Frequency (IF), as well as all control signals to synchronize Transmit and Receive Switches in all channels. In addition a phase control board needs to be designed in order to phase locked all local oscillators through all the TR Modules. When the whole radar is constructed it will be used to explore new methods to improve observation, detection and prediction of atmospheric phenomena.

REFERENCES

- [1] Tom M. Hyltin, "The Beginning of Solid State Radars", IEEE Transactions on Aerospace and Electronic Systems Vol. 36, NO. 3 July 2000.
- [2] David N. McQuiddy, Jr. , "Solid State Radar Path to GaAs", Texas Instrument Incorporated, IEEE MTT-S Digest, 1982.
- [3] Alfred Y. Harper, "Solid State Phased Array Radar", U.S. Army Advanced Ballistic Missile Defense Agency, Washington, DC.
- [4] L.P Ligthhart, L.R Nieuwkerk, "An X-Band solid-state FM-CW Weather Radar", IEEE proceedings, Vol. 137, Pt. F, No.6, December 1990.
- [5] Marcel P.J Gaudreau, Jeffrey A. Casey, J. Michael Mulvaney, Michael A. Kempkes, "Solid State Radars Modulators", Diversified Technologies Inc, Bedford MA. 2000 IEEE.
- [6] Marcel P.J Gaudreau, Jeffrey A. Casey, Timothy J. Hawkey, J. Michael Mulvaney, Michael A. Kempkes, "Solid State, High PRF RADAR Modulators", IEEE International Radar Conference, 2000.
- [7] J.D Hay, E.A Kerstenbeck, D.G Rahn, "The Explanatory Development if a High Power S Band Solid State RADAR Transmitter", IEEE International Radar Conference, 1900.
- [8] Raymond Wexler, Joséph Weinstein, "Rainfall Intensities and Attenuation of Centimeter Electromagnetic Waves", Proceedings of the I.R.E, Unpublished Manuscript.
- [9] F.S Marzano, G. Ferrauto, "Relation Between weather radar equation and first-order backscattering theory" European Geosciences Union 2003.
- [10] Brian R. McGee, R.M. Nelms, "Powering Solid State Radar T/R Module Arrays from a Fuel Cell Using and Isolated Cuk Converter.", IEEE 2004. pp. 1853-1857.
- [11] E.B. Brown, E.R Brown, "Retrodirective Noise-Correlating Radar at X-band: First Demonstration of Small Target Detection." IEEE 2005. pp. 1769-1722.
- [12] Francesc Junyent, V. Chandrasekar, H. Bluestein, M. French, "High Resolution Dual-Polarization Radar Observation of Tornados: Implications for Radar Development and Tornado Detection.", IEEE 2005. pp. 2034-2037.

- [13] Toshiaki Kozu, Kenji Nakamura, Robert Maneghini, Wayne C. Bonczyk., “Dual Parameter Radar Rainfall Measurement From Space: A Tets Result From an Aircraft Experiment.”, IEEE 1991, pp. 690-702.
- [14] Vega Cartagena, M.A., “Student Developed Meteorological Radar Network for the western part of Puerto Rico: First Node”, M.S. Thesis, University of Puerto Rico at Mayagüez, May 2007.
- [15] Collaborative Adaptive Sensing of the Atmosphere (CASA) Engineering Research Center, “Overview” [Online]. Available from <http://www.casa.umass.edu>, 2003.
- [16] Marrero, V., “Dual Polarized Microstrip Antenna Array for the Off the Grid Radar”, M.S. Thesis, University of Puerto Rico at Mayagüez, May 2007.
- [17] Castaneda, H., “Phase Shifter System Using Vector Modulator for Phased Array Radar Modulation”, M.S. Thesis, University of Puerto Rico at Mayagüez, May 2006.
- [18] P. Peebles, Jr., Radar Principles, 1st ed., Wiley Inter-Science: New York, 1998.
- [19] Bringi, V.N., and V. Chandrasekar, Polarimetric Doppler Radar, 1st ed., Cambridge University Press: Cambridge, UK, 2001.
- [20] Pozar, D.M., Microwave Engineering, 2nd ed., Wiley: New York, 1998.
- [21] Constantine A. Balanis, Antenna Theory Analysis and Design, 2nd ed., Wiley: New York, 1997.
- [22] Fawaz T Ulaby, Richard K Moore, Adrian K Fung, Microwave Remote Sensing Fundamentals and Radiometry, Vol I, Wesley: New York, 1981.
- [23] Merrill Sholnik, Radar handbook, Second Edition, McGraw-Hill: Boston, 1990.
- [24] Doviak Richard, Doppler Radar and Weather Observations, Second Edition, Dover Publications Inc: Mineola, New York 1993.
- [25] The Hong Kong Observatory. What is a Weather Radar? [Online] Available http://www.hko.gov.hk/education/edu01met/wxrad/ele_radar_e.htm, April 22, 2004.

- [26] Hughes John. Radar Basics [Online] Available
http://superdarn.gi.alaska.edu/photos/PARS2006/Lectures/PPT/Hughes_PPT.ppt,
August 1, 2006.
- [27] Vega, M.A., Colóm, J., Orama, L., “Student Developed Meteorological Radar Network for Western Puerto Rico”, 49th Midwest Symposium on Circuits and Systems, August 2006.
- [28] Stiles Jim, Minimum Detectable Signal. [Online] Available
<http://www.itc.ku.edu/~jstiles/622/handouts/Minimum%20Detectable%20Signal.pdf>,
November 1, 2006.
- [29] Hittite Microwave Corporation, “HMC631LP3/631LP3E GaAs HBT Vector Modulator 1.8-2.7GHz” pp.10-58.
- [30] Ligthart, L.P, and Nieuwkerk, L.R: “FM-CW radar for studies in the lower troposphere”. J.Atmos and Oceanic Technologies., Special issue on lower tropospheric profiling, 1989,6,(5),pp.798-808.
- [31] Ligthart, L.P, and Nieuwkerk, L.R: “An X-Band solid state FM-CW weather radar”.IEEE proceedings, Vol 137, Pt. F, No.6, December 1990,pp.418-426.
- [32] David G. C. Luck, “Frequency Modulated Radars” McGraw-Hill, New York, 1949, 466 pages.


```

dBZe = 10*log10(Ze);

Ze1db = (((6.75*(2^14))*log(2)).*(r.^2).*(lambda^2)*p1db)/A;
dBZe1db = 10*log10(Ze1db);

plot(r,dBZe,'b-')                % Plots.
xlabel('Range (km)')
ylabel('dBZe')
title('Radar Range Sensitivity')
%grid on
hold on
%legend('Min Ze',-1);

figure(2)                        % Dynamic Range Plot.
plot(r,dBZe1db,'r-')
xlabel('Range (km)')
ylabel('dBZe')
title('Receiver Dynamic Range')
%grid on
hold on
plot(r,dBZe,'b-')
%legend('Max Ze','Min Ze',-1)

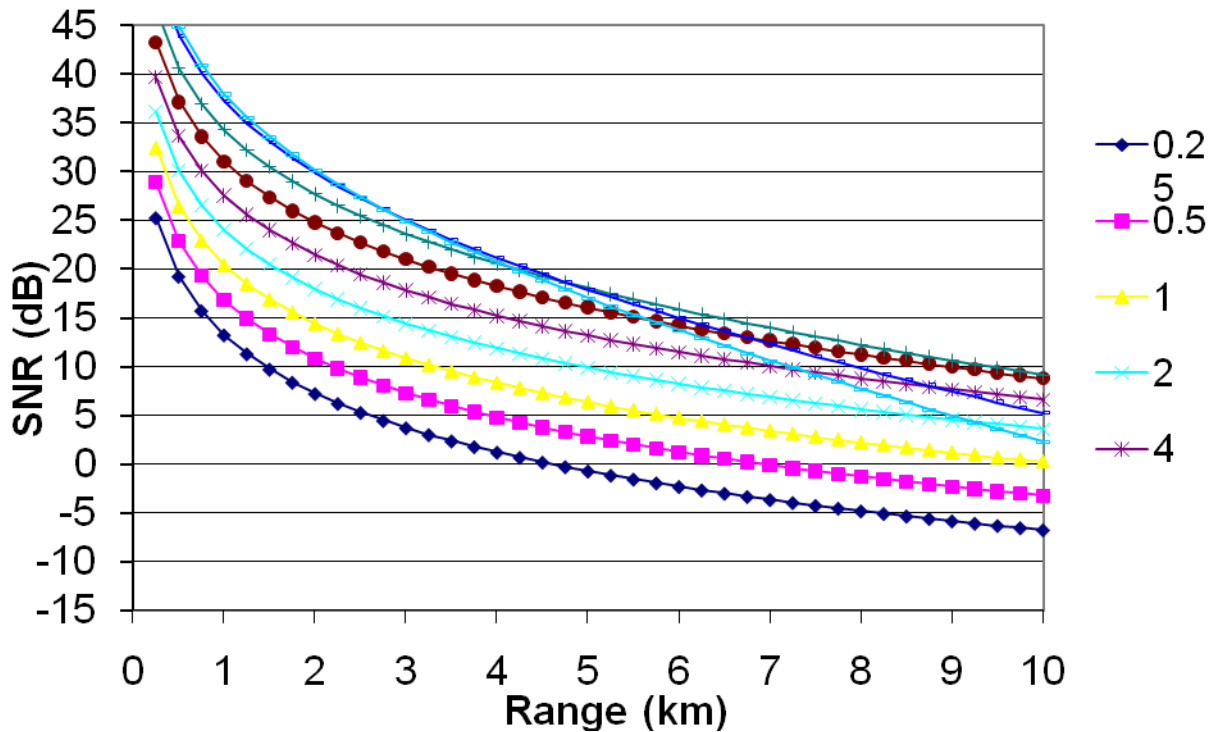
```

USING ROSENFELD RELATION

	0.25	0.5	1	2	4	8	16	32	40
	47.37	108.82	250.00	574.35	1319.51	3031.43	6964.40	16000.00	20912.79
	16.75	20.37	23.98	27.59	31.20	34.82	38.43	42.04	43.20
Range (km)	0.002	0.004	0.010	0.023	0.054	0.124	0.286	0.663	0.868
0.25	25.27572	28.88685	32.49638	36.10217	39.69934	43.27655	46.80761	50.23189	51.29212
0.5	19.25419	22.86409	26.47078	30.07	33.65198	37.19405	40.64381	43.88001	44.83755
0.75	15.73143	19.34011	22.94395	26.53661	30.10339	33.61032	36.97878	40.0269	40.88175
1	13.23172	16.83917	20.44018	24.02627	27.57786	31.04965	34.3368	37.19684	37.949
1.25	11.29258	14.89881	18.49698	22.0765	25.6129	29.04954	32.2554	34.92735	35.57683
1.5	9.708025	13.31302	16.90835	20.48131	24.00252	27.40402	30.52857	33.01244	33.55923
1.75	8.368155	11.97193	15.56442	19.13081	22.63683	26.00318	29.04643	31.34222	31.78632
2	7.207382	10.80993	14.39958	17.9594	21.45023	24.78144	27.74338	29.8511	30.19251
2.25	6.183397	9.784714	13.37153	16.92478	20.40042	23.69648	26.57713	28.49676	28.73549
2.5	5.267313	8.867402	12.45138	15.99807	19.45851	22.71943	25.51878	27.25033	27.38637
2.75	4.438525	8.037387	11.61852	15.15865	18.6039	21.82967	24.54772	26.09119	26.12454
3	3.68182	7.279455	10.85775	14.39131	17.82137	21.012	23.64874	25.00413	24.9348
3.25	2.985643	6.582051	10.15751	13.6845	17.09937	20.25485	22.8103	23.97761	23.80558
3.5	2.341015	5.936196	9.508815	13.02924	16.42892	19.54926	22.0234	23.00263	22.72791
3.75	1.740817	5.334771	8.904551	12.41841	15.80289	18.88809	21.28093	22.07208	21.69468
4	1.179308	4.772035	8.338976	11.84627	15.21556	18.26561	20.57715	21.18022	20.70013
4.25	0.651795	4.243295	7.807397	11.30812	14.66222	17.67713	19.90737	20.32236	19.73958
4.5	0.154389	3.744662	7.305926	10.80008	14.13899	17.11876	19.26769	19.4946	18.80913
4.75	-0.31617	3.272878	6.831304	10.31889	13.64261	16.58723	18.65487	18.69369	17.90554
5	-0.76263	2.825189	6.380776	9.861798	13.17032	16.0798	18.06614	17.91688	17.02604
5.25	-1.18735	2.399242	5.95199	9.426445	12.71978	15.59412	17.49915	17.16181	16.16828
5.5	-1.59235	1.993013	5.542922	9.010811	12.28895	15.12814	16.95187	16.42646	15.33024
5.75	-1.97939	1.604748	5.151819	8.613141	11.87609	14.68014	16.42257	15.70907	14.51016
6	-2.34999	1.232919	4.777151	8.231906	11.47967	14.24857	15.90969	15.00812	13.70652
6.25	-2.7055	0.876182	4.417576	7.865764	11.09833	13.83209	15.41192	14.32226	12.91797
6.5	-3.0471	0.533354	4.071909	7.51353	10.73091	13.42952	14.92804	13.6503	12.14333
6.75	-3.37584	0.203384	3.739101	7.174155	10.37634	13.03981	14.45703	12.99121	11.38155
7	-3.69266	-0.11466	3.418215	6.846702	10.0337	12.66202	13.99794	12.34404	10.63169
7.25	-3.9984	-0.42162	3.108416	6.530336	9.702138	12.29532	13.54994	11.70796	9.892922
7.5	-4.2938	-0.71825	2.808951	6.224304	9.380914	11.93895	13.11227	11.08221	9.164484
7.75	-4.57954	-1.00522	2.519142	5.927929	9.069347	11.59224	12.68426	10.46611	8.445702
8	-4.85624	-1.28315	2.238376	5.640596	8.766823	11.25457	12.26529	9.859063	7.735964
8.25	-5.12445	-1.55259	1.966097	5.36175	8.472785	10.92539	11.8548	9.260499	7.034712
8.5	-5.38469	-1.81405	1.701798	5.090883	8.186727	10.60419	11.4523	8.669915	6.341439
8.75	-5.6374	-2.06799	1.445015	4.827534	7.908186	10.2905	11.05731	8.086848	5.655684
9	-5.88303	-2.31484	1.195326	4.571278	7.636738	9.983912	10.66942	7.510874	4.977022
9.25	-6.12195	-2.55499	0.952341	4.321727	7.371995	9.684025	10.28823	6.941604	4.305065
9.5	-6.35452	-2.78879	0.715704	4.078522	7.113599	9.390485	9.913391	6.378682	3.639454
9.75	-6.58107	-3.01657	0.485084	3.841335	6.86122	9.102962	9.544567	5.821777	2.979861
10	-6.80192	-3.23864	0.260176	3.609861	6.614554	8.821152	9.181455	5.270585	2.325981

Rain Rate (mm/h)
Z
dBZ
Kr

Single Pulse SNR vs Range for Different Rain Rates (mm/hr) using $Z=250R^{1.2}$



Input Section		
f	9.5	radar frequency (GHz)
Pt	19.2	peak transmitted power (W)
Pmin	-110	minimum detectable signal (dBm)
Ga	24	antenna gain (dB)
HBW	6	Horizontal Beamwidth (degrees)
VBW	6	Vertical Beamwidth (degrees)
pw	10	pulse width (μ s)
PRI	100	pulse repetition interval (μ s)

APPENDIX C.

RADAR BUILD OF MATERIAL

RECEIVER						
COMPANY	PIECE PART #	QTY PER POL	POL	CHANNELS	TOTAL QTY	DESCRIPTION
DORADO	31MS95	N/A	2	24	24	20Db CIRCULATOR
HITTITE	HMC564LC4	3	2	24	144	LNA-17dB, 9.5GHz
Mouser	581-04023A101F 04023A101FAT2A	3			432	Capacitors, 0402pkg, 25W, 100pF, pp739
Mouser	581-TACL225K010V TACL225K010XTA	2			288	Capacitors, 10V, 2.2uF, pp824
MINI-CIRCUIT	BP2U	1	2	24	48	POWER SPLITTER
HITTITE	HMC568LC5	1	2	24	48	DOUBLE MIXER, DOWNCONVERTER, 9-12GHz
Mouser	581-04023A101F 04023A101FAT2A	3			144	Capacitors, 0402pkg, 25W, 100pF, pp739
Mouser	581-0402YC102K 0402YC102KAT2A	3			144	Capacitor, 0402pkg, 16V, 1000pF, pp739
Mouser	581-TAJA225K010 TAJA225K010R	3			144	Capacitor, Case A, 2.2uF, *(polarity), pp824
HITTITE	HMC340LP5E	1	2	24	48	DOUBLE MIXER, DOWNCONVERTER, 1.7-4.5GHz
HITTITE	HMC548LP3	2	2	24	96	LNA-19dB, 2.4GHz
Mouser	581-04023A101F 04023A101FAT2A	2			192	150 pF Capacitor, 0402 Pkg.
Mouser	581-0402YC102K 0402YC102KAT2A	1			96	Capacitor, 0402pkg, 16V, 1000pF, pp739
Mouser	80-C0402C183K8K C0402C183K8RACTU	1			96	18,000 pF Capacitor, 0402 Pkg. PP.747
	516-1589-2-ND MSA-0311-TR1G	1			96	Filter, Amotech AMOBP1575P02-A1 2.5 dB loss @ 1575 MHz
HITTITE	HMC505LP4	1	2	24	48	OSCILLATOR, 7.1GHz
HITTITE	HMC385LP4	1	2	24	48	OSCILLATOR 2.4GHZ,

		2	2	24	96	QUADRATURE HYBRIDS
TOTAL PER RECEIVER BOARD		31			2232	

TRANSMITTER						
HITTITE	HMC521LC4	1	2	24	48	DOUBLE MIXER, UPCONVERTER, DC-3.5GHz
HITTITE	HMC340LP5E	1	2	24	48	DOUBLE MIXER, UPCONVERTER, 1.7-4.5GHz
MINI-CIRCUIT	BP2U	1	2	24	48	POWER SPLITTER
HITTITE	HMC590LP5	2	2	24	96	21 dB POWER AMPLIFIER
Mouser	581-04023A101F 04023A101FAT2A	6			576	Capacitors, 0402pkg, 25W, 100pF, pp739
Mouser	581-TACL225K010V TACL225K010XTA	6			576	Capacitors, 10V, 2.2pF, pp824
HITTITE	HMC487LP5	3	2	24	144	20 dB POWER AMPLIFIER
Mouser	581-04023A101F 04023A101FAT2A	6			864	Capacitors, 0402pkg, 25W, 100pF, pp739
Mouser	581-TACL225K010V TACL225K010XTA	6			864	Capacitors, 10V, 2.2pF, pp824
HITTITE	HMC505LP4	1	2	24	48	OSCILLATOR, 7.1GHz
HITTITE	HMC385LP4	1	2	24	48	OSCILLATOR,
DESIGNED	N/A	2	2	24	96	QUADRATURE HYBRIDS
TOTAL PER TRANSMITTER BOARD		36			3456	

VECTOR MODULATOR						
HITTITE	HMC631LP3	1	2	24	48	VECTOR MODULATOR, 1.8-2.7GHz
Mouser	581-TACK475M003Q TACK475M003QTA	1			48	Capacitors Tantalum, 4.7uF, pp824
Mouser	581-04023A101F 04023A101FAT2A	4			288	Capacitors, 0402pkg, 25W, 100pF, pp739
Murata / Digi-Key	81-LDB212G4005C LDB212G4005C-001	1			48	Balun, 0805pkg,
HITTITE	HMC221LP4E	2	2	12	432	SWITCHES, DC-3GHz

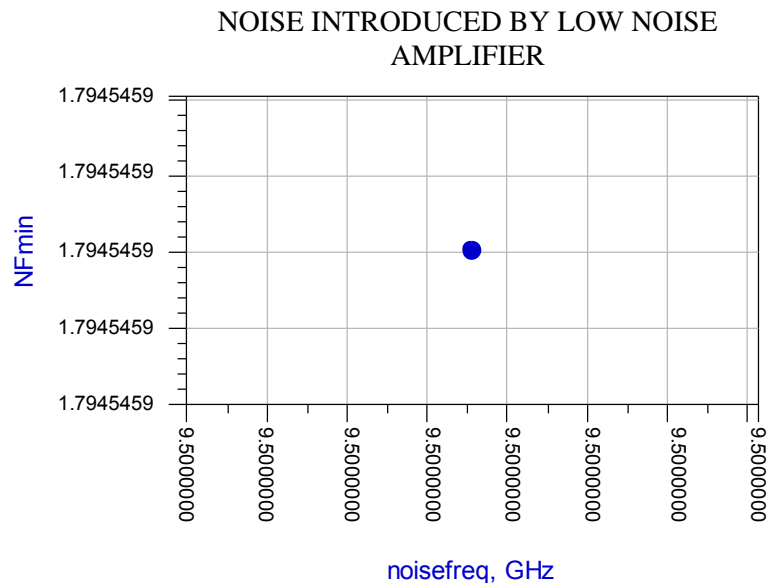
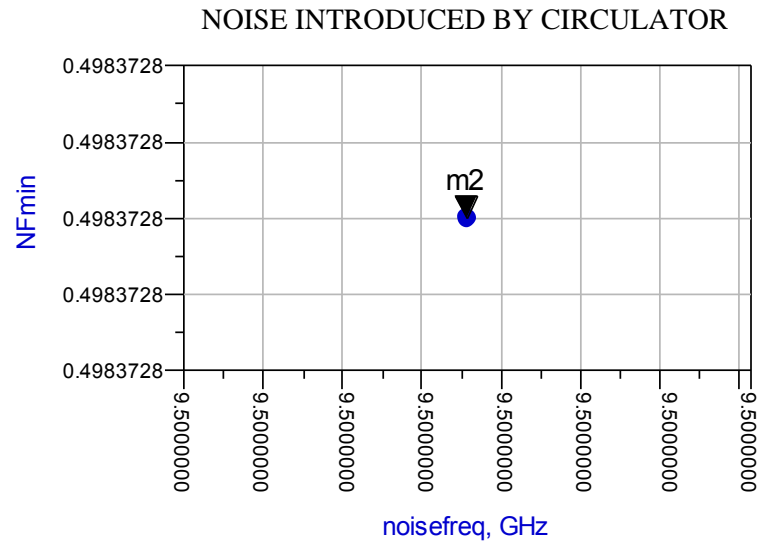
Mouser	581-04025C331K 04025C331KAT2A	3			144	330 pF capacitor, 0402 Pkg.
TOTAL PER VECTOR MODULATOR BOARD		12			1872	

CALIBRATION						
MA-COM	AT-635	1	2	24	48	VARIABLE ATTENUATOR
HITTITE	HMC607LP4E	2	2	24	96	HIGH ISOLATION SWITCH 60dB
NOISECOM	NC1128A	1	2	24	48	NOISE SOURCE
DESIGNED	N/A	1	2	24	48	DIRECTIONAL COUPLER
TOTAL PER CALIBRATION BOARD		5			240	

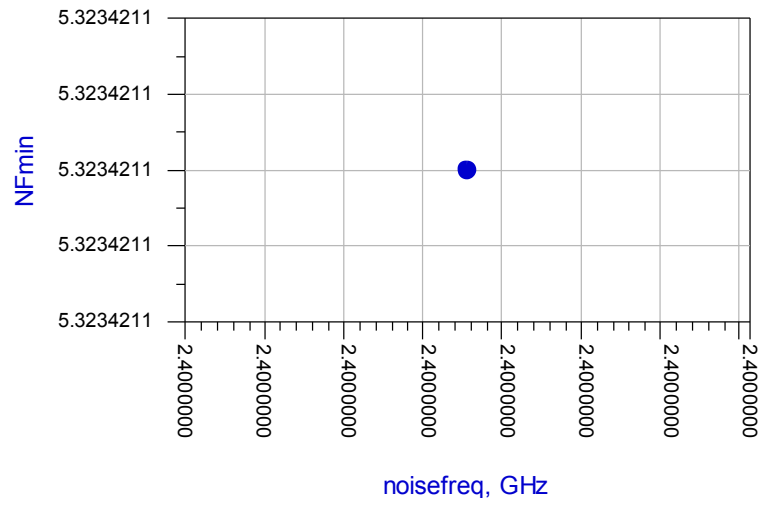
PHASED LOCKED LOOP						
HITTITE	HMC700LP4	1	2	24	48	PHASE LOCKED LOOP
HITTITE	HMC550LP4	1	2	24	48	OSCILLATOR, 7.1GHZ
HITTITE	HMC385LP4	1	2	24	48	OSCILLATOR 2.4GHZ,
HITTITE	HMC590LP5	2	2	24	96	21 dB POWER AMPLIFIER
Mouser	581-04023A101F 04023A101FAT2A	6			576	Capacitors, 0402pkg, 25W, 100pF, pp739
Mouser	581-TACL225K010V TACL225K010XTA	6			576	Capacitors, 10V, 2.2pF, pp824
TOTAL PER OSCILLATOR BOARD		17			1392	

APPENDIX D.

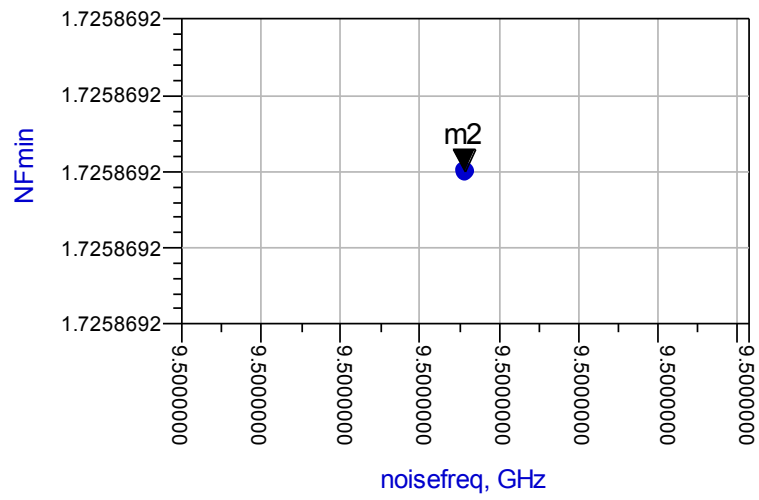
NOISE FIGURE



NOISE INTRODUCED BY MIXER
INCLUDING 90 HYBRID



NOISE INTRODUCED BY ISOLATING
SWITCH



APPENDIX E.

TR MODULE COST

RECEIVER						
COMPANY	PIECE PART #	QTY PER POL	POL	PRICE PER PIECE	COST PER CHANNEL	DESCRIPTION
HITTITE	HMC564LC4	3	2	20.94	125.64	LNA-17dB, 9.5GHz
Mouser	581-04023A101F 04023A101FAT2A	3	2	0.64	3.84	Capacitors, 0402pkg, 25W, 100pF, pp739
Mouser	581- TACL225K010V TACL225K010XTA	2	2	1.63	6.52	Capacitors, 10V, 2.2uF, pp824
MINI-CIRCUIT	BP2U	1	2	4.95	9.9	POWER SPLITTER
HITTITE	HMC568LC5	1	2	33.08	66.16	DOUBLE MIXER, Downconverter, 9-12GHz
Mouser	581-04023A101F 04023A101FAT2A	3	2	0.64	3.84	Capacitors, 0402pkg, 25W, 100pF, pp739
Mouser	581-0402YC102K 0402YC102KAT2A	3	2	0.33	1.98	Capacitor, 0402pkg, 16V, 1000pF, pp739
Mouser	581-TAJA225K010 TAJA225K010R	3	2	0.32	1.92	Capacitor, Case A, 2.2uF, *(polarity), pp824
HITTITE	HMC340LP5E	1	2	10.74	21.48	DOUBLE MIXER, Upconverter, 1.7-4.5GHz
HITTITE	HMC548LP3	2	2	2.9	11.6	LNA-19dB, 2.4GHz
Mouser	581-04023A101F 04023A101FAT2A	2	2	0.33	1.32	150 pF Capacitor, 0402 Pkg.
Mouser	581-0402YC102K 0402YC102KAT2A	1	2	0.33	0.66	Capacitor, 0402pkg, 16V, 1000pF, pp739
Mouser	80-C0402C183K8K C0402C183K8RACTU	1	2	0.37	0.74	18,000 pF Capacitor, 0402 Pkg. PP.747

Amotech	<i>AMOBP1575P02-A1</i>	1	2	0.5	1	Filter, Amotech AMOBP1575P02-A1 2.5 dB loss @ 1575 MHz
	<i>516-1589-2-ND MSA-0311-TR1G</i>	1	2	1.36	2.72	Filter, Amotech AMOBP1575P02-A1 2.5 dB loss @ 1575 MHz
HITTITE	HMC505LP4	1	2	11.75	23.5	OSCILLATOR, 7.1GHz
HITTITE	HMC385LP4	1	2	6.59	13.18	OSCILLATOR,
		2	2		0	QUADRATURE HYBRIDS
TOTAL COST PER RECEIVER BOARD		32	2		296	

VECTOR MODULATOR

HITTITE	HMC631LP3	1	2	12.92	25.84	VECTOR MODULATOR, 1.8-2.7GHz
Mouser	<i>581-TACK475M003Q TACK475M003QTA</i>	1	2	0.7	1.4	<i>Capacitors Tantalum, 4.7uF, pp824</i>
Mouser	<i>581-04023A101F 04023A101FAT2A</i>	4	2	0.64	5.12	<i>Capacitors, 0402pkg, 25W, 100pF, pp739</i>
Murata / Digi-Key	<i>81-LDB212G4005C LDB212G4005C-001</i>	1	2	0.45	0.9	<i>Balun, 0805pkg,</i>
HITTITE	HMC221LP4E	2	2	1.12	4.48	SWITCHES, DC-3GHz
Mouser	<i>581-04025C331K 04025C331KAT2A</i>	3	2	0.33	1.98	<i>330 pF capacitor, 0402 Pkg.</i>
TOTAL PER VECTOR MODULATOR BOARD		55	2		39.72	

TRANSMITTER

HITTITE	HMC521LC4	1	2	20.03	40.06	DOUBLE MIXER, UPCPNVERTER, DC-3.5GHz
HITTITE	HMC340LP5E	1	2	10.74	21.48	DOUBLE MIXER, Upconverter, 1.7-4.5GHz
MINI-CIRCUIT	BP2U	1	2	4.95	9.9	POWER SPLITTER
HITTITE	HMC487LP5	3	2	69.49	416.94	POWER AMPLIFIER
Mouser	581-04023A101F 04023A101FAT2A	6	2	0.64	7.68	Capacitors, 0402pkg, 25W, 100pF, pp739
Mouser	581- TACL225K010V TACL225K010XTA	6	2	1.63	19.56	Capacitors, 10V, 2.2pF, pp824
HITTITE	HMC505LP4	1	2	11.75	23.5	OSCILLATOR, 7.1GHz
HITTITE	HMC385LP4	1	2	6.59	13.18	OSCILLATOR,
		2	2		0	QUADRATURE HYBRIDS
TOTAL PER TRANSMITTER BOARD		82	2		552.3	

CALIBRATION

MA-COM	AT-635	1	2	1	2	VARIABLE ATTENUATOR
HITTITE	HMC232LP4E	2	2	30.51	122.04	
NOISECOM	NC1128A	1	2		0	NOISE SOURCE
		1	2		0	DIRECTIONAL COUPLER
TOTAL PER CALIBRATION BOARD		108	2		124.04	

